

The climate and vegetation of Europe, North Africa and the Middle East during the Last Glacial Maximum (21,000 years BP) based on pollen data

Basil A.S. Davis¹, Marc Fasel², Jed O. Kaplan³, Emmanuele Russo⁴, Ariane Burke⁵

¹Institute of Earth Surface Dynamics, University of Lausanne, Lausanne, 1015, Switzerland

²enviroSPACE lab, Institute for Environmental Sciences, University of Geneva, Geneva, 1211, Switzerland

³Department of Earth Sciences, The University of Hong Kong, Hong Kong, Peoples Republic of China

⁴Department of Environmental Systems Science, ETH Zurich, Zurich, 8092, Switzerland

⁵Laboratoire d'Ecomorphologie et de Paleoanthropologie, Departement d'Anthropologie, Universite de Montreal, Montreal, Quebec, H3C 3J7, Canada

Correspondence to: Basil A. S. Davis (basil.davis@unil.ch)

Abstract. Pollen data represents one of the most widely available and spatially-resolved sources of information about the past land cover and climate of the Last Glacial Maximum (21,000 years BP). Previous pollen data compilations for Europe, the Mediterranean and the Middle East however have been limited by small numbers of sites and poor dating control. Here we present a new compilation of pollen data from the region that improves on both the number of sites (63) and the quality of the chronological control. Data has been sourced from both public data archives and published (digitized) diagrams. Analysis is presented based on a standardized pollen taxonomy and sum, with maps shown for the major pollen taxa, biomes and total arboreal pollen, as well as quantitative reconstructions of forest cover and winter, summer and annual temperatures and precipitation. The reconstructions are based on the modern analogue technique (MAT) adapted using PFT scores, and with a modern pollen dataset taken from the latest Eurasian Modern Pollen Database (~8000 samples). A site-by-site comparison of MAT and Inverse Modelling methods shows little or no significant difference between the methods for the LGM, indicating that no-modern-analogue and low CO₂ conditions during the LGM do not appear to have had a major effect on MAT transfer function performance. Previous pollen-based climate reconstructions using modern pollen datasets show a much colder and drier climate for the LGM than both Inverse Modelling and climate model simulations, but our new results suggest much greater agreement. Differences between our latest MAT reconstruction and those in earlier studies can be largely attributed to bias in the small modern dataset previously used, and differences in the method itself (Brewer et al. 2008, Salonen et al. 2019). We also find that quantitative forest cover reconstructions show more forest than that previously suggested by biome reconstructions, but less forest than that suggested by simple percentage arboreal pollen, although uncertainties remain large. Overall, we find that LGM climatic cooling/drying was significantly greater in winter than in summer, but with large site to site variance that emphasizes the importance of topography and other local factors in controlling the climate and vegetation of the LGM.

46 **1 Introduction**

47

48 During the Last Glacial Maximum (LGM) ~21,000 years BP (Mix et al., 2001), the climate,
49 vegetation and landscape of Europe and its surrounding regions were very different than
50 today. Scandinavia and a large part of the British Isles were covered by a single ice sheet,
51 with separate ice sheets covering the Alps and Pyrenees, while many smaller and lower
52 mountainous areas were also glaciated (Ehlers et al. 2011). As a result of this global build-up
53 of ice on land, sea levels were around 120 meters lower than today, resulting in the retreat of
54 Atlantic and Mediterranean coastlines and the emergence on land of the English Channel and
55 North Sea basin. Falling sea levels also led to the disconnection of the Black Sea from the
56 Mediterranean, and a subsequent drop in Black Sea water levels as evaporation exceeded
57 inflow (Arslanov et al. 2007). On land, permafrost and periglacial processes occurred
58 immediately to the south of the Scandinavian ice sheet, while the massive discharge of glacial
59 clays and sands provided material to be redeposited by the wind as belts of loess across
60 northern France, Benelux, Germany and central Europe (Lehmkuhl et al. 2021). Under these
61 cooler and drier climatic conditions, forests are thought to have retreated to the relative
62 shelter of Southern Europe and the Mediterranean, while relatively unproductive steppe and
63 tundra dominated the region north of the Alps (Grichuk 1992).

64

65 This traditional view of the LGM has been established for many years, but many details
66 concerning the climate and vegetation of the LGM remain debated. Much of this debate
67 concerns information derived from the pollen record, which represents one of the most
68 widely available and spatially-resolved sources of information concerning LGM vegetation
69 and climate, and the primary terrestrial proxy used to evaluate climate models in the
70 Palaeoclimate Modelling Intercomparison Project (PMIP) (Bartlein et al., 2011; Braconnot et
71 al., 2019; Harrison et al., 2014).

72

73 For example, climate model simulations continue to indicate a climate that is less cold and
74 more humid than pollen-based reconstructions (Jost et al., 2005). These results are similar to
75 reconstructions based on glaciological modelling (Allen et al., 2008b). On the other hand, the
76 pollen-based reconstructions that show the greatest disagreement with climate models have
77 themselves been criticized for not considering the possible effect of low atmospheric CO₂ on
78 the physiological relationship between plants and climate (Ramstein et al., 2007). Methods
79 that use modern pollen samples are based on the assumption that the relationship between
80 vegetation and climate remains the same through time, and that this is independent of change
81 in CO₂ concentration. Studies have shown however that plant growth processes and plant
82 resilience are sensitive to CO₂ concentration, and particularly water-use efficiency which
83 would make plants more drought sensitive in low CO₂ environments (Cowling & Sykes
84 1999). Atmospheric CO₂ during the LGM was around 190 ppm, some 100 ppm lower than
85 the pre-industrial period, and 200 ppm lower than the levels experienced in the last 50 years.
86 Concerns about the effects of lower CO₂ during the LGM has directly led to the development
87 of pollen-climate reconstruction methods that can take account of CO₂ effects, either through
88 use of a process-based vegetation model run in inverse mode (Guiot et al. 2000, Guiot et al.
89 2009), or through the use of a correction algorithm (Prentice et al. 2017; Cleator et al., 2020).
90 Pollen-climate reconstructions based on inverse modelling that account for these low CO₂
91 effects show less cooling and drying and consequently greater agreement with climate
92 models (Ramstein et al., 2007; Wu et al., 2007; Izumi & Bartlein., 2016; Wu et al. 2019).

93

94 Further data-model discrepancies have also been highlighted concerning LGM vegetation
95 cover. Earlier pollen synthesis studies, especially those that applied the biomisation method

96 (Elenga et al., 2000) give the impression that non-glaciated areas of LGM Europe were
97 dominated by treeless steppe, while vegetation models driven by climate model simulations
98 indicate large areas of forest and woodlands (Binney et al., 2017; Kaplan et al., 2016;
99 Velasquez et al., 2021). The apparent data-model discrepancy associated with steppe has led
100 to the suggestion that early humans, which are not included in vegetation models, could have
101 reduced the forest cover with only a relatively moderate use of fire because of the cold
102 climate and slow speed of vegetation recovery (Kaplan et al., 2016). This debate is important
103 because of studies that have shown the sensitivity of the climate system to vegetation
104 boundary conditions during the LGM (Ludwig et al., 2017; Velasquez et al., 2021). This
105 suggests that accurate knowledge of the vegetation cover during the LGM is a necessary
106 prerequisite to understanding the role of other influences on the climate system at this time.
107

108 More recent pollen and macrofossil studies from eastern Central Europe have shown that at
109 least in this region there existed areas of open boreal forest and woodland with some
110 temperate broadleaf species (Kuneš et al., 2008; Willis and Van Andel, 2004). The evidence
111 of forest, and particularly elements of temperate broadleaf forest, north of the Alps has come
112 to represent a challenge to the traditional view that forest species only survived the LGM in
113 sheltered refugia far to the south of the Fenoscandian ice sheet and close to the moderating
114 influence of the Mediterranean Sea. The presence of micro-refugia north of the Alps is
115 important because it would represent a very different baseline for understanding the later rate
116 and route of plant migrations under the rapid warming that occurred during the Late Glacial
117 to Holocene transition (Douda et al., 2014; Giesecke, 2016; Krebs et al., 2019; Nolan et al.,
118 2018), as well as understanding patterns of present-day genetic diversity (Normand et al.,
119 2011; Svenning et al., 2008). Modelling studies have shown difficulty in supporting the very
120 high rates of postglacial expansion that would be necessary for southern refugia (Feurdean et
121 al., 2013, Nogués-Bravo et al. 2018).
122

123 Much of this debate has been informed by an increasing number of LGM pollen studies from
124 an ever-broader geographical area, and especially from an increasing number of studies from
125 north of the Alps. Nevertheless, the synthesis of these studies into a single narrative is made
126 difficult by several factors, for instance: different taxonomic definitions, pollen percentages
127 calculated from non-standardized pollen sums, and quantitative analyses such as climate
128 reconstructions that are based on different training sets and methodologies. This has led to
129 some modelling studies ignoring the pollen record completely, on the basis that data from the
130 LGM is too scarce (Janská et al., 2017). Where standardized methods have been applied to
131 multiple LGM pollen records, poor dating control has resulted in the inclusion of many
132 records that may not actually be from the selected LGM time window. This is particularly
133 important because the 21 ± 2.0 ka time slice commonly used to represent the LGM period in
134 PMIP data-model comparisons and other synthesis studies (MARGO members, 2009;
135 Bartlein et al., 2011) occurs immediately after the glacial maxima in the Alps around 26-23
136 ka (Heiri et al., 2014; Spötl et al., 2021) and Heinrich stadial HS-2 (24.3-26.5), whilst also
137 being closely followed by Heinrich stadial HS-1 (15.6-18.0 ka) (Sanchez-Goñi & Harrison,
138 2010). These closely associated time periods can therefore be expected to represent both a
139 different vegetation and climate than the LGM itself.
140

141 For example, of the 18 European pollen records used in the PMIP benchmarking dataset
142 (Bartlein et al., 2011), 10 fall into the worst class ('poor') in the COHMAP chronological
143 quality classification scheme if relative dating such as pollen correlation is excluded. More
144 recent synthesis studies have also relied heavily on records from the European Pollen
145 Database (EPD) which currently has 116 records with samples of LGM age (as of June

146 2022). Many of these records however are based on chronologies that are considered reliable
147 for the Holocene (Giesecke et al., 2014), but have large uncertainties for the LGM as a result
148 of 1) excessive extrapolation back in time from Holocene age dates, 2) the use of pollen
149 correlation or other relative dating despite poorly defined regional biostratigraphy, or 3) the
150 inappropriate use of radiocarbon dates contaminated with old carbon. We found that 104 of
151 these 116 EPD records (Neotoma, 2021) fall into the worst class ('poor') in the COHMAP
152 chronological quality classification.

153

154 Here we address these problems using a new synthesis of LGM pollen records from
155 throughout Europe, the Mediterranean and the Middle East (EurMedMidEst) based on
156 rigorous quality control criteria. Records were compiled from an extensive review of public
157 databases and archives, and the scientific literature. Pollen records were selected according to
158 the robustness of their chronological control around the PMIP LGM time-window (21 ± 2
159 ka), and combined into a single dataset based on a harmonized taxonomy and standardized
160 pollen sum. The dataset was then analysed so that standardised maps could be produced to
161 show the distribution of the major pollen taxa, biomes and total arboreal pollen at the LGM.
162 In addition, quantitative reconstructions of forest cover as well as winter, summer and annual
163 temperatures and precipitation were undertaken using a modified version of the standard
164 Modern Analogue Technique (MAT) (Guiot et al. 1989), utilizing the latest Eurasian Modern
165 Pollen Database v2 dataset. These climate reconstructions are compared and evaluated
166 against previous LGM pollen-climate reconstructions, as well as reconstructions based on
167 other proxies. The dataset and results are fully documented and the complete data files are
168 provided in the supplementary information.

169

170 **2 Methods**

171

172 **2.1 Pollen Data**

173

174 LGM fossil pollen data from Europe and bordering regions including North Africa and the
175 Middle East were selected and collated into a single standardized project database. This data
176 was sourced from the EPD/Neotoma database (Williams et al., 2021), the Pangaea data
177 archive, publications in scientific journals, and from the original authors. We selected LGM
178 pollen sites/data according to strict quality control criteria. Where possible, primary raw
179 pollen counts were used where this was available. Where the original electronic data was not
180 available, the data was digitized from the published diagram. Overall we have included 63
181 records in our study, of which 35 were digitized and 28 consisted of the original pollen
182 counts (Table 1).

183

184 The distribution of the 63 sites reflects the distribution of suitable archives, with fewer
185 records available from climatically or environmentally challenging regions (Fig. 1). High
186 rates of erosion and a drier and colder climate during the LGM reduced the number of
187 suitable anoxic sediment sinks for pollen preservation, especially in Central Europe between
188 the Scandinavian and Alpine ice sheets. Nevertheless, our dataset includes sites from this
189 region, as well as North Africa and eastern Central Europe through to Iran, although most
190 sites are located in an arc across eastern Spain, the Alps, and Italy. Lakes sites are the most
191 numerous archive and tend to be located in the more sheltered and topographically favourable
192 regions of Southern Europe and the Mediterranean. Peat is the next most important archive,
193 followed by alluvial and colluvial sediments, as well as cave sites, the later also often being
194 known for their archaeological significance. Sites located at the ice margins that appear to be
195 under the ice reflect uncertainties in the location of the ice margin both in time and space

196 during the LGM, as well as the fact that the selected time window for this study (21 ± 2 ka) is
197 later than the maximum ice advance in some regions (Hughes and Gibbard, 2015). For
198 completeness, we also include 7 marine records which have the advantage of more
199 continuous deposition and often better dating over the LGM period, but which are prone to
200 taphonomic biases compared to terrestrial records. These biases are discussed later in this
201 section.

202

203 LGM pollen records were selected according to a number of quality control criteria, but
204 primary amongst these was the existence of sufficient independent chronological control
205 points to accurately identify samples that would fall within the 21 ± 2 ka BP time-slice of
206 interest. We have used all of the samples within this time frame where the samples have been
207 available in electronic form, else we have used the sample closest to the target time (21 ka
208 BP). For records taken from the EPD we have used the latest Bayesian age-depth models
209 where these were available (Giesecke et al., 2014), otherwise we have used the dates and
210 chronology proposed by the original authors. We classified chronologies according to the
211 COHMAP chronological quality scheme for the LGM period (Anderson et al., 1988; Yu and
212 Harrison, 1995), which classifies record quality from 1-6 depending on whether a date falls
213 within 2000 14C years (or less) of the time being assessed, or whether bracketing dates fall
214 within 6000 and 8000 14C years (or less) about the time being assessed (Table A1).
215 Chronologies based on dates that fall outside of these limits fall into COHMAP class 7, and
216 are regarded as ‘poorly dated’ with respect to the LGM. Importantly, we have only included
217 radiometric and other absolute dates (such as varves) in this assessment, and have excluded
218 dates based on correlation with regional pollen records. These pollen-based stratigraphic
219 dates have been widely used in previous LGM studies, but do not include estimates of
220 uncertainty and are generally regarded as unreliable at this time given the sparsity of well
221 dated pollen sites and samples on which to base any correlation (Giesecke et al., 2014).

222

223 All records that were classified as poorly dated (COHMAP class 7) were subsequently
224 excluded from our analysis. This has meant that many of the pollen records used in previous
225 studies were excluded, including 16 of the 26 LGM records used by PMIP and associated
226 studies in Europe (Bartlein et al., 2011; Elenga et al., 2000; Tarasov et al. 2000, Jost et al.,
227 2005; Peyron et al., 1998; Wu et al., 2007; Cleator et al., 2020). We also excluded 104 of the
228 116 records in the EPD with samples that fall within our LGM time window. Many of these
229 EPD pollen records have been used in more recent studies, although the exact record (EPD
230 Entity number) is often not stated. We estimate that we have excluded 16 of the 17 European
231 sites used by Binney et al. (2017) (this study only included sites above latitude 40N), 5 of the
232 6 European sites used by Allen et al. (2010), 28 of the 33 sites used by Cao et al. (2019) and
233 27 of the 71 sites used by Kaplan et al. (2016).

234

235 Other quality control criteria were also used in the selection of LGM pollen records.
236 Published pollen diagrams that only included a small part of the terrestrial pollen assemblage,
237 or only presented summary taxa, were excluded. Records were also excluded where the
238 dating information was incomplete, for instance where radiocarbon dating uncertainties were
239 not published or where it was not possible to determine if the date shown was in calibrated or
240 uncalibrated radiocarbon years.

241

242 The modern pollen data for the climate and tree cover reconstructions were sourced from the
243 latest version 2 of the Eurasian Modern Pollen Database (Davis et al., 2020), which is
244 managed as part of the EPD. The EMPD2 includes 8133 modern pollen samples from across
245 the Palearctic biogeographic region from Europe to the far East of Asia. The taxa from both

246 the fossil and modern pollen data were consolidated into 120 of the most commonly-
247 occurring terrestrial taxa types. This taxa list was designed to be compatible with the
248 biomisation scheme used in our study (Peyron et al., 1998; Tarasov et al., 2000) and that used
249 in the Holocene mapping study of Brewer et al. (2017). The count of *Larix* was amplified by
250 a factor of 10 due to its low pollen representation (Edwards et al. 2000, Bigelow et al. 2003,
251 Tarasov et al. 1998, 2000, 2013, Binney et al., 2017).

252

253 **2.2 Biomisation**

254

255 We converted pollen assemblages to biomes based on the European biomisation scheme of
256 Peyron et al (1998), which in turn is based on Prentice et al. (1996). The method is described
257 in detail in Collins et al. (2012). We expanded the number of taxa included in the biomisation
258 procedure proposed by Peyron et al (1998) to include taxa from the Northern Eurasian
259 biomisation procedure of Tarasov et al. (1998). The inclusion of additional Northern Eurasian
260 taxa reflects recent evidence that modern analogues of LGM vegetation occur in parts of
261 Siberia (Magyari et al., 2014a). The biomisation procedure (Prentice et al. 1996) assigns each
262 taxa to a plant functional type (PFT) and calculates a score for each of these PFT's based on
263 the sum of the square root of the percentage of each of the taxa included in that PFT. To
264 reduce the influence of long-distance transport, taxa below 0.5% are removed at the start of
265 the procedure. Each biome is then assigned one or more PFT's and a score for each biome is
266 calculated as the sum of the associated PFT scores. The biome with the highest score is then
267 viewed as the dominant biome. Where the highest score is the same for more than one biome,
268 the dominant biome is decided based on a hierarchy of unique PFT's. Peyron et al. (1998)
269 also included a procedure for distinguishing warm and cold steppe biomes based on re-
270 assigning certain steppe PFT's according to the presence or otherwise of PFT's indicative of
271 cold or warm conditions. Following the Biome6000 project (Elenga et al., 2000) and Allen et
272 al. (2010), we did not apply this additional procedure and present only the merged steppe
273 biome. In summary, the biomisation procedure categorised 39 arboreal pollen taxa and 39
274 non-arboreal taxa into 22 plant functional types (PFT's), which were then combined into 12
275 biomes.

276

277 **2.3 Quantitative climate reconstruction**

278

279 We reconstructed climate from pollen data based on a ~~standard~~-modified Modern Analogue
280 Technique (MAT) (Guiot et al. 1989) that used PFT scores to match fossil samples with
281 modern pollen samples (as used by Davis et al., 2003). "Other methods using PFT scores and
282 artificial neural network techniques have been developed to reconstruct the climate of Europe
283 during the LGM from pollen data (Peyron et al. (1998) and Jost et al (2005). PFT scores have
284 been used in previous large-scale European pollen-based climate reconstructions for the
285 Holocene (Davis et al., 2003; Mauri et al., 2014, 2015), where performance was found to be
286 better than the conventional approach based on individual taxa (eg Marsicek et al., 2018). A
287 particular advantage of the PFT approach for the LGM is that it can help overcome problems
288 associated with vegetation (pollen) assemblages that may have no modern analogue (Davis et
289 al. 2003). This can be a problem during the LGM when the climate and environment could be
290 expected to be very different from today, and when many taxa formed unusual vegetation
291 assemblages as a result of their forced retreat to sheltered refugia locations. The problem of
292 modern analogues is also addressed in our reconstruction by using the latest EMPD2 modern
293 pollen dataset. The EMPD2 provides a large number of potential modern analogues for many
294 different LGM vegetation types and climates found today across the Palearctic region. PFT
295 scores were calculated according to the methods outlined already in the Biomisation section,

296 then normalized so that each sample was proportional to every other sample (Juggins and
297 Birks, 2012).

298
299 The MAT method was applied using the Rioja program for R (Juggins, 2020). The modern
300 pollen data was taken from the latest version 2 of the EMPD (as detailed earlier). The
301 EMPD2 includes 8133 samples, which is considerably larger than the modern datasets used
302 in previous LGM pollen-based reconstructions. For instance, Peyron et al. (1998) used a
303 modern pollen dataset of 683 samples, which was updated by Jost et al (2005) to include an
304 additional 185 samples. These datasets were also mainly taken from the steppes of Kazakstan
305 and Mongolia, while the EMPD2 covers a much wider area, spanning most of the Eurasian
306 Palearctic region (Davis et al., 2020). The size and distribution of the modern training set in
307 climate and vegetation space is important because in order for the method to work
308 effectively, it is necessary to have samples representative of the likely vegetation and climate
309 space that could be occupied by the fossil assemblage (Turner et al. 2021, Chevalier et al.,
310 2020; Salonen et al. 2012, Juggins, 2013).

311
312 A known problem with MAT is the role of spatial auto-correlation in providing
313 unrealistically low estimates of uncertainty (Chevalier et al., 2020; Telford and Birks, 2009).
314 This results from the fact that closely analogous modern pollen samples can also be located
315 closely in physical space, and therefore in climate space. To reduce this problem it is possible
316 to exclude closely located samples from the analogue matching process using a filter based
317 on a set distance (h-block filter) (Telford and Birks, 2009). While this approach can help,
318 there are also three main problems associated with it. The first is error substitution, since
319 removing samples also reduces the number of potential analogues, creating a different source
320 of error that is not easy to categorise. Secondly, multiple samples taken from the same
321 location are actually a strength of pollen training sets, since they are more likely to capture
322 the full range of the assemblage diversity associated with a given climate. Thirdly, current
323 methods that limit spatial range such as the h-block filter only do so on the horizontal axis,
324 and do not consider the fact that samples can also be found at different elevations. In hilly or
325 mountainous regions samples can therefore be excluded because they are closely located in
326 horizontal space, but in fact they actually occupy very different climates and vegetation
327 associations, contradicting the logical premise of the h-block filter. It was therefore decided
328 not to apply this filter.

329
330 Uncertainties for the pollen-climate reconstructions were calculated using a standard method
331 for MAT (Juggins 2020) based on the spread of the climates associated with the best modern
332 pollen analogues used for each fossil sample. The closer the climates of the best modern
333 pollen analogues (6 in the case of this study) then the smaller are the calculated uncertainties
334 assigned to the reconstructed climate of the fossil pollen sample.

335
336 Climate reconstructions are presented as anomalies. These have been calculated with respect
337 to modern climate (1970-2000 average) at each core site location using WorldClim 2 (Fick
338 and Hijmans, 2017) (Table A2), which was also used to assign the modern climate for the
339 modern pollen samples in the transfer function (Davis et al., 2020).

340 **2.4 Marine pollen records**

341
342
343 We have included marine pollen records in our analysis for reasons explained below, but it is
344 important that these records should be viewed with caution, particularly when used for biome
345 and quantitative MAT reconstructions, and when compared with terrestrial records from

346 different archives. Biomisation methods have been applied to individual marine pollen
347 records (Combourieu Nebout et al., 2009), as well as multi-site synthesis studies such as the
348 ACER project (ACER project members et al., 2017). However, marine records were
349 specifically excluded from the Biome6000 project (Elenga et al., 2000). Similarly,
350 quantitative climate methods have been applied to individual marine pollen records
351 (Combourieu Nebout et al., 2009; Fletcher et al., 2010), as well as multi-site synthesis studies
352 (Sánchez Goñi et al., 2005; Brewer et al., 2008; Salonen et al., 2021). However, marine
353 records have also been specifically excluded from other major pollen-climate studies
354 (Cheddadi et al., 1996; Davis et al., 2003; Marsicek et al., 2018), as well as quantitative forest
355 cover reconstructions (Zanon et al. 2018).

356
357 Discussion on the advantages and problems associated with marine records can be found
358 elsewhere (Chevalier et al., 2020; Daniau et al., 2019), but are reviewed briefly here where
359 relevant to the methodologies applied in this study. Marine sedimentary records provide
360 continuous and well dated pollen records for the LGM that are often lacking from many
361 terrestrial regions, especially in arid areas with few alternative anaerobic sediment sinks.
362 Conversely however, pollen source areas for marine sites may be many hundreds of
363 kilometers from the coring site and may be liable to change through time in response to
364 changes in distance to the coastline, rates of river discharge and ocean and atmospheric
365 dynamics. This can theoretically give rise to changes in the vegetation shown in the pollen
366 assemblage recorded at the marine site without any actual change in climate or other
367 environmental pressure. The large and indeterminable source area of marine records also
368 mean that it is difficult to apply quantitative MAT reconstruction methods, not least because
369 the mean climate or forest cover of the source area is almost impossible to determine. In
370 addition, the fossil pollen record and the modern pollen dataset to which it is being compared
371 are composed largely of terrestrial lakes and bog sites with much smaller and more
372 homogeneous source areas. This creates a series of problems, the more obvious of which is
373 the calculation of anomalies, since we cannot assume that the modern climate at the (marine)
374 coring site location is representative of the (terrestrial) source area. In this study we have
375 taken the closest point on land as the modern climate for the calculation of anomalies, but
376 provide the absolute values for all sites so that these can be recalculated if necessary (Table
377 A2). The next problem is that the large source area may capture a combination of different
378 vegetation types that is not going to be represented in a modern pollen dataset based on
379 samples from terrestrial sites with much smaller source areas, for instance a mixture of
380 coastal and mountain vegetation, or even vegetation from different continents (Magri and
381 Parra, 2002). However, in our analysis we did not find any sample from a marine record (or
382 terrestrial record) that did not have a reasonable modern analogue in our training set (chord
383 distance <0.3)(Huntley, 1990), even though we did not adjust the pollen assemblage for the
384 over-representation of *Pinus* (and other Pinaceae) in the marine pollen samples.

385
386 Typically, the Pinaceae component is excluded from the terrestrial pollen sum when
387 calculating percentages for marine pollen samples, and in some cases has been excluded
388 entirely from the samples used in marine pollen-climate reconstructions (Combourieu Nebout
389 et al., 2009). The problem with excluding *Pinus* is two-fold, the first is that *Pinus* often
390 represents the main forest forming tree in the Koeppen Csb climate zone on the Atlantic coast
391 where many marine sites are located (García-Amorena et al., 2007), as well as representing
392 the most abundant tree taxa in Europe during the LGM (Figure A10).

393
394 The effect of excluding Pinaceae on the biomisation algorithm and MAT climate
395 reconstruction process has not been widely investigated. We therefore decided to evaluate

396 this problem for 1) biomisation, and 2) pollen-climate reconstruction. In table S3 we show
397 the biomisation results for 8213 modern pollen samples taken from the EMPD2 modern
398 pollen database. Using this as the control, we then artificially varied the amount of Pinaceae
399 (*Pinus*, *Abies* and *Picea*) in the assemblage of each pollen sample and compiled the results
400 (Table S3). This shows quite clearly that removing all of the Pinaceae has a much more
401 profound effect on the biomisation process than artificially inflating the amount of Pinaceae
402 (as might be expected in a marine sample where Pinaceae can be over-represented). Even
403 when Pinaceae was artificially inflated by as much as 400% of the original value, the biomes
404 were changed in only 2348 samples, compared to 5860 samples if all the Pinaceae was
405 removed entirely. In terms of the effects on individual biomes, removing the Pinaceae
406 considerably increased the amount of CLDE, STEP and TUND, whilst greatly reducing the
407 amount of XERO, almost eliminating the amount of TAIG, and completely eliminating the
408 COCO biome. In contrast, the effect of inflating the amount of Pinaceae tended to be more
409 evenly distributed between the biomes, with the biggest increase seen in TUND and biggest
410 decrease in STEP. This suggests that even if the over-representation of Pinaceae was quite
411 extreme in marine pollen samples, the effect on biome classification (and by definition, the
412 underlying PFT scores) is less than removing Pinaceae completely from the pollen
413 assemblage.

414
415 In a second test, we compared the reconstruction of LGM climate from marine pollen
416 samples when Pinaceae was included, and excluded. The results are shown in table S4 and
417 indicate reconstructed temperatures are generally 1-2C cooler, and precipitation slightly
418 higher when Pinaceae is excluded. The differences between the two methods however are
419 small, and generally less than half of the uncertainties, suggesting that differences are
420 statistically indistinguishable when considered in the context of the overall uncertainties.

421
422 In summary we find that including Pinaceae in the biomisation process is less likely to lead to
423 miss-assignment of the biome than excluding Pinaceae, except in extreme cases of over-
424 representation. Percentages of Pinaceae in the LGM marine samples range on average
425 between 23-88%, suggesting that while Pinaceae was high at some sites, it does not appear to
426 completely overwhelm the assemblage as might be expected if over-representation was to be
427 a significant problem. We also find that including Pinaceae in the pollen assemblage of the
428 LGM marine pollen samples gives pollen-climate reconstructions that are statistically
429 indistinguishable from those obtained by excluding Pinaceae from the assemblage. Including
430 Pinaceae in marine samples also provides compatibility with terrestrial samples, particularly
431 when calculating and plotting pollen taxa percentages. For these reasons we have included
432 Pinaceae in the analysis of all marine pollen samples in this study, although it is important to
433 recognize that Pinaceae in such samples can be subject to over-representation and that the
434 results presented here from marine sites should consequently be viewed with caution.

435 436 437 **2.54 Quantitative tree cover reconstruction**

438
439 It has long been recognized that the proportional representation of individual pollen taxa in a
440 pollen assemblage does not necessarily reflect the proportion of land area covered by that
441 taxa in the pollen source area surrounding the sample site (Davis 1963, Gaillard et al. 2010,
442 Zanon et al. 2018). These differences can be caused by variations in pollen productivity,
443 differential transport, deposition and preservation of pollen grains, and even the ease or
444 otherwise of the identification of pollen grains themselves. This can make the interpretation

445 of pollen taxa percentages difficult, even for relatively simple questions such as the
446 proportion of forest to non-forest in the landscape.

447
448 There have been two main methods developed to account for this quantification problem, one
449 using a physical modelling technique (PMT) based on estimates of pollen production for
450 individual taxa (Gaillard et al., 2010), and the other using a MAT very similar to that used in
451 pollen-climate reconstructions (Williams and Jackson, 2003). Both approaches have been
452 widely applied during the Holocene in Europe (Zanon et al., 2018), but we know of no
453 previous study that has applied either of these approaches to the LGM. The LGM presents a
454 number of challenges, not least the problem of potential missing vegetation analogues, as
455 well as low atmospheric CO₂, which has been shown to influence pollen productivity (Leroy
456 and Arpe, 2007).

457
458 Here we use the MAT to provide quantitative estimates of forest cover, following the
459 approach of Zanon et al. (2018) who applied this method to the Holocene pollen record of
460 Europe. We apply MAT in exactly the same way as for the climate reconstructions described
461 earlier, including the use of PFT scores to match fossil and modern pollen samples. Instead of
462 modern climate values, we assigned an estimate of modern forest cover to each of our
463 modern pollen sites. To do this we use a high resolution (~100m) remote sensing dataset
464 derived from satellite observations (Hansen et al., 2013). Zanon et al. (2018) have shown that
465 the MAT calibrated in this way gives comparable results to the PMT approach in Europe, at
466 least for the Holocene. One of the main differences however is that the PMT is designed to
467 provide estimates of the proportions of different taxa, whereas the MAT (as applied here) is
468 designed to provide estimates of the proportion of forest cover. Where the PMT can only
469 reconstruct the proportion of forest forming trees, irrespective of their size, the MAT
470 (following Zanon et al. 2018) is calibrated specifically to reconstruct forest composed of trees
471 over 5m tall. This follows the FAO definition of forest as “land spanning more than 0.5
472 hectares with trees higher than 5 meters and a canopy cover of more than 10 percent, or trees
473 able to reach these thresholds in situ” (FAO Terms and definitions 2020
474 <http://www.fao.org/3/I8661EN/i8661en.pdf>).

475 476 **2.6.5 Maps**

477
478 We present our results in the form of maps that include the main physiographic features of
479 the LGM in the study area. The maps are based on the WGS84 projection. Coastlines reflect
480 LGM sea level at 120m below present, while ice sheets are based on Ehlers et al. (2011).
481 Modern national country boundaries are also included for reference.

482 483 **2.6 Marine pollen records**

484
485 ~~We have included marine pollen records in our analysis for reasons explained below, but it is~~
486 ~~important that these records should be viewed with caution, particularly when used for biome~~
487 ~~and quantitative MAT reconstructions, and when compared with terrestrial records from~~
488 ~~different archives. Biomisation methods have been applied to individual marine pollen~~
489 ~~records (Combourieu Nebout et al., 2009), as well as multi-site synthesis studies such as the~~
490 ~~ACER project (ACER project members et al., 2017). However, marine records were~~
491 ~~specifically excluded from the Biome6000 project (Elena et al., 2000). Similarly,~~
492 ~~quantitative climate methods have been applied to individual marine pollen records~~
493 ~~(Combourieu Nebout et al., 2009; Fletcher et al., 2010), as well as multi-site synthesis studies~~
494 ~~(Sánchez Goñi et al., 2005; Brewer et al., 2008; Salonen et al., 2021). However, marine~~

495 records have also been specifically excluded from other major pollen-climate studies
496 (Cheddadi et al., 1996; Davis et al., 2003; Marsicek et al., 2018), as well as quantitative forest
497 cover reconstructions (Zanon et al. 2018).

498
499 Discussion on the advantages and problems associated with marine records can be found
500 elsewhere (Chevalier et al., 2020; Daniau et al., 2019), but are reviewed briefly here where
501 relevant to the methodologies applied in this study. Marine sedimentary records provide
502 continuous and well-dated pollen records for the LGM that are often lacking from many
503 terrestrial regions, especially in arid areas with few alternative anaerobic sediment sinks.
504 Conversely however, pollen source areas for marine sites may be many hundreds of
505 kilometers from the coring site and may be liable to change through time in response to
506 changes in distance to the coastline, rates of river discharge and ocean and atmospheric
507 dynamics. This can theoretically give rise to changes in the vegetation shown in the pollen
508 assemblage recorded at the marine site without any actual change in climate or other
509 environmental pressure. The large and indeterminable source area of marine records also
510 mean that it is difficult to apply quantitative MAT reconstruction methods, not least because
511 the mean climate or forest cover of the source area is almost impossible to determine. In
512 addition, the fossil pollen record and the modern pollen dataset to which it is being compared
513 are composed largely of terrestrial lakes and bog sites with much smaller and more
514 homogeneous source areas. This creates a series of problems, the more obvious of which is
515 the calculation of anomalies, since we cannot assume that the modern climate at the (marine)
516 coring site location is representative of the (terrestrial) source area. In this study we have
517 taken the closest point on land as the modern climate for the calculation of anomalies, but
518 provide the absolute values for all sites so that these can be recalculated if necessary (Table
519 A2). The next problem is that the large source area may capture a combination of different
520 vegetation types that is not going to be represented in a modern pollen dataset based on
521 samples from terrestrial sites with much smaller source areas, for instance a mixture of
522 coastal and mountain vegetation, or even vegetation from different continents (Magri and
523 Parra, 2002). However, in our analysis we did not find any sample from a marine record (or
524 terrestrial record) that did not have a reasonable modern analogue in our training set (chord
525 distance < 0.3) (Huntley, 1990), even though we did not adjust the pollen assemblage for the
526 over-representation of *Pinus* (and other Pinaceae) in the marine pollen samples.

527
528 Typically, the Pinaceae component is excluded from the terrestrial pollen sum when
529 calculating percentages for marine pollen samples, and in some cases has been excluded
530 entirely from the samples used in marine pollen-climate reconstructions (Combourieu-Nebout
531 et al., 2009). The problem with excluding *Pinus* is two-fold, the first is that *Pinus* often
532 represents the main forest-forming tree in the Koeppen Csb climate zone on the Atlantic coast
533 where many marine sites are located (García-Amorena et al., 2007), as well as representing
534 the most abundant tree taxa in Europe during the LGM (Figure A3eA5).

535
536 The effect of excluding Pinaceae on the biomisation algorithm and MAT climate
537 reconstruction process has not been widely investigated. We therefore decided to evaluate
538 this problem for 1) biomisation, and 2) pollen-climate reconstruction. In table S3 we show
539 the biomisation results for 8213 modern pollen samples taken from the EMPD2 modern
540 pollen database. Using this as the control, we then artificially varied the amount of Pinaceae
541 (*Pinus*, *Abies* and *Picea*) in the assemblage of each pollen sample and compiled the results
542 (Table S3). This shows quite clearly that removing all of the Pinaceae has a much more
543 profound effect on the biomisation process than artificially inflating the amount of Pinaceae
544 (as might be expected in a marine sample where Pinaceae can be over-represented). Even

545 when Pinaceae was artificially inflated by as much as 400% of the original value, the biomes
546 were changed in only 2348 samples, compared to 5860 samples if all the Pinaceae was
547 removed entirely. In terms of the effects on individual biomes, removing the Pinaceae
548 considerably increased the amount of CLDE, STEP and TUND, whilst greatly reducing the
549 amount of XERO, almost eliminating the amount of TAIG, and completely eliminating the
550 COCO biome. In contrast, the effect of inflating the amount of Pinaceae tended to be more
551 evenly distributed between the biomes, with the biggest increase seen in TUND and biggest
552 decrease in STEP. This suggests that even if the over-representation of Pinaceae was quite
553 extreme in marine pollen samples, the effect on biome classification (and by definition, the
554 underlying PFT scores) is less than removing Pinaceae completely from the pollen
555 assemblage.

556
557 In a second test, we compared the reconstruction of LGM climate from marine pollen
558 samples when Pinaceae was included, and excluded. The results are shown in table S4 and
559 indicate reconstructed temperatures are generally 1-2C cooler, and precipitation slightly
560 higher when Pinaceae is excluded. The differences between the two methods however are
561 small, and generally less than half of the uncertainties, suggesting that differences are
562 statistically indistinguishable when considered in the context of the overall uncertainties.

563
564 In summary we find that including Pinaceae in the biomisation process is less likely to lead to
565 miss-assignment of the biome than excluding Pinaceae, except in extreme cases of over-
566 representation. Percentages of Pinaceae in the LGM marine samples range on average
567 between 23-88%, suggesting that while Pinaceae was high at some sites, it does not appear to
568 completely overwhelm the assemblage as might be expected if over-representation was to be
569 a significant problem. We also find that including Pinaceae in the pollen assemblage of the
570 LGM marine pollen samples gives pollen-climate reconstructions that are statistically
571 indistinguishable from those obtained by excluding Pinaceae from the assemblage. Including
572 Pinaceae in marine samples also provides compatibility with terrestrial samples, particularly
573 when calculating and plotting pollen taxa percentages. For these reasons we have included
574 Pinaceae in the analysis of all marine pollen samples in this study, although it is important to
575 recognize that Pinaceae in such samples can be subject to over-representation and that the
576 results presented here from marine sites should consequently be viewed with caution.

577 578 579 **3. Results**

580 581 **3.1 Vegetation & Biomes**

582
583 Results of the biomisation analysis shows that steppe (STEP) was the most common biome at
584 the LGM across the study area, occurring at 36 out of 63 sites, indicating that the landscape
585 was largely dominated by cool temperate grasslands across much of western Central Europe,
586 central and eastern Mediterranean, as well as North Africa and the Middle East (Fig. 2).
587 However, at the same time we also find that there were a significant number of sites where
588 we find that woody and forest biomes occur, more particularly in southern and eastern Iberia,
589 northern Italy and central eastern Europe. The most dominant of these forest and woody
590 biomes are taiga (TAIG) in the north, and cool-mixed forest (COMX) and xerophytic
591 woodlands (XERO) in the south.

592
593 As would be expected, the dominance of STEP biomes is generally reflected in low arboreal
594 pollen percentages across the same areas/sites (Fig. 3 & 4). Exceptions to this rule can be

595 found at marine sites such as [MD99-2331 site #3] and [MD01-2430 site #58] where STEP is
596 reconstructed despite arboreal pollen percentages of 71 and 80 percent respectively. This
597 apparent contradiction illustrates some of the idiosyncrasies of the biomisation method,
598 especially when applying the method to marine pollen samples. In this case it is important to
599 remember that the AP% is calculated from the sum of the percentages of each relevant taxa,
600 but the score for each biome is the sum of the square root of the percentages of each of its
601 constituent taxa. This results in biomes with taxa with large percentage values scoring
602 proportionally smaller, and biomes with taxa with small percentage values scoring
603 proportionally larger. For example, a single taxa at 50% has a square root of 7.07, but the
604 sum of the square roots of 10 taxa each at 5% is 22.36 even though the sum of the
605 percentages is the same 50%. This effect can be particularly pronounced in marine pollen
606 samples because they are usually dominated by a single taxa (*Pinus*) that forms a high
607 percentage of the total assemblage. Since there are often more non-arboreal taxa than
608 arboreal taxa in a pollen assemblage, the non-arboreal taxa can dominate in the biomisation
609 process even if collectively their percentage of the assemblage is a lot less than the arboreal
610 taxa, resulting in a non-arboreal biome such as STEP having the highest biome score.

611
612 Of the main arboreal biomes, Taiga (TAIG) is the dominant biome at 3 sites at the eastern
613 end of the Alpine ice sheet, as well as at a site just to the north in northern Germany and a
614 site in Slovakia, while Cool Conifer Forest (COCO) is found at 1 site close to the
615 Scandinavian ice sheet in Lithuania. Cool Mixed Forest (COMX) is found much more widely
616 at 8 sites south of the Alps from south-west Iberia to Romania, with Xerophytic Scrub
617 (XERO) occurring at 8 sites with a similar distribution but not as far east or west. Cold
618 Mixed Forest (CLMX) occurs at just two sites in Georgia and the Alboran Sea at the far east
619 and west of the study area, while Warm Mixed Forest (WAMX) is the dominant biome at just
620 1 site in Southern Spain. We do not record Temperate Deciduous Forest (TEDE), Tundra
621 (TUND) or Desert (DESE) as the dominant biome at any site at the LGM, although they do
622 occur as sub-dominant biomes.

623
624 An alternative picture of LGM tree-cover is provided by the MAT reconstructions (Fig. 4).
625 MAT performance statistics for tree cover are shown in table 2, based on an evaluation using
626 the modern training set. This shows a relatively large root mean square error (RMSE) of
627 21.03. and an R2 of 0.52 that is not as good as for the MAT climate analysis, but overall the
628 results are comparable with previous MAT tree cover studies (Zanon et al., 2018). In general,
629 the MAT values (site average 34%) show forest-cover around 16% less than that suggested
630 from AP% (site average 50%) (Fig. A1), although sites with very low AP% also show higher
631 values based on MAT. These differences are consistent with comparisons between MAT and
632 AP% in Zanon et al (2018), although it should be noted that uncertainties related to the MAT
633 reconstructions are large ($\pm 23\%$). Zanon et al (2018) found that the differences between
634 MAT and AP% were greatest over Northern Europe and in Arctic and sub-Arctic climate
635 regions that are likely to be comparable to many areas of Europe during the LGM. These
636 regions today are associated with tree-forming taxa such as Birch that fail to grow to a height
637 of 5m or more, developing only as shrubs or krummholz forms.

638
639 Pollen taxa percentages are shown in supplementary figure A2, and distribution maps of the
640 33 most common taxa are shown in the supplementary figures [A3a](#)[A3-f](#)[A8](#). Of the 21
641 arboreal taxa, *Pinus* generally has the highest values and is the most widespread, being
642 present at all 63 sites. Other acicular arboreal taxa include *Juniperus*, which also has a wide
643 distribution across EurMedMidEst although at lower values. The rest of the acicular arboreal
644 taxa have more regional distributions. *Picea* is found mainly to the north of the study region,

645 away from the Mediterranean, whilst *Abies* is generally found more to the south. *Larix* occurs
646 only in the central European area including the northern edge of the Po plain just south of the
647 Alps, whilst *Cedrus* is found mainly across south and west Europe in locations much further
648 north than its Holocene and modern distribution which is confined mainly to Morocco and
649 Lebanon (Collins et al., 2012). Temperate broadleaf arboreal taxa which also include cold-
650 tolerant species such as *Betula* and *Salix* are relatively widely spread across the
651 EurMedMidEst during the LGM, while less drought tolerant taxa such as *Alnus*, *Carpinus* and
652 *Corylus* are found more to the south-west through to the north-east. Other temperate
653 broadleaf arboreal taxa such as *Quercus* (deciduous) and *Ulmus* have a much more southern
654 distribution, with *Fraxinus*, *Olea*, and *Quercus* (evergreen) being more prevalent in the
655 south-west. In contrast, *Fagus* occurs more to centre and the east, while *Tilia* is found even in
656 more northern locations of central Europe. The remaining arboreal taxa are more shrubby and
657 drought adapted, with *Ephedra* and particularly *Ephedra fragilis* having a southern
658 distribution, whilst the more cold adapted *Hippophae* being found even in the north of central
659 Europe (similar to *Tilia*).

660
661 The main non-arboreal taxa generally indicate cool, dry and environmentally disturbed
662 conditions across much of the EurMedMidEst. The most widely distributed taxon is Poaceae,
663 which like *Pinus*, is found in all records. Other non-arboreal taxa with a widespread
664 distribution include Rubiaceae, Apiaceae and Asteraceae (Asteroideae), while *Plantago*,
665 Cayophyllaceae, Brassicaceae and Asteraceae (Cichorioideae) have a more southern and
666 western distribution. *Thalictrum* can be found mostly at sites in the centre of the
667 EurMedMidEst, along with *Helianthemum* which also extends to sites in the south-west.
668 Other taxa such as *Chenopodiaceae* and *Artemisia* have a more southern distribution,
669 reflecting their preference for drier and less cold climates.

670

671 **3.2 Climate reconstruction evaluation**

672

673 Evaluation of transfer function performance based on the modern training set is presented in
674 table 2. This shows that root mean square error predicted (RMSEP) values were smallest for
675 summer temperatures (2.21C), and largest for winter temperature (3.35C), with mean annual
676 temperatures in between (2.28C). The weaker performance for winter temperatures largely
677 reflects the much greater range of winter temperatures in the training set. In turn, this
678 contributes to a better R2 performance for winter temperatures (0.91) than annual
679 temperatures (0.9) and summer temperatures (0.81). Overall R2 performance for precipitation
680 is weaker than for temperature, which is typical because of the higher spatial variability of
681 precipitation compared to temperature. Summer precipitation has the strongest R2
682 performance (0.75) compared to winter and annual precipitation (both 0.69), as well as
683 smaller RMSE values (52mm) than winter (78mm).

684

685 Given the widespread occurrence of steppe during the LGM, we also undertook a separate
686 evaluation of transfer function performance in this type of environment. For this we used a
687 subset of 1588 pollen samples from the EMPD2 that are classified with the steppe pollen-
688 biome (Davis et al. 2020). The results indicate (Table A5) little difference in performance
689 compared to the full dataset, with a small decrease in performance in annual and summer
690 seasons in both precipitation and temperature, and a slight increase in performance in winter.

691

692 The results overall indicate good transfer function performance especially for temperature,
693 and are comparable with those found in other continental scale pollen-climate studies
694 (Bartlein et al., 2011). It is important to remember though that comparisons between studies

695 can only be made with caution because results are often heavily dependent on the nature of
696 the modern pollen dataset used as the training set, ~~which is not the same in all studies~~
697 (Juggins, 2013), as well as the method used (Salonen et al. 2019, Brewer et al. 2008, Peyron
698 et al., 2013).

699

700

701 **3.3 Climate reconstruction**

702

703 Reconstructed LGM temperatures indicate an overall mean annual cooling of $-7.2 \pm 3.3\text{C}$,
704 with a greater cooling of around $-9.3 \pm 4.5\text{C}$ in winter and $-5.0 \pm 3.2\text{C}$ in summer (Fig. 5). All
705 sites apart from Lake Van [site #62] in eastern Turkey show cooler temperatures at the LGM
706 compared to modern (Fig. 6), and even at this site cooler conditions fall within the
707 uncertainties. With greater cooling in winter compared to summer, the difference in
708 temperature between winter and summer also increased (shown by positive anomalies) at
709 most (but not all) sites (Fig. 6). This increase in continentality was around $+4.2\text{C}$ on average
710 across all sites (Fig. 5).

711

712 We reconstruct an overall decline in mean annual precipitation of around $-91 \pm 270\text{mm}$ (-
713 13%) at the LGM. Most of this decline is in winter ($-38 \pm 90\text{mm}$) (-21%), while in summer a
714 small increase is shown ($10 \pm 57\text{mm}$) (6%), although uncertainties are large (Fig. 7).

715 Compared to temperature there is significant seasonal and spatial variability in positive and
716 negative precipitation anomalies (Fig. 8). Positive anomalies appear more predominant in
717 eastern and southern Spain and in central eastern Europe in both summer and winter, while
718 positive anomalies are found more generally in summer across sites in Southern Europe and
719 the Mediterranean. These more positive summer anomalies also reflect a relative shift from
720 winter to summer in the seasonality of precipitation in this region.

721

722 **4.0 Discussion**

723

724 Before we consider the results of our analysis it is important to provide some context in terms
725 of European LGM geography and environment, which was very different from today (Fig. 1).
726 Major ice sheets covered Scandinavia and much of the UK, the Alps, and the Pyrenees. Sea
727 level was 120m lower, resulting in much of the North Sea and English Channel becoming dry
728 land, and the European coastline extending over 100 km out into the Atlantic and
729 Mediterranean, especially around the Bay of Biscay and Adriatic. The Black Sea was no
730 longer connected to the Mediterranean, and was smaller with a water level around 100m
731 lower than today (Genov, 2016). These changes in sea or water level had two main
732 consequences, the first being that the marine sites were closer to land, and therefore closer to
733 (low lying) terrestrial vegetation and (pollen carrying) river discharge points than they are
734 today. The second consequence of lower seas levels is that terrestrial pollen sites were
735 located further from the moderating effect of the ocean than they are today, resulting in a
736 localised modification of the climate experienced by the site irrespective of regional or global
737 changes (Geiger, 1960).

738

739 The maps used in our analysis shows the maximum ice sheet at $21\text{k} \pm 2\text{k}$ (Ehlers et al., 2011).
740 The precise geographical location of the ice sheet is difficult to resolve at a fine spatial scale,
741 however, which explains why some sites close to the ice margin appear to be actually located
742 under the ice (for example sites Kersdorf-Briesen site #46 & Mickunai site #54). The
743 resolution of the map also shows the occurrence of permanent ice not only to the north and
744 over the Alps, but also on many subsidiary areas of high ground across central and southern

745 Europe, including areas such as the Pyrenees, Massif Central, Vosges and Carpathian
746 Mountains. While global ice volume may have peaked ~21 ka individual ice sheets in Europe
747 and other areas are known to have reached their maximum extent at different times (Hughes
748 et al., 2016). The larger ice sheets are likely to have had a significant influence on regional
749 climate and environmental conditions across Europe, but the smaller ice sheets had similar if
750 more localized impacts as well. Surrounding each ice sheet would have been an unglaciated
751 area of active peri-glacial processes and newly created and unstable ground. This would
752 include outwash plains, impounded lakes and recently drained lake beds, seasonally and
753 sporadically flooded areas, moraines, kettle holes and other glaciological and peri-glacial
754 features. Soils in these areas would be non-existent or skeletal, and vegetation would find it
755 difficult to obtain nutrients and water for survival, irrespective of the prevailing climatic
756 conditions. Outside of these areas, permafrost is also likely to have been present, particularly
757 north of the Alps (Vandenberghe et al., 2014), which would also act as an impediment to
758 vegetation growth.

759

760 In terms of regional climate, the major ice sheets would have provided significant barriers to
761 westerly atmospheric circulation, or even north-south circulation in the case of the Alps and
762 Pyrenees. As well as representing a physical obstruction, the thermodynamic response of the
763 atmosphere to these high, cold obstructions would have been to encourage the formation of
764 areas of semi-permanent high pressure, similar to those found today for instance over the
765 Greenland ice sheet. In addition, the Laurentide ice sheet located over North America would
766 have generated downstream effects over Europe (COHMAP, 1988). These physical and
767 thermodynamic effects would have affected the direction of storm tracks, as well as more
768 local climatic effects commonly associated with ice sheets such as strong katabatic winds
769 (Kageyama, et al. 2021, Velasquez et al. 2021, Luetscher et al. 2015, Lefort et al. 2019)

770

771 **4.1 Vegetation Cover**

772

773 The nature and extent of forest cover during the LGM remains a matter of considerable
774 debate. Vegetation models driven by LGM climate model simulations generally indicate
775 extensive areas of boreal forest north of the Alps, and a mix of temperate and warm-
776 temperate woodland to the south across southern Europe and much of the Mediterranean.
777 Treeless areas such as steppe are mainly confined to those areas where it is also found today,
778 namely inland Iberia, Ukraine, southern Russia and Turkey, while tundra is found to the
779 north close to the Scandinavian Ice Sheet (Allen et al., 2010; Cao et al., 2019; Prentice et al.,
780 2011; Velasquez et al., 2021).

781

782 Evaluation of these vegetation-model simulations against data has been largely based on
783 comparison with compilations of pollen-biome reconstructions (Prentice et al., 2011; Allen et
784 al., 2010; Cao et al., 2019; Velasquez et al., 2021). Early studies were based on only a limited
785 number of sites from southern Europe, and showed steppe at all sites in contradiction with
786 model simulations (Elenga et al. 2000). More recent pollen compilations have included more
787 sites especially to the north that have revealed a more mixed picture of vegetation cover, with
788 forest biomes at some sites both south and north of the Alps that appear more consistent with
789 model simulations (Binney et al., 2017; Cao et al., 2019). However, many of these pollen
790 sites used in these studies were assigned an LGM age based on poor or incorrect dating
791 control, and likely date to MIS3, the Late-Glacial or even the Holocene. Nevertheless, based
792 on our compilation of more securely dated LGM pollen sites, we also show a wider
793 distribution of forest biomes particularly in Iberia, northern Italy and Central Europe,

794 although with greater areas of steppe than suggested by the models over the remaining
795 regions.

796

797 However, the interpretation of biome reconstructions requires care since the forest cover and
798 vegetation composition may not be as clear as the dominant biome suggests. For instance, we
799 find that steppe is still reconstructed as the dominant biome at some sites despite arboreal
800 pollen forming 70-80% of the pollen assemblage. In addition, it is important to remember
801 that pollen-biomes are based only on the proportion of taxa that can form forest and
802 woodland, while these taxa may in fact exist only as shrubs or stunted krummholz forms in
803 the challenging climate and environment of the LGM. Alternatively, similar conditions may
804 favour low-lying non-arboreal taxa forms with poor pollen dispersion or even insect
805 pollinated taxa forms that may be poorly represented in the pollen assemblage, giving greater
806 prominence to arboreal taxa whose pollen may be the result of long-distance transport
807 particularly *Pinus*. However there also appear to be plenty of samples with low or even very
808 low (<20%) arboreal percentages, so not all sites in open areas may be affected by long-
809 distance transport of *Pinus* in the same way.

810

811 Quantitative MAT based reconstructions of forest cover can overcome some of these
812 problems, where they can be detected, based on the composition of the pollen assemblage
813 when compared with the modern land-cover. Chord-distance measurements of the match
814 between fossil and modern pollen assemblages indicate good LGM analogues exist in our
815 large Eurasian modern pollen dataset. The results of the MAT forest cover reconstruction
816 indicates that forest cover was low but not entirely devoid of woodland in most areas, similar
817 to the modern boreal forests of Siberia and consistent with a steppe-tundra-woodland mosaic
818 proposed by many authors (e.g. Birks and Willis, 2008; Willis and Van Andel, 2004). This is
819 confirmed in an analysis of the most commonly found modern analogue ecoregions for LGM
820 pollen samples at each site (Table A6). Uncertainties are large, but for comparison the MAT
821 site-average of 33% forest cover is slightly less than the average today over the Boreal region
822 of Europe (43%) and slightly more than the average today over Mediterranean region (27%)
823 (Zanon et al. 2018).

824

825 By calculating the percentage of each of the taxa in each LGM pollen sample using a
826 standardized pollen sum, we are able to make direct comparisons between different LGM
827 pollen records and their taxa percentages (Figure A2, A3). The results show a preponderance
828 of boreal forest taxa to the north of the Alps, consistent with biome results mentioned earlier.
829 *Pinus* is the most common forest forming taxa in this boreal zone, together with *Picea*, and
830 including *Larix* to the east and *Abies* to the west. The occurrence of *Betula* and *Juniperus*
831 also suggests shrubby elements consistent with arctic shrub-tundra, although high Poaceae
832 and other herbaceous taxa such as *Artemisia* and *Chenopodiaceae* indicate more steppe than
833 tundra. Other deciduous taxa found north of the Alps include cold tolerant generalists such as
834 *Corylus* and *Alnus*, as well as low percentages of relatively thermophilous taxa in the east,
835 such as *Carpinus* and *Tilia*.

836

837 These results are consistent with charcoal (Magyari et al., 2014a; Willis and Van Andel,
838 2004), malacological (Juříčková et al., 2014), biomarkers (Zech et al., 2010) and genetic
839 evidence (Stivriņš et al., 2016; Willis and Van Andel, 2004) that the main forest region north
840 of the Alps was in the eastern region of Central Europe around the Carpathian basin. This
841 was also an area where cold and moisture sensitive deciduous taxa were also able to survive
842 (Magyari et al., 2014), although evidence of temperate taxa found in the pollen record has yet
843 to be supported by charcoal and macrofossil records (Feurdean et al., 2014). Our pollen

844 evidence indicates an open taiga or cool mixed forest that extended in central and eastern
845 Europe to areas close to the Scandinavian and Alpine ice caps, as proposed by Willis and Van
846 Andel (2004) and Huntley and Allen (2003), although whether this represents isolated
847 pockets of forest or an extended open steppe-forest is difficult to determine (Kuneš et al.,
848 2008). Even steppe or tundra areas in western Europe show a low but significant presence of
849 the pollen of tree taxa at sites close to the ice sheets that are unlikely to be solely the result of
850 long distance transport or reworking (Kelly et al., 2010). The presence of woodland in these
851 areas is also supported by mammalian remains, for instance at Kents Cavern in SW England
852 (Stewart and Lister, 2001).

853
854 Overall however, our results clearly show a much greater predominance of thermophilous
855 and moisture sensitive deciduous taxa south of the Alps, particularly in Iberia and Northern
856 Italy, where temperate broadleaf forests survived in sheltered refugia (Kaltenrieder et al.,
857 2009). Most of these appear to be in hilly areas with the ability to generate orographic rainfall
858 (Monegato et al., 2015), on south facing slopes to make the most of the sun's radiant energy
859 and located above the valley floor to escape frost and flooding. We might also expect these
860 areas to be sheltered from cold northerly winds, and benefit from relatively mild and moisture
861 laden winds coming from the Mediterranean Sea. For instance, the presence of woodland and
862 low glacier altitudes along the southern slopes of the Alps around the Po Valley and Trentino
863 region is consistent with strong orographic rains generated by southerly and easterly winds
864 that today can be generated by low pressure located south of the Alps in the Gulf of Genoa,
865 and consistent with a southerly storm track around the Alps (Kehrwald et al., 2010; Luetscher
866 et al., 2015). Generally, as might be expected, areas of forest reconstruct similar or increased
867 precipitation compared to today, and areas of steppe indicate decreased precipitation (see next
868 section).

869
870 Independent evidence of LGM vegetation is provided by archaeozoological data. This data
871 supports the palynological evidence for the existence of forest and woodland refugia across
872 the ice-free areas of Europe at latitudes north of the Alps. For instance, large vertebrates in
873 these areas show patterns of extirpation and extinction in response to shifts in climate and
874 vegetation cover that is different for different species, indicating a variety of environments
875 and niches (Lister and Stuart, 2008; Stewart and Lister, 2001). As with the pollen record, the
876 presence of temperate adapted large vertebrate taxa within the glacial landscape of Western
877 Europe also suggests the existence of temperate "micro-refugia" (Stewart and Lister, 2001),
878 consistent with suggestions that temperate arboreal taxa were not entirely extirpated from the
879 region during the LGM (Magri, 2010). Further east, mammal assemblages indicate
880 generalized loss of forest components in the East European Plain (Demay et al. 2021,
881 Puzachenko et al., 2021) which is consistent with our data indicating low forest cover in this
882 region. In other areas, evidence of the prevailing land cover at the LGM comes from studies
883 of small vertebrate communities, which have a closer affinity to the prevailing environment
884 than large vertebrates (López-García and Blain, 2020) that have the propensity to migrate
885 large distances, often on a seasonal basis. These studies of small vertebrate assemblages also
886 support the existence of temperate "micro-refugia" in France (Royer et al., 2016) and the
887 existence of woodland components in many regions across Southern Europe including parts
888 of Iberia (Bañuls-Cardona et al., 2014) Italy (Berto et al., 2019) and the Balkan Peninsula
889 (Mauch Lenardić et al., 2018).

890
891 Other paleobotanical evidence also supports our land cover reconstruction. Schafer et al.
892 (2016) suggest leaf wax patterns from palaeosols in Spain may indicate the presence of
893 drought intolerant deciduous trees and more humid conditions during the LGM. Significantly,

894 none of the pollen sites indicate that temperate broadleaf forests were dominant, and
895 broadleaf temperate taxa always appear part of a mixed woodland together with cold or
896 aridity adapted evergreen and needleleaf taxa, including typical Mediterranean taxa. This type
897 of mixed vegetation probably extended to the Balkans where the hilly terrain and proximity
898 to the Mediterranean would appear to have provided favourable climatic conditions, although
899 we still lack LGM sites from this region. At sites in central and southern Italy and east
900 through Greece and Turkey to the Middle East (and including North Africa), the vegetation
901 appears drier with a greater prevalence of steppe. Only a site in Georgia at the edge of the
902 Caucasian mountains indicates the presence of significant amounts of forest (mainly *Pinus*), a
903 result that was also found by Tarasov et al. (2000), and probably linked to favourable
904 orographic precipitation and proximity to the Black Sea.

905
906 Comparison with LGM land cover from vegetation modelling studies driven by climate
907 model simulations indicate a much wider presence of forest than that shown by the pollen
908 data (Kaplan et al., 2016). Data-model agreement appears to be closest over eastern-central
909 Europe where pollen indicates the presence of open **b**Boreal forest, and over south-west
910 Europe with the presence of cool mixed temperate forest, including broadleaf deciduous and
911 thermophilous elements (Prentice et al., 2011; Allen et al., 2010; Cao et al., 2019; Velasquez
912 et al., 2021). Nevertheless, agreement still appears to be weak over western-central Europe
913 and Southern and Eastern Europe through to the Middle East, where pollen data continues to
914 indicate widespread steppe. One proposed explanation for this data-model discrepancy has
915 been the role of fire (including man-made fire) in maintaining forest openness, a factor
916 influencing forest cover that is not included in most vegetation models (Kaplan et al., 2016).
917 In the Carpathian basin Magyari et al. (2014a) noted that charcoal increased as forest cover
918 declined, suggesting that wildfires played a role in decreasing forest cover during the LGM.
919 Other studies have noted low levels of charcoal and therefore fires during the LGM, although
920 these tend to be from steppe areas with low biomass and fuel availability (Connor et al.,
921 2013; Kaltenrieder et al., 2009). Recent LGM vegetation simulations that include fire indicate
922 much lower values of forest cover than those without fire over western central Europe, while
923 forest remains in central eastern Europe (~~see figure 6 in~~ Velasquez et al., 2021). This appears
924 closer to the data, but the values are perhaps too low compared with our MAT
925 reconstructions here (Figure 4).

926

927 **4.2 Climate**

928

929 **4.2.1 Comparison with previous pollen-based reconstructions**

930

931 The climate of the LGM is generally considered to have been cooler and drier than today, but
932 data-model comparisons continue to highlight important discrepancies, not only in the degree
933 of cooling and drying but also in their seasonal and spatial distribution. Data-model
934 comparisons over Europe have mainly used pollen-based climate reconstructions, especially
935 the Paleoclimate Modelling Intercomparison Project (PMIP/CMIP) (Kageyama et al., 2021,
936 Bartlein et al., 2011; Harrison et al., 2015; Kageyama et al., 2006; Braconnot et al 2007 ;
937 Braconnot et al 2012, Cleator et al 2020). The most commonly used reconstructions have
938 been based on two main methods, a neural-network methodology (ANN) of Peyron et al.
939 (1998) and Jost et al. (2005), and an Inverse Modelling approach (INV) applied by Wu et al.
940 (2007). The ANN method uses modern pollen samples and does not include any correction
941 for CO₂ effects, being similar in these respects with the MAT method used in this study. In
942 contrast the INV method does not use modern pollen samples, but instead uses a process-
943 based vegetation model run in inverse mode (Guiot et al. 2000). Ordinarily, a vegetation

944 model will use climate as an input to generate a vegetation as an output, but in inverse mode
945 the model is reconfigured so that the input climate (and CO₂) can be varied iteratively until
946 the closest match is found between the vegetation simulated by the model (represented by
947 PFT scores) and the fossil pollen assemblage (also represented by PFT scores). ~~to generate~~
948 ~~climate as an output given a particular vegetation (pollen) assemblage as an input.~~ One of the
949 advantages of the INV method is that CO₂ can also be varied as an input, and therefore the
950 effect of changes in CO₂ on the vegetation, and therefore reconstructed climate, can be
951 investigated. Comparison of these ANN and INV reconstructions have shown important
952 differences, with the INV reconstruction generally not as cold and somewhat drier than ANN
953 (Wu et al. 2007). These differences between pollen-climate methods have often been
954 attributed to CO₂ effects (Wu et al. 2007) but this is not clear since there may be other
955 factors, such as the size and location of the training set used in the ANN reconstruction.

956
957 We make a comparison with these earlier reconstructions based on 10 sites/records in our
958 dataset which we identified as also being included in these earlier studies (Fig. 9). While we
959 were able to identify the site and data source, as well as the time window, we were unable to
960 establish if the the data represented a single sample or the mean of multiple samples within a
961 time-window or the exact depth of those samples, or the actual sediment core in the case of
962 multiple cores from the same site. While these aspects are unknown, it seems likely that the
963 pollen data we used in our analysis was very similar if not identical in most cases, and
964 reconstructed biomes for these sites from our pollen dataset are identical to the biomes
965 reconstructed using the earlier pollen dataset (Elenga et al., 2000).

966
967 We compare our MAT with the ANN and INV reconstructions in figure 9. On average across
968 all 10 records, the MAT and INV methods give almost identical results for both anomalies of
969 mean annual temperature (MAT -6.6C, INV -7.2C) and precipitation (MAT 158mm, INV
970 165mm). Uncertainties are also similar for both methods. In contrast, the ANN method gives
971 much cooler mean annual temperature anomalies (ANN -13.9C) and drier precipitation
972 anomalies (ANN -474mm). On a site by site basis the MAT and INV methods show closer
973 agreement for temperatures than precipitation, although precipitation has proportionally
974 larger uncertainties. The reconstructions based on these two methods are close enough that
975 the uncertainties overlap at all sites for both temperature and precipitation, except the
976 precipitation reconstruction at Lac de Bouchet (site #25). The reason for this is not clear, but
977 there could easily be minor differences with the pollen data analysed by Wu et al. (2007) in
978 their INV reconstruction since the pollen record (Reille and de Beaulieu, 1988) includes
979 multiple cores each with many different samples covering the LGM period.

980
981 This comparison shows that our MAT reconstructions are very similar to the INV method,
982 but not as cold or dry as the ANN method. This has two main implications. The first is that
983 our reconstructions indicate greater agreement with the results of climate model simulations
984 since climate models indicate temperatures closer to the INV reconstructions (Latombe et al.,
985 2018) than the ANN reconstructions (Jost et al., 2005; Kageyama et al., 2006). The difference
986 between our MAT and earlier ANN reconstructions is likely the result of the modern pollen
987 datasets used, since the ANN reconstruction was based on a considerably smaller number of
988 samples taken mainly from the cold dry steppes of Kazakstan and Mongolia.

989
990 The second implication is that the MAT method may not be significantly impacted by the
991 effects of lower CO₂ (Cowling and Sykes, 1999; Prentice and Harrison, 2009; Williams et
992 al., 2000) or indeed insolation changes during the LGM, since the MAT results are similar to
993 those based on the INV method which specifically takes account of these non-climatic factors

994 (Wu et al., 2007). This would suggest that MAT could also work well for pollen-based
995 climate reconstructions on longer glacial-interglacial timescales where insolation and CO₂
996 vary significantly from their modern values. This is consistent with the findings of Pini et al.
997 (2021) who applied a correction algorithm developed by Prentice et al. (2017) and Cleator et
998 al. (2020) to a MAT reconstruction of mean annual precipitation at Lake Fimon in Northern
999 Italy. This shows a very small correction of 0mm to 30mm for samples across the LGM time-
1000 window, which indicates that CO₂ is not a very significant factor in influencing this type of
1001 reconstruction, at least compared to the overall uncertainties (+/- 200mm) of the
1002 reconstruction itself. The uncertainties associated with the correction algorithm are not
1003 discussed, but given that inputs include estimates of both LGM temperature and cloud cover,
1004 it seems likely that these could be significant. Importantly, both Pini et al (2021) and Cleator
1005 et al (2020) specifically exclude the necessity of applying a correction algorithm to
1006 temperature reconstructions, since they consider only hydrological variables to be affected by
1007 changes in atmospheric CO₂.

1008
1009

1010 **4.2.2 Comparison with climate reconstructions based on other proxies**

1011

1012 **4.2.2.1 Temperature**

1013

1014 Proxies that are not based on plants should remain unaffected by the CO₂ problem during the
1015 LGM, and provide an alternative basis for evaluating pollen-based reconstructions. Samartin
1016 et al. (2016) reconstructed LGM summer temperatures based on chironomid remains from
1017 Lago della Costa (site #34) in Northern Italy. They also undertook pollen analysis on the
1018 same samples down the core, allowing us to make a sample-by-sample comparison between
1019 the chironomid temperature record and our MAT reconstruction (Fig. 10). Our pollen-climate
1020 reconstruction is for JJA mean temperate, while the chironomid reconstruction is for July
1021 mean temperature, with the anomalies based on the modern equivalent JJA and July mean
1022 temperatures respectively. The average anomaly values for all 8 samples reconstructed by the
1023 pollen-climate MAT are $-10.2 \pm 3.5\text{C}$, and for the chironomids $-9.5 \pm 3.0\text{C}$. This indicates
1024 that pollen and chironomid average summer temperature reconstructions are very similar on
1025 average, taking into account the overlapping uncertainties, while also showing a strong
1026 similarity on a sample-by-sample basis throughout the time-series.

1027

1028 Other reconstructions based on other proxies provide a basis for more general regional
1029 comparisons (Figure A4, Figure A9, A5). We reconstruct both summer and winter
1030 temperatures and show that cooling in winter was greater than in summer at most sites,
1031 associated with an increase in continentality (increased temperature difference between
1032 summer and winter). A similar seasonal pattern of temperature change has also been shown
1033 in other studies that reconstruct both summer and winter LGM temperatures, including
1034 Prud'homme et al. (2016) using d18O analysis of earthworm calcite granules at Nussloch
1035 near the French-German border, Bañuls-Cardona et al. (2014) using faunal remains of small
1036 mammals at 4 locations in western Spain, and Ferguson et al. (2011) who examined seasonal
1037 temperature change using d18O and Mg/Ca analysis of limpet shells at Gibraltar in southern
1038 Spain. The increase in continentality at Nussloch (Prud'homme et al., 2016) was
1039 reconstructed at between 11.6 to 15.6 °C, comparable at the lower end with nearby pollen
1040 sites [La Grotte Walou site #28] $10.4 \pm 5.8 \text{ °C}$ and [Bergsee site #29] $7.9 \pm 5.7 \text{ °C}$. The faunal
1041 sites in western Spain studied by Bañuls-Cardona et al. (2014) gave much reduced increases
1042 in continentality, but nevertheless similar to nearby pollen sites. For instance at Valdavara 5.1
1043 °C [MD99-2331 site #3] $5.2 \pm 3.1 \text{ °C}$, El Miron 1.2 °C [Tourbiere de l'Estarres site #19] $5.1 \pm$

1044 6.2 °C, El Portalon 0.9C [Torrecilla de Valmadrid site #16] 2.8 ± 1.8 °C and Cueva de
1045 Maltrvieso 6.1C [SU81-18 site #2] 4.8 ± 3.4 °C. Further south at Gibraltar the limpet-based
1046 study of Ferguson et al. (2011) also shows a relatively small increase of 2 °C. The nearest
1047 pollen site [Gorham Cave site #5] however shows a larger increase of 4.7 ± 2.3 °C, although
1048 differences could be expected given the different temporal resolution of annual laminae on
1049 mollusk shells compared to pollen assemblages that reflecting much slower changes in trees
1050 and other long-lived flora.

1051
1052 Summer temperatures were warm enough during the LGM over the Alpine areas that Swiss
1053 lakes were largely ice free in summer, while glacier ELA's around the time of the LGM
1054 suggest summers were -6.5 to -7.7 °C cooler compared to the LIA (Heiri et al., 2014). This
1055 cooling was similar to that found at Nussloch some 200km north of the Swiss border by
1056 Prud'homme et al. (2016), who reconstructed anomalies of -6 to -8 ± 4 °C from $\delta^{18}O$
1057 analysis of earthworm calcite granules (representing warm season May-September
1058 temperatures). Slightly less cooling was found close by at the nearby site of Achenheim
1059 where analysis of Mollusc assemblages gave summer (August) cooling estimates of -3.5 to -
1060 6.5 °C based on MAT (Rousseau, 1991), and -5.5 to -9.5 °C based on the Mutual Climatic
1061 Range method (Moine et al., 2002). These reconstructions appear somewhat cooler than
1062 nearby pollen sites [La Grotte Walou site #28] -1.4 ± 3.6 °C and [Bergsee site #29] -2.7 ± 5.1
1063 °C, although comparable with the pollen site [Pilsensee site #32] -7.3 ± 5.0 °C 200 km further
1064 east. Similar differences also occur at the site of Les Echets on the western edge of the Alps
1065 where a diatom based reconstruction of summer (July) temperatures (Ampel et al., 2010)
1066 indicated a greater cooling (-10.5 to -11.5 °C) than our pollen reconstruction [Les Echets G
1067 site #27] $(-4 \pm 2.7$ °C). However, the authors caution that the results were based on poor
1068 analogues and rare taxa, as well as a small training set of only 90 lakes in Switzerland.

1069
1070 South of the Alps, other proxies show the opposite relationship with the pollen
1071 reconstructions. For instance, at Lago della Costa in the Po valley, a summer (July)
1072 temperature chironomid reconstruction by Samartin et al. (2016) is around 1-2 °C less cool
1073 than the pollen reconstruction (JJA) for the same site [Lago della Costa site #34] $-11.4 \pm$
1074 2.7 °C, although both reconstructions fall within their respective uncertainty ranges (Figure 8).
1075 In the Pindus Mountains in Greece, Hughes et al. (2006) estimated LGM summer
1076 temperature anomalies of -7 °C based on glacier modelling, which is comparable with that
1077 reconstructed at the nearest pollen site [Ioannina site #51] -7.7 ± 2.8 °C. In Spain the analysis
1078 of small mammal remains by Bañuls-Cardona et al. (2014) shows similarly less cooling in
1079 summer or even warmer than present positive anomalies compared to the nearest pollen sites,
1080 such as Valdavara 1.4 °C [MD99-2331 site #3] -2.3 ± 2.8 °C, El Miron -2.3 °C [Tourbiere de
1081 l'Estarres site #19] -5.7 ± 5.4 °C, El Portalon 0.8 °C [Torrecilla de Valmadrid site #16] $-2.6 \pm$
1082 1.1 °C and Cueva de Maltrvieso -1.1C [SU81-18 site #2] -10.4 ± 2.8 °C. Further south at
1083 Gibraltar, the limpet-based study of Ferguson et al. (2012) suggests an anomaly of around -7
1084 °C, which is a greater cooling than the pollen reconstruction from this location [Gorham Cave
1085 site #5] -1.3 ± 2.2 °C, although comparable with other pollen sites slightly further east.

1086
1087 Winter temperature reconstructions from non-pollen proxies show a similar pattern in relation
1088 to pollen reconstructions as for summer temperatures. North of the Alps at Achenheim,
1089 Prud'homme et al. (2016) use $\delta^{18}O$ on earthworm remains to reconstruct particularly cold
1090 winter anomalies of -17.6 to -23.6 °C compared to nearby pollen sites [La Grotte Walou site
1091 #28] -11.8 ± 8.0 °C and [Bergsee site #29] -10.6 ± 6.3 °C. South of the Alps in Spain, the
1092 analysis by Bañuls-Cardona et al (2014) based on the remains of small mammals shows less
1093 cooling in winter compared to the nearest pollen sites, in particular Valdavara -3.7 °C

1094 [MD99-2331 site #3] -7.5 ± 3.4 °C , El Miron -3.5 °C [Tourbiere de l'Estalles site #19] -10.8
1095 ± 7.0 °C, El Portalon -0.1 °C [Torrecilla de Valmadrid #16] -5.4 ± 2.5 °C and Cueva de
1096 Maltrvieso -7.2 °C [SU81-18 site #2] -15.2 ± 4.0 °C. And again, in southern Spain at Gibraltar,
1097 analysis of limpet shells by Ferguson et al (2011) suggests winter cooling of around -9 °C
1098 while the pollen reconstruction suggests [Gorham Cave site #5] -6.0 ± 2.5 °C, although sites
1099 further east indicate cooler conditions.

1100

1101 A number of additional proxies have also been used to reconstruct LGM mean annual
1102 temperature. Heyman et al. (2013) applied glacier mass balance modelling at sites located in
1103 the smaller mountain regions north of the Alps. These are generally slightly cooler than our
1104 pollen-based reconstructions at sites close to the Vosges Mountains -12.7 ± 2.0 °C and Black
1105 Forest -11.4 ± 2.3 °C [Bergsee site #29] -8.2 ± 3.3 °C, Bavarian Forest -10.7 ± 2.2 [Pilsensee
1106 site #32] -9.2 ± 1.2 °C and Giant Mountains -8.5 ± 1.8 [Kersdorf-Briesen site #46] -7.3 ± 0.3
1107 °C. These values obtained by Heyman et al. (2013) are warmer than Pud'homme et al. (2016)
1108 who estimated annual mean temperature anomalies of -15.1 to -19.1 °C based on $\delta 18\text{O}$ of
1109 earthworm calcite at the Nussloch site just north of the Vosge and Black Forest. The annual
1110 temperatures reconstructed by Heyman et al. (2013) are also around 2°C warmer than Allen et
1111 al. (2008) who applied a similar, although simpler method to over 29 different mountainous
1112 regions across Europe that had been glaciated during the LGM. Since glacier mass balance is
1113 a function of both snowfall and temperature, these estimated temperatures vary according to
1114 estimated changes in precipitation. For instance, mean annual temperature estimates by Allen
1115 et al. (2008a) are much cooler than reconstructed by pollen, with an average anomaly of -13.2
1116 °C for the 29 sites assuming a 40% reduction in precipitation, but this is reduced to -11.8 °C
1117 assuming the same precipitation as modern. *These average anomalies across all sites*
1118 *calculated by Allen et al (2008a) compare with an average temperature anomaly of -7.2 °C*
1119 *across all 63 of our pollen sites. This compares with -7.2 °C for our 63 pollen sites.* The
1120 glacier mass balance modelling by Allen et al. (2008a) assumes a seasonal distribution of
1121 precipitation that is similar to the present day, and does not consider increases in winter
1122 precipitation or mean annual precipitation above present day levels. Both of these are
1123 suggested by the pollen data in some regions, and both could explain glacier extent found
1124 during the LGM based on less extreme temperature anomalies more comparable with the
1125 pollen data. Mean annual temperatures have also been reconstructed from the Paris basin area
1126 in Eastern France by Bekaert et al. (2023) using the Noble gas proxy. The authors suggest an
1127 LGM temperature anomaly of -9.1 ± 0.9 °C although this is actually dated to 25.6 ± 0.5 k,
1128 which is earlier than our $21 \text{k} \pm 2.0 \text{k}$ time window that we adopt here. The sample closest to
1129 21k is at 21.9 ± 0.5 k and suggests slightly warmer temperatures at -7.77 °C, which compares
1130 well with our pollen reconstructions nearby at [Bergsee site #29] -8.2 ± 3.3 °C and [La Grotte
1131 Walou site #28] -6.6 ± 3.1 °C.

1132

1133 To the east of the Alps in the Panonian basin, mean annual temperature anomaly estimates
1134 have been made from noble gas measurements on groundwater ranging from -2 to -4 °C
1135 (Stute and Deak, 1990) up to -9 °C (Varsányi et al., 2011). These are similar to estimates
1136 ranging from -2 to -9 °C from oxygen isotope ratios from mammoth tooth enamel (Kovács et
1137 al., 2012) and are comparable with nearby pollen sites [Feher Lake site #50] -8.2 ± 3.3 °C and
1138 [Kokad site #52] -4.5 ± 2.3 °C. On a broader scale, Sanchi et al (2014) estimated LGM
1139 cooling in the Danube and Dneiper basins based on Lipid biomarkers in a core from the
1140 Black Sea and came up with similar mean annual temperature anomalies between -6 to -10
1141 °C, which again are comparable with pollen sites from the region that range from
1142 [Nagymohos site #48] -10.5 ± 4.1 °C to [Straldzha site #57] -4.3 ± 5.8 °C.

1143

1144 Further south and west, García-Amorena et al. (2007) reported mean annual temperature
1145 anomalies of -2.0 to -11.3 °C at LGM sites along the Portuguese coast, based on an indicator
1146 species method using plant macrofossils. This is similar to the closest marine pollen sites off
1147 the coast, which recorded values of [MD95-2039 site #1] -10.5 ± 4.6 °C and [MD99-2331 site
1148 #3] -5.3 ± 2.9 °C. Meanwhile, in the far east of the study area, Zaarur et al. (2016) estimated a
1149 mean annual temperature anomaly of around -3 °C based on clumped isotope analysis of
1150 *Melanopsis* shells from LGM sediments in the Sea of Galilee. This limited cooling appears
1151 similar to the nearest pollen site [Lake Zeribar site #63] where we reconstruct a cooling of -
1152 2.2 ± 4.6 °C.

1153
1154 Reconstructions of LGM sea surface temperatures (SST's) provide yet another source of
1155 comparison with our terrestrial pollen-based reconstructions, although many of the physical
1156 processes controlling surface sea temperatures such as upwelling, surface mixing, surface
1157 currents, stratification and thermal inertia through the seasonal cycle, represent quite different
1158 processes to those controlling surface temperatures over land, particularly at the sub-regional
1159 scale. Nevertheless, the Atlantic coastal waters of Iberia and the waters throughout the
1160 Mediterranean Sea include many SST sites that lie in relative proximity to our terrestrial
1161 pollen-sites, allowing us to make a comparison at the largest scale. Within this area the
1162 MARGO database (MARGO Members, 2009) includes 13 Alkenone, 2 Mg/Ca and 41
1163 Foraminifera based SST records of mean annual temperature, with the Foraminifera records
1164 also providing an additional 41 winter (JFM) and summer (JAS) SST estimates. We compare
1165 the SST records with the 36 closest terrestrial pollen records which fall within a box of -11 to
1166 35 degrees longitude and 32 to 43 degrees latitude containing all of the SST records. A
1167 simple site average indicates a mean annual SST anomaly of -5.5 ± 1.0 °C which is relatively
1168 close to the value of -7.2 ± 3.4 °C obtained from the terrestrial pollen sites [sites #1-4, 5, 7-
1169 24, 25, 26, 30, 35-38, 41, 47, 51, 53, 56-59]. Interestingly the inter-site variance (standard
1170 deviation of the reconstructed temperatures across all sites) is almost identical for the two
1171 datasets, 2.57 °C for the SST sites and 2.63 °C for the pollen sites, despite representing very
1172 different environments, proxies and uncertainties. However, when we look at the seasonal
1173 temperature anomalies, we find very different results. Site averaged winter SST anomalies
1174 are -3.7 ± 1.1 °C compared to -9.3 ± 4.2 °C for winter temperatures from terrestrial pollen
1175 sites, while in summer the values are reversed, -7.0 ± 0.8 °C compared to -5.38 ± 3.3 °C
1176 respectively. This suggests that SST's experienced greater cooling in summer compared to
1177 winter, which is the opposite to that generally found in terrestrial seasonal temperature
1178 reconstructions throughout the region, although this is consistent with model simulations
1179 (Mikolajewicz, 2011).

1180 1181 **4.2.2.2 Precipitation**

1182
1183 Few proxies apart from pollen provide quantitative reconstructions of precipitation during the
1184 LGM. Glacier mass balance modelling includes assumptions about precipitation in order to
1185 derive temperatures (Allen et al., 2008a), but neither is independent of the other. Hughes et
1186 al. (2006) estimate from glacier modelling that mean annual precipitation during the LGM at
1187 sites in the Pindus mountains in Greece was around 2300 ± 200 mm, which they consider to
1188 be similar to the present day (>2000 mm). A small change in precipitation compared to
1189 modern values is also indicated by the nearest pollen site, which is around 47 km to the south
1190 [Ioannina #51], and indicates a mean annual precipitation anomaly of -152 ± 294 mm,
1191 representing just 15% of the modern value. A larger reduction in mean annual precipitation of
1192 -45% (maximum) is reconstructed by García-Amorena et al. (2007) based on plant
1193 macrofossil remains from sites on the Portuguese coast. In comparison, the closest pollen

1194 sites record values which are a little lower, ranging from [MD95-2039 site #1] -22% to
1195 [MD99-2331 site #3] -34%. Further north in south-west Germany, Prud'homme et al. (2018)
1196 reconstructed mean annual precipitation from the delta ^{13}C of earthworm calcite granules at
1197 Fussloch. They estimate a field site average of 333 (159-574) mm/yr at the LGM, which
1198 represents an anomaly of -503 mm/yr (-60%) relative to the modern precipitation of 836
1199 mm/yr. This is comparable with the closest pollen site [Bergsee #29] with an anomaly of -
1200 540 mm/yr.

1201
1202 As with glaciers, lake levels reflect changes in moisture balance that includes the effects of
1203 both temperature (via evapotranspiration) and precipitation, rather than just precipitation.
1204 They also represent semi-quantitative data at best, with changes often described relative to
1205 the modern or other baseline. There are few lake level records available north of the Alps, but
1206 to the south, many records indicate high lake levels in areas such as Spain (Lacey et al., 2016;
1207 Moreno et al., 2012; Vegas et al., 2010), Italy (Belis et al., 1999; Giraudi, 2017), Greece and
1208 Turkey (Harrison et al., 1996; Reimer et al., 2009) and the Middle East (Kolodny et al., 2005;
1209 Lev et al., 2019). These lake records are also supported by evidence of higher river levels in
1210 Morocco (El Amrani et al., 2008). The cause of the higher lake levels has been the subject of
1211 some debate, since many pollen records (and especially early biome reconstructions) show
1212 steppe vegetation that would suggest aridity that appears incompatible with higher lake
1213 levels. Prentice et al. (1992) proposed that the co-existence of steppe vegetation and high lake
1214 levels could be possible if precipitation increased outside of the summer growing season,
1215 while summers themselves were drier and cooler with decreased evaporation. However, the
1216 results of our analysis tend to indicate the opposite in regions with higher lake levels, with
1217 increased summer rainfall and decreased winter rainfall. In addition, the increase in summer
1218 precipitation was enough to compensate for the decrease in winter rainfall, leading to an
1219 overall increase in mean annual precipitation at many pollen sites in Spain and Greece for
1220 instance. This together with depressed temperatures and consequently decreased evaporation
1221 could explain the higher lake levels, whilst also limiting the growth of trees as a result of
1222 cooler temperatures and prolonged aridity outside of the summer season. Davis & Stevenson
1223 (2007) also note a differential hydrological response between summer and winter rainfall in
1224 the Mediterranean during the Holocene that may also provide an explanation. In this case
1225 sporadic summer storms may result in high rates of runoff that may fill run-off fed lakes, but
1226 low rates of soil moisture recharge that fails to benefit vegetation in the same way winter
1227 rainfall does.

1228
1229 Overall, we reconstruct only a small reduction in precipitation during the LGM of around
1230 91mm (13%) averaged over all sites, which is less than the ~200mm reduction based on the
1231 sites in the pollen-climate compilation used by PMIP (Bartlein et al., 2011). Since our
1232 precipitation reconstruction on average matches that of the INV reconstruction by Wu et al
1233 (2007), we can attribute much of the difference to the greater aridity shown in the ANN
1234 reconstruction by Peyron et al and Jost et al (2005) (see figure 9). As with temperature, this is
1235 probably a reflection of the modern training set used in the ANN reconstruction which is
1236 much smaller than our training set and is largely taken from the arid steppes of Kazakhstan
1237 and Mongolia. However, it is also important to recognize the significant spatial variability in
1238 precipitation, which means that a simple average of different sets of sites from different
1239 regions may not accurately reflect the change in LGM precipitation at the European scale.
1240 Nevertheless, one of the most consistent signals in our dataset is for an increase in summer
1241 precipitation over many areas of Southern Europe and the Mediterranean. This is also found
1242 in climate models, where it has been attributed to an increase in convection-driven
1243 precipitation, although the amount of precipitation generated by this mechanism varies

1244 significantly between models (Beghin et al., 2016). It may seem counter-intuitive to see an
1245 increase in reconstructed precipitation in the same regions where we also find a
1246 preponderance of steppe or xerophytic biomes and taxa, including *Artemisia* and
1247 *Chenopodiaceae*. This is attributable to the fact that climate can change quite markedly with
1248 necessarily invoking a major change in vegetation, and especially the pollen biome. For
1249 instance, a semi-arid climate ranges from 250-500mm rainfall a year, so we could expect a
1250 semi-arid vegetation to be dominant even if the rainfall increases 250mm (100%).

1251
1252 A more consistent response in models is for an increase in winter precipitation across
1253 Southern Europe and the Mediterranean related to a stronger and more southerly displaced jet
1254 stream, with winter precipitation also accounting for much of the change in mean annual
1255 precipitation (Beghin et al., 2016). Our reconstruction of winter precipitation however shows
1256 less support for this scenario with a more general decrease in winter precipitation apart from
1257 southern and eastern Iberia, and with summer precipitation generally more important in those
1258 sites that show an overall increase in mean annual precipitation. This may not necessarily
1259 contradict the models in terms of the strength and position of the winter jet stream, but may
1260 instead indicate that models over-estimate the amount of moisture being carried westward
1261 from the cold North Atlantic along the storm track, especially across the far northern
1262 Mediterranean. The increase in winter precipitation across southern and eastern Iberia is
1263 however entirely consistent with a strengthened and more southerly jet stream, which also
1264 brings increased winter precipitation to the region today as a result of blocking over northern
1265 Europe/Atlantic and a negative NAO (Vicente-Serrano et al., 2011).

1266
1267 Other areas that show an increase in winter precipitation include pollen sites around the
1268 eastern end of the Alps. This is consistent with a recent study by Spötl et al (2021) who
1269 argued, on the basis of cryogenic carbonates preserved in a cave in Austria, that heavy winter
1270 (and autumn) precipitation was a significant factor in driving LGM glaciation in the region.
1271 The seasonally specific nature of this precipitation is also supported by the same pollen sites,
1272 which do not show any increase in summer precipitation at this time.

1273 1274 **5.0 Conclusions**

1275
1276 We have reconstructed the climate and vegetation cover across Europe, North Africa and the
1277 Middle East at the time of the LGM based on 63 pollen records. These records were selected
1278 using strict quality control criteria, with particular attention paid to dating control, which led
1279 to the exclusion of many records that have been used in previous studies. This fully
1280 documented dataset represents the most chronologically precise and spatially resolved view
1281 of LGM climate and vegetation during the PMIP benchmarking time window at 21 ± 2 ka.
1282 Nevertheless, it is important to recognize that there are still significant spatial gaps in pollen
1283 sites especially north of the Alps, the Balkans, Turkey and the Middle East, and we continue
1284 to have only a partial understanding of the LGM over these areas.

1285
1286 One of the key questions concerning the vegetation landscape of the LGM in Europe has
1287 been the extent to which forest rather than steppe covered the continent, and to what extent
1288 temperate elements could be found north of the classical refugia areas of Southern Europe
1289 and the Mediterranean. Our results show that although steppe and tundra was extensive at the
1290 time of the LGM, areas of open forest also occurred in many regions, particularly (but not
1291 exclusively) in Iberia, northern Italy and Central Europe. These forest or woodland stands are
1292 likely to have been located in environmentally favourable areas, with good soils, elevated
1293 rainfall and shelter from cold, desiccating winds. In those areas where woodland existed,

1294 **b**Boreal taxa generally dominated north and east of the Alps, while temperate and
1295 thermophilous (mainly drought adapted) taxa were generally confined to areas south of the
1296 Alps and around the Mediterranean. The temperate deciduous forests that compose the
1297 climax community in many areas of Europe today were displaced to the south and reduced to
1298 a partnership role with **b**Boreal elements. Overall our new reconstruction indicates greater
1299 agreement with model land cover simulations, but models still appear to over-estimate the
1300 amount of forest and woodland over areas such as France and the Benelux, Greece, Turkey
1301 and the Far East.

1302
1303 Another key question about the LGM concerns the ability of climate models to simulate the
1304 climate of this period and whether pollen-based climate reconstructions which show
1305 disagreement with models have been biased by the effects of low CO₂ on plant physiology.
1306 We find that our new pollen-climate reconstruction shows much closer agreement with
1307 climate models than previous reconstructions that did not take account of low CO₂ effects.
1308 We also find close agreement with previous reconstructions that did take account of CO₂
1309 effects. Since our MAT method itself does not specifically take account of low CO₂ effects,
1310 this would suggest that this problem is not a significant hindrance to MAT performance at the
1311 time of the LGM, at least not compared to other uncertainties. Instead, we suggest that the
1312 main factor in the performance of pollen-climate transfer functions that use modern analogue
1313 methods is the provision of a large enough modern pollen dataset with suitable LGM
1314 analogues.

1315
1316 This conclusion is supported by comparison with climate reconstructions based on other
1317 proxies. We found little difference between our MAT reconstruction and a Chironomid-based
1318 summer temperature record based on a downcore sample by sample comparison, as well as
1319 comparisons with records from a variety of other proxies at a regional scale. However, it is
1320 notable that some studies using glacier mass balance modelling methods indicate LGM
1321 temperatures that are much cooler than our pollen-based reconstruction. The reasons behind
1322 this are not clear, but our pollen-based results indicate higher than present precipitation in
1323 some areas that could potentially explain low elevation glacier ELA's without the need for
1324 such cold temperatures.

1325
1326 We also find that although our pollen-based reconstruction and those of SST's generally
1327 agree in terms of mean annual temperatures, SST's indicate greater cooling in summer
1328 compared to winter, while terrestrial records indicate greater cooling in winter compared to
1329 summer. These seasonal differences are also reproduced in climate models, and probably
1330 reflect the different processes driving seasonal temperature change in the terrestrial and
1331 marine domain.

1332
1333 Our reconstructions of precipitation show large spatial and seasonal variability, but generally
1334 indicate less overall aridity than previously suggested from smaller scale studies which
1335 sampled less of the spatial domain. We find that in some regions of Southern Europe
1336 precipitation may actually have been greater than present, especially in summer, but also in
1337 winter in southern and eastern Iberia and around the southern slopes of the Alps. This may
1338 have important implications in understanding the development of LGM glaciation, which
1339 may be less a function of temperature than previously supposed. This could also help better
1340 explain the observed asynchronous nature of glaciation even within relatively small regions
1341 such as Europe, as a result of more localized controls on ice sheet development such as
1342 precipitation.

1343

1344 We hope that this new continental-scale dataset of climate and vegetation reconstructions will
1345 provide an improved baseline for data-model comparisons and other studies that will allow us
1346 to better understand the complex LGM environment.
1347

1348

1349 **Code/Data availability**

1350

1351 All of the data shown in the figures together with the fossil and modern pollen datasets will
1352 be made available on pangaea.de once the review process has been completed and these
1353 datasets are therefore no longer subject to change.
1354

1354

1355 **Author contribution**

1356

1357 BASD designed the study, undertook the analysis and wrote the manuscript. MF and ER
1358 designed and prepared the maps. JOK and AB reviewed the manuscript and provided
1359 additional input.
1360

1360

1361 **Competing interests**

1362

1363 The authors declare that they have no conflict of interest.
1364

1364

1365 **Acknowledgements**

1366

1367 This work was supported by a grant from the Fonds de Recherche du Québec Société et
1368 Culture (2019-SE3-254686) to AB. Data were obtained from the European Pollen Database
1369 (EPD), based within the Neotoma Paleoecology Database (<http://www.neotomadb.org>). The
1370 work of data contributors, data stewards, and the Neotoma and EPD community is gratefully
1371 acknowledged. We dedicate this paper in memory of Eric Grimm, whose tireless work for the
1372 EPD and Neotoma helped make this study possible.
1373

1373

1374
1375
1376
1377

References

- 1378 ACER project members, Goñi, M. F. S., Desprat, S., Daniau, A. L., Bassinot, F. C., Polanco-
1379 Martínez, J. M., Harrison, S. P., Allen, J. R. M., Scott Anderson, R., Behling, H., Bonnefille,
1380 R., Burjachs, F., Carrión, J. S., Cheddadi, R., Clark, J. S., Combourieu-Nebout, N., Mustaphi,
1381 C. J. C., Debusk, G. H., Dupont, L. M., Finch, J. M., Fletcher, W. J., Giardini, M., González,
1382 C., Gosling, W. D., Grigg, L. D., Grimm, E. C., Hayashi, R., Helmens, K., Heusser, L. E.,
1383 Hill, T., Hope, G., Huntley, B., Igarashi, Y., Irino, T., Jacobs, B., Jiménez-Moreno, G.,
1384 Kawai, S., Peter Kershaw, A., Kumon, F., Lawson, I. T., Ledru, M. P., Lézine, A. M., Mei
1385 Liew, P., Magri, D., Marchant, R., Margari, V., Mayle, F. E., Merna Mckenzie, G., Moss, P.,
1386 Müller, S., Müller, U. C., Naughton, F., Newnham, R. M., Oba, T., Pérez-Obiol, R., Pini, R.,
1387 Ravazzi, C., Roucoux, K. H., Rucina, S. M., Scott, L., Takahara, H., Tzedakis, P. C., Urrego,
1388 D. H., Van Geel, B., Guido Valencia, B., Vandergoes, M. J., Vincens, A., Whitlock, C. L.,
1389 Willard, D. A. and Yamamoto, M.: The ACER pollen and charcoal database: A global
1390 resource to document vegetation and fire response to abrupt climate changes during the last
1391 glacial period, *Earth Syst. Sci. Data*, 9(2), 679–695, doi:10.5194/essd-9-679-2017, 2017.
1392
- 1393 Allen, J. R. M., Hickler, T., Singarayer, J. S., Sykes, M. T., Valdes, P. J. and Huntley, B.:
1394 Last glacial vegetation of northern Eurasia, *Quat. Sci. Rev.*, 29(19–20), 2604–2618,
1395 doi:10.1016/j.quascirev.2010.05.031, 2010.
- 1396
- 1397 Allen, R., Siegert, M. J. and Payne, A. J.: Reconstructing glacier-based climates of LGM
1398 Europe and Russia – Part 2 : A dataset of LGM precipitation / temperature relations derived
1399 from degree-day modelling of palaeo glaciers, , 249–263, 2008a.
- 1400
- 1401 Allen, R., Siegert, M. J. and Payne, A. J.: Reconstructing glacier-based climates of LGM
1402 Europe and Russia – Part 3 : Comparison with previous climate reconstructions, , (1999),
1403 265–280, 2008b.
- 1404
- 1405 Ampel, L., Bigler, C., Wohlfarth, B., Risberg, J., Lotter, A. F. and Veres, D.: Modest summer
1406 temperature variability during DO cycles in western Europe, *Quat. Sci. Rev.*, 29(11–12),
1407 1322–1327, doi:10.1016/j.quascirev.2010.03.002, 2010.
- 1408
- 1409 El Amrani, M., Macaire, J. J., Zarki, H., Bréhéret, J. G. and Fontugne, M.: Contrasted
1410 morphosedimentary activity of the lower Kert River (northeastern Morocco) during the Late
1411 Pleistocene and the Holocene. Possible impact of bioclimatic variations and human action,
1412 *Comptes Rendus - Geosci.*, 340(8), 533–542, doi:10.1016/j.crte.2008.05.004, 2008.
- 1413
- 1414 Anderson, P. M., Barnosky, C. W., Bartlein, P. J., Behling, P. J., Brubaker, L., Cushing, E. J.,
1415 Dodson, J., Dworetsky, B., Guetter, P. J., Harrison, S. P., Huntley, B., Kutzbach, J. E.,
1416 Markgraf, V., Marvel, R., McGlone, M. S., Mix, A., Moar, N. T., Morley, J., Perrott, R. A.,
1417 Peterson, G. M., Prell, W. L., Prentice, I. C., Ritchie, J. C., Roberts, N., Ruddiman, W. F.,
1418 Salinger, M. J., Spaulding, W. G., Street-Perrott, F. A., Thompson, R. S., Wang, P. K., Webb,
1419 T., Winkler, M. G. and Wright, H. E.: Climatic changes of the last 18,000 years:
1420 Observations and model simulations, *Science* (80-.), 241(4869), 1043–1052,
1421 doi:10.1126/science.241.4869.1043, 1988.
- 1422

1423 Arpe, K., Leroy, S. A. G. and Mikolajewicz, U.: A comparison of climate simulations for the
1424 last glacial maximum with three different versions of the ECHAM model and implications
1425 for summer-green tree refugia, *Clim. Past*, 91–114, doi:10.5194/cp-7-91-2011, 2011.
1426

1427 Arslanov, K. A., Dolukhanov, P. M. and Gei, N. A.: Climate, Black Sea levels and human
1428 settlements in Caucasus Littoral 50,000-9000 BP, *Quat. Int.*, 167–168, 121–127,
1429 doi:10.1016/j.quaint.2007.02.013, 2007.
1430

1431 Bañuls-Cardona, S., López-García, J. M., Blain, H. A., Lozano-Fernández, I. and Cuenca-
1432 Bescós, G.: The end of the Last Glacial Maximum in the Iberian Peninsula characterized by
1433 the small-mammal assemblages, *J. Iber. Geol.*, 40(1), 19–27,
1434 doi:10.5209/rev_JIGE.2014.v40.n1.44085, 2014.
1435

1436 Bartlein, P. J., Harrison, S. P., Brewer, S., Connor, S., Davis, B. A. S., Gajewski, K., Guiot,
1437 J., Harrison-Prentice, T. I., Henderson, A., Peyron, O., Prentice, I. C., Scholze, M., Seppä, H.,
1438 Shuman, B., Sugita, S., Thompson, R. S., Viau, A. E., Williams, J. and Wu, H.: Pollen-based
1439 continental climate reconstructions at 6 and 21 ka: A global synthesis, *Clim. Dyn.*, 37(3),
1440 775–802, doi:10.1007/s00382-010-0904-1, 2011.
1441

1442 de Beaulieu, J.-L. and Reille, M.: Pollen analysis of a long upper Pleistocene continental
1443 sequence in a Velay maar (Massif Central, France), *Palaeogeogr. Palaeoclimatol. Palaeoecol.*,
1444 80(1), 35–48, 1990.

1445 Beghin, P., Charbit, S., Kageyama, M., Combourieu-Nebout, N., Hatté, C., Dumas, C. and
1446 Peterschmitt, J. Y.: What drives LGM precipitation over the western Mediterranean? A study
1447 focused on the Iberian Peninsula and northern Morocco, *Clim. Dyn.*, 46(7–8), 2611–2631,
1448 doi:10.1007/s00382-015-2720-0, 2016.
1449

1450 Bekaert, D. V., Blard, P.-H., Raoult, Y., Pik, R., Kipfer, R., Seltzer, A. M., Legrain, E., and
1451 Marty, B.: Last glacial maximum cooling of 9 °C in continental Europe from a 40 kyr-long
1452 noble gas paleothermometry record, *Quaternary Sci. Rev.* 310,
1453 108123, <https://doi.org/10.1016/j.quascirev.2023.108123>, 2023
1454

1455 Belis, C. A., Lami, A., Guilizzoni, P., Ariztegui, D. and Geiger, W.: The late Pleistocene
1456 ostracod record of the crater lake sediments from Lago di Albano (Central Italy): Changes in
1457 trophic status, water level and climate, *J. Paleolimnol.*, 21(2), 151–169,
1458 doi:10.1023/A:1008095805748, 1999.
1459

1460 Berto, C., López-García, J. M. and Luzi, E.: Changes in the Late Pleistocene small-mammal
1461 distribution in the Italian Peninsula, *Quat. Sci. Rev.*, 225,
1462 doi:10.1016/j.quascirev.2019.106019, 2019.
1463

1464 Bigelow, N.H., Brubaker, L.B., Edwards, M.E., Harrison, S.P., Prentice, I.C., Anderson,
1465 P.M., Andreev, A.A., Bartlein, P.J., Christiansen, T.R., Cramer, W., Kaplan, J.O., Lozhkin,
1466 A.V., Matveyeva, N.V., Murray, D.F., McGuire, A.D., Razzhivin, V.Y., Ritchie, J.C., Smith,
1467 B., Walker, D.A., Gajewski, K., Wolf, V., Holmqvist, B.H., Igarashi, Y., Kremenetskii, K.,
1468 Paus, A., Pisaric, M.F.J., Volkova, V.S.: Climate change and arctic ecosystems: 1. Vegetation
1469 changes north of 55 N between the last glacial maximum, mid-Holocene, and present. *J.*
1470 *Geophys. Res.* 108 (D19), 8170. doi.org/10.1029/2002JD002558, 2013.
1471

- 1472 Binney, H., Edwards, M., Macias-Fauria, M., Lozhkin, A., Anderson, P., Kaplan, J. O.,
1473 Andreev, A., Bezrukova, E., Blyakharchuk, T., Jankovska, V., Khazina, I., Krivonogov, S.,
1474 Kremenetski, K., Nield, J., Novenko, E., Ryabogina, N., Solovieva, N., Willis, K. and
1475 Zernitskaya, V.: Vegetation of Eurasia from the last glacial maximum to present: Key
1476 biogeographic patterns, *Quat. Sci. Rev.*, 157, 80–97, doi:10.1016/j.quascirev.2016.11.022,
1477 2017.
- 1478
1479 Birks, H. J. B. and Willis, K. J.: Alpines, trees, and refugia in Europe, *Plant Ecol. Divers.*,
1480 1(2), 147–160, doi:10.1080/17550870802349146, 2008.
- 1481
1482 Bonatti, E.: Pollen sequence in the lake sediments. In: *Ianula: an account of the history and*
1483 *development of the Lago di Monterosi, Latium, Italy*, in *Trans. Am. phil. Soc.*, vol. 60, edited
1484 by G. E. Hutchinson, pp. 26–31., 1970.
- 1485
1486 Braconnot, P., Harrison, S.P., Kageyama, M., Bartlein, P.J., Masson-Delmotte, V., Abe-
1487 Ouchi, A., Otto-Bliesner, B., and Zhao, Y.: Evaluation of climate models using
1488 palaeoclimatic data, *Nat. Clim. Change*, 2, 417–424, doi:10.1038/nclimate1456, 2012.
- 1489
1490 Brewer, S., Guiot, J., Sánchez-Goñi, M. F. and Klotz, S.: The climate in Europe during the
1491 Eemian: a multi-method approach using pollen data, *Quat. Sci. Rev.*, 27(25–26), 2303–2315,
1492 doi:10.1016/j.quascirev.2008.08.029, 2008.
- 1493
1494 Brewer, S., Giesecke, T., Davis, B. A. S., Finsinger, W., Wolters, S., Binney, H., de
1495 Beaulieu, J. L., Fyfe, R., Gil-Romera, G., Kühl, N., Kuneš, P., Leydet, M. and Bradshaw, R.
1496 H.: Mapping Lateglacial and Holocene European pollen data: The maps, *J. Maps*, 13(2), 921–
1497 928, doi:10.1080/17445647.2016.1197613, 2017.
- 1498
1499 Camuera, J., Jiménez-Moreno, G., Ramos-Román, M. J., García-Alix, A., Toney, J. L.,
1500 Anderson, R. S., Jiménez-Espejo, F., Bright, J., Webster, C., Yanes, Y. and Carrión, J. S.:
1501 Vegetation and climate changes during the last two glacial-interglacial cycles in the western
1502 Mediterranean: A new long pollen record from Padul (southern Iberian Peninsula), *Quat. Sci.*
1503 *Rev.*, 205, 86–105, doi:10.1016/j.quascirev.2018.12.013, 2019.
- 1504
1505 Cao, X., Tian, F., Dallmeyer, A. and Herzschuh, U.: Northern Hemisphere biome changes
1506 (>30°N) since 40 cal ka BP and their driving factors inferred from model-data comparisons,
1507 *Quat. Sci. Rev.*, 220, 291–309, doi:10.1016/j.quascirev.2019.07.034, 2019.
- 1508
1509 Carrión, J. S.: Late quaternary pollen sequence from Carihuela Cave, southern Spain, *Rev.*
1510 *Palaeobot. Palynol.*, 71(1–4), doi:10.1016/0034-6667(92)90157-C, 1992.
- 1511
1512 Carrión, J. S.: Patterns and processes of Late Quaternary environmental change in a montane
1513 region of southwestern Europe, *Quat. Sci. Rev.*, 21, 2047–2066, 2002.
- 1514
1515 Carrión, J. S., Finlayson, C., Fernández, S., Finlayson, G., Allué, E., López-Sáez, J. A.,
1516 López-García, P., Gil-Romera, G., Bailey, G. and González-Sampériz, P.: A coastal reservoir
1517 of biodiversity for Upper Pleistocene human populations: palaeoecological investigations in
1518 Gorham’s Cave (Gibraltar) in the context of the Iberian Peninsula, *Quat. Sci. Rev.*, 27(23–
1519 24), 2118–2135, doi:10.1016/j.quascirev.2008.08.016, 2008.
- 1520

1521 Cheddadi, R., Yu, G., Guiot, J., Harrison, S. P. and Colin Prentice, I.: The climate of Europe
1522 6000 years ago, *Clim. Dyn.*, 13(1), 1–9, 1996.

1523

1524 Chevalier, M., Davis, B. A. S., Heiri, O., Seppä, H., Chase, B. M., Gajewski, K., Lacourse,
1525 T., Telford, R. J., Finsinger, W., Guiot, J., Köhl, N., Maezumi, S. Y., Tipton, J. R., Carter, V.
1526 A., Brussel, T., Phelps, L. N., Dawson, A., Zanon, M., Vallé, F., Nolan, C., Mauri, A., de
1527 Vernal, A., Izumi, K., Holmström, L., Marsicek, J., Goring, S., Sommer, P. S., Chaput, M.
1528 and Kupriyanov, D.: Pollen-based climate reconstruction techniques for late Quaternary
1529 studies, *Earth-Science Rev.*, 210, doi:10.1016/j.earscirev.2020.103384, 2020.

1530

1531 Cleator, S. F., Harrison, S. P., Nichols, N. K., Colin Prentice, I. and Roulstone, I.: A new
1532 multivariable benchmark for Last Glacial Maximum climate simulations, *Clim. Past*, 16(2),
1533 699–712, doi:10.5194/cp-16-699-2020, 2020.

1534

1535 COHMAP,: Climatic changes of the last 18,000 years: observations and model
1536 simulations. *Science*, 241, 1043-1052, 1988.

1537

1538 Collins, P. M., Davis, B. A. S. and Kaplan, J. O.: The mid-Holocene vegetation of the
1539 Mediterranean region and southern Europe, and comparison with the present day, *J.*
1540 *Biogeogr.*, 39(10), doi:10.1111/j.1365-2699.2012.02738.x, 2012.

1541

1542 Combourieu Nebout, N., Peyron, O., Dormoy, I., Desprat, S., Beaudouin, C., Kotthoff, U.
1543 and Marret, F.: Rapid climatic variability in the west Mediterranean during the last 25 000
1544 years from high resolution pollen data, *Clim. Past*, 5(3), 503–521, doi:10.5194/cp-5-503-
1545 2009, 2009.

1546

1547 Connor, S. E., Ross, S. A., Sobotkova, A., Herries, A. I. R., Mooney, S. D., Longford, C. and
1548 Iliev, I.: Environmental conditions in the SE Balkans since the Last Glacial Maximum and
1549 their influence on the spread of agriculture into Europe, *Quat. Sci. Rev.*, 68, 200–215,
1550 doi:10.1016/j.quascirev.2013.02.011, 2013.

1551

1552 Cowling, S. A. and Sykes, M. T.: Physiological significance of low atmospheric CO₂ for
1553 plant-climate interactions, *Quat. Res.*, 52(2), 237–242, doi:10.1006/qres.1999.2065, 1999.

1554

1555 Damblon, F.: L'enregistrement palynologique de la sequence pléistocène et holocène de la
1556 grotte Walou, in *La grotte Walou à Trooz (Belgique)*, edited by C. Draily, S. Pirson, and M.
1557 Toussaint, pp. 84–129, Service public de Wallonie (Etudes et Documents, Archéologie, 21).,
1558 2011.

1559

1560 Daniau, A.-L., Desprat, S., Aleman, J. C., Bremond, L., Davis, B., Fletcher, W., Marlon, J.
1561 R., Marquer, L., Montade, V., Morales-Molino, C., Naughton, F., Rius, D. and Urrego, D. H.:
1562 Terrestrial plant microfossils in palaeoenvironmental studies, pollen, microcharcoal and
1563 phytolith. Towards a comprehensive understanding of vegetation, fire and climate changes
1564 over the past one million years, *Rev. Micropaleontol.*, 63, doi:10.1016/j.revmic.2019.02.001,
1565 2019.

1566

1567 Davis, B. A. S. and Stevenson, A. C.: The 8.2 ka event and Early-Mid Holocene forests, fires
1568 and flooding in the Central Ebro Desert, NE Spain, *Quat. Sci. Rev.*, 26(13–14),
1569 doi:10.1016/j.quascirev.2007.04.007, 2007.

1570

- 1571 Davis, B. A. S., Brewer, S., Stevenson, A. C., Guiot, J., Allen, J., Almqvist-Jacobson, H.,
1572 Ammann, B., Andreev, A. A., Argant, J., Atanassova, J., Balwierz, Z., Barnosky, C. D.,
1573 Bartley, D. D., De Beaulieu, J. L., Beckett, S. C., Behre, K. E., Bennett, K. D., Berglund, B.
1574 E. B., Beug, H.-J., Bezusko, L., Binka, K., Birks, H. H., Birks, H. J. B., Björck, S.,
1575 Bliakheartchouk, T., Bogdel, I., Bonatti, E., Bottema, S., Bozilova, E. D. B., Bradshaw, R.,
1576 Brown, A. P., Brugiapaglia, E., Carrion, J., Chernavskaya, M., Clerc, J., Clet, M., Coûteaux,
1577 M., Craig, A. J., Cserny, T., Cwynar, L. C., Dambach, K., De Valk, E. J., Digerfeldt, G.,
1578 Diot, M. F., Eastwood, W., Elina, G., Filimonova, L., Filipovitch, L., Gaillard-Lemdhal, M.
1579 J., Gauthier, A., Göransson, H., Guenet, P., Gunova, V., Hall, V. A. H., Harmata, K., Hicks,
1580 S., Huckerby, E., Huntley, B., Huttunen, A., Hyvärinen, H., Ilves, E., Jacobson, G. L., Jahns,
1581 S., Jankovská, V., Jóhansen, J., Kabailiene, M., Kelly, M. G., Khomutova, V. I., Königsson,
1582 L. K., Kremenetski, C., Kremenetskii, K. V., Krisai, I., Krisai, R., Kvavadze, E., Lamb, H.,
1583 Lazarova, M. A., Litt, T., Lotter, A. F., Lowe, J. J., Magyari, E., Makohonienko, M.,
1584 Mamakowa, K., Mangerud, J., Mariscal, B., Markgraf, V., McKeever, Mitchell, F. J. G.,
1585 Munuera, M., Nicol-Pichard, S., Noryskiewicz, B., Odgaard, B. V., Panova, N. K.,
1586 Pantaleon-Cano, J., Paus, A. A., Pavel, T., Peglar, S. M., Penalba, M. C., Pennington, W.,
1587 Perez-Obiol, R., et al.: The temperature of Europe during the Holocene reconstructed from
1588 pollen data, *Quat. Sci. Rev.*, 22(15–17), doi:10.1016/S0277-3791(03)00173-2, 2003.
- 1589
1590 Davis, B. A. S., Chevalier, M., Sommer, P., Carter, V. A., Finsinger, W., Mauri, A., Phelps,
1591 L. N., Zanon, M., Abegglen, R., Åkesson, C. M., Alba-Sánchez, F., Scott Anderson, R.,
1592 Antipina, T. G., Atanassova, J. R., Beer, R., Belyanina, N. I., Blyakharchuk, T. A., Borisova,
1593 O. K., Bozilova, E., Bukreeva, G., Jane Bunting, M., Clò, E., Colombaroli, D., Combourieu-
1594 Nebout, N., Desprat, S., Di Rita, F., Djamali, M., Edwards, K. J., Fall, P. L., Feurdean, A.,
1595 Fletcher, W., Florenzano, A., Furlanetto, G., Gaceur, E., Galimov, A. T., Gałka, M., García-
1596 Moreiras, I., Giesecke, T., Grindean, R., Guido, M. A., Gvozdeva, I. G., Herzschuh, U.,
1597 Hjelle, K. L., Ivanov, S., Jahns, S., Jankovska, V., Jiménez-Moreno, G., Karpínska-Kołaczek,
1598 M., Kitaba, I., Kołaczek, P., Lapteva, E. G., Latałowa, M., Lebreton, V., Leroy, S., Leydet,
1599 M., Lopatina, D. A., López-Sáez, J. A., Lotter, A. F., Magri, D., Marinova, E., Matthias, I.,
1600 Mavridou, A., Mercuri, A. M., Mesa-Fernández, J. M., Mikishin, Y. A., Milecka, K.,
1601 Montanari, C., Morales-Molino, C., Mrotzek, A., Sobrino, C. M., Naidina, O. D., Nakagawa,
1602 T., Nielsen, A. B., Novenko, E. Y., Panajiotidis, S., Panova, N. K., Papadopoulou, M.,
1603 Pardoe, H. S., Pędziszewska, A., Petrenko, T. I., Ramos-Román, M. J., Ravazzi, C., Rösch,
1604 M., Ryabogina, N., Ruiz, S. S., Sakari Salonen, J., Sapelko, T. V., Schofield, J. E., Seppä, H.,
1605 Shumilovskikh, L., Stivrins, N., Stojakowits, P., Svitavska, H. S., Święta-Musznicka, J.,
1606 Tantau, I., Tinner, W., Tobolski, K., Tonkov, S., Tsakiridou, M., et al.: The Eurasian Modern
1607 Pollen Database (EMPD), version 2, *Earth Syst. Sci. Data*, 12(4), 2423–2445,
1608 doi:10.5194/essd-12-2423-2020, 2020.
- 1609
1610 Davis M.B.: On the theory of pollen analysis. *American Journal of Sciences*, 26, 897–912,
1611 1963.
- 1612
1613 Demay, L., Julien, M.A., Anghelinu, M., Shydlovskiy, P.S., Koulakovska, L.V., P’ean, S.,
1614 Stupak, D.V., Vasyliiev, P.M., Ob’ada, T., Wojtal, P., Belyaeva, V.I.: Study of human
1615 behaviors during the Late Pleniglacial in the East European Plain through their relation to the
1616 animal world. *Quat. Int.* <https://doi.org/10.1016/j.quaint.2020.10.047>, 2021.
- 1617
1618 Douda, J., Doudová, J., Drašnarová, A., Kuneš, P., Hadincová, V., Krak, K., Zákavský, P.
1619 and Mandák, B.: Migration patterns of subgenus *Alnus* in Europe since the last glacial
1620 maximum: A systematic review, *PLoS One*, 9(2), doi:10.1371/journal.pone.0088709, 2014.

1621
1622 Duprat-Oualid, F., Rius, D., Bégeot, C., Magny, M., Millet, L., Wulf, S. and Appelt, O.:
1623 Vegetation response to abrupt climate changes in Western Europe from 45 to 14.7k cal a BP:
1624 the Bergsee lacustrine record (Black Forest, Germany), *J. Quat. Sci.*, 32(7), 1008–1021,
1625 doi:10.1002/jqs.2972, 2017.

1626
1627 Dupre Ollivier, M.: *Palinología y paleoambiente- nuevos datos españoles referencias*,
1628 Universidad de Valencia., 1988.

1629
1630 Edwards, M. E., Anderson, P. M., Brubaker, L. B., Ager, T., Andreev, A. A., Bigelow, N. H.,
1631 Cwynar, L. C., Eisner, W. R., Harrison, S. P., Hu, F.-S., Jolly, D., Lozhkin, A. V.,
1632 MacDonald, G. M., Mock, C. J., Ritchie, J. C., Sher, A. V., Spear, R. W., Williams, J. & Yu,
1633 G.: Pollen-based biomes for Beringia 18,000, 6000 and 0 14C yr bp. *Journal of*
1634 *Biogeography*, 27, 521– 554, doi: [10.1046/j.1365-2699.2000.00426.x](https://doi.org/10.1046/j.1365-2699.2000.00426.x), 2000.

1635
1636 Ehlers, J., Gibbard, P. L. and Hughes, P. D.: *Quaternary Glaciations - Extent and Chronology*
1637 *A Closer Look*, edited by J. Ehlers, P. L. Gibbard, and P. D. Hughes, Elsevier., 2011.

1638
1639 Elenga, H., Peyron, O., Bonnefille, R., Jolly, D., Cheddadi, R., Guiot, J., Andrieu, V.,
1640 Bottema, S., Buchet, G., De Beaulieu, J. L., Hamilton, A. C., Maley, J., Marchant, R., Perez-
1641 Obiol, R., Reille, M., Riollet, G., Scott, L., Straka, H., Taylor, D., Van Campo, E., Vincens,
1642 A., Laarif, F. and Jonson, H.: Pollen-based biome reconstruction for southern Europe and
1643 Africa 18,000 yr BP, *J. Biogeogr.*, 27(3), 621–634, doi:10.1046/j.1365-2699.2000.00430.x,
1644 2000.

1645
1646 Ferguson, J. E., Henderson, G. M., Fa, D. A., Finlayson, J. C. and Charnley, N. R.: Increased
1647 seasonality in the Western Mediterranean during the last glacial from limpet shell
1648 geochemistry, *Earth Planet. Sci. Lett.*, 308(3–4), 325–333, doi:10.1016/j.epsl.2011.05.054,
1649 2011.

1650
1651 Feurdean A, Bhagwat SA, Willis KJ, Birks HJB, Lischke H, Hickler T.: Tree migration-rates:
1652 narrowing the gap between inferred post-glacial rates and projected rates. *PLoS ONE* 8:
1653 e71797, 2013.

1654
1655 Feurdean, A., Perşoiu, A., Tanţău, I., Stevens, T., Magyari, E. K., Onac, B. P., Marković, S.,
1656 Andrić, M., Connor, S., Fărcaş, S., Gałka, M., Gaudeny, T., Hoek, W., Kolaczek, P., Kuneš,
1657 P., Lamentowicz, M., Marinova, E., Michczyńska, D. J., Perşoiu, I., Płóciennik, M.,
1658 Słowiński, M., Stancikaite, M., Sumegi, P., Svensson, A., Tămaş, T., Timar, A., Tonkov, S.,
1659 Toth, M., Veski, S., Willis, K. J. and Zernitskaya, V.: Climate variability and associated
1660 vegetation response throughout Central and Eastern Europe (CEE) between 60 and 8ka, *Quat.*
1661 *Sci. Rev.*, 106, 206–224, doi:10.1016/j.quascirev.2014.06.003, 2014.

1662
1663 Fick, S. E. and Hijmans, R. J.: WorldClim 2: new 1-km spatial resolution climate surfaces for
1664 global land areas, *Int. J. Climatol.*, 37(12), 4302–4315, doi:10.1002/joc.5086, 2017.

1665
1666 Fletcher, W. J., Goni, M. F. S., Peyron, O. and Dormoy, I.: Abrupt climate changes of the last
1667 deglaciation detected in a Western Mediterranean forest record, *Clim. Past*, 6(2), 245–264,
1668 doi:10.5194/cp-6-245-2010, 2010.

1669

- 1670 Gaillard, M. J., Sugita, S., Mazier, F., Trondman, A. K., Broström, A., Hickler, T., Kaplan, J.
1671 O., Kjellström, E., Kokfelt, U., Kuneš, P., Lemmen, C., Miller, P., Olofsson, J., Poska, A.,
1672 Rundgren, M., Smith, B., Strandberg, G., Fyfe, R., Nielsen, A. B., Alenius, T., Balakauskas,
1673 L., Barnekow, L., Birks, H. J. B., Bjune, A., Björkman, L., Giesecke, T., Hjelle, K., Kalnina,
1674 L., Kangur, M., Van Der Knaap, W. O., Koff, T., Lageras, P., Latałowa, M., Leydet, M.,
1675 Lechterbeck, J., Lindbladh, M., Odgaard, B., Peglar, S., Segerström, U., Von Stedingk, H.
1676 and Seppä, H.: Holocene land-cover reconstructions for studies on land cover-climate
1677 feedbacks, *Clim. Past*, 6(4), 483–499, doi:10.5194/cp-6-483-2010, 2010.
- 1678
1679 García-Amorena, I., Gómez Manzaneque, F., Rubiales, J. M., Granja, H. M., Soares de
1680 Carvalho, G. and Morla, C.: The Late Quaternary coastal forests of western Iberia: A study of
1681 their macroremains, *Palaeogeogr. Palaeoclimatol. Palaeoecol.*, 254(3–4), 448–461,
1682 doi:10.1016/j.palaeo.2007.07.003, 2007.
- 1683
1684 Genov, I.: The Black Sea level from the Last Glacial Maximum to the present time, *Geol.*
1685 *Balc.*, 45(1–3), 3–19, 2016.
- 1686
1687 Giesecke, T.: Did thermophilous trees spread into central Europe during the Late Glacial?,
1688 *New Phytol.*, 212(1), 15–18, doi:10.1111/nph.14149, 2016.
- 1689
1690 Giesecke, T., Davis, B., Brewer, S., Finsinger, W., Wolters, S., Blaauw, M., de Beaulieu, J.-
1691 L., Binney, H., Fyfe, R. M., Gaillard, M.-J., Gil-Romera, G., van der Knaap, W. O., Kuneš,
1692 P., Köhl, N., van Leeuwen, J. F. N., Leydet, M., Lotter, A. F., Ortu, E., Semmler, M. and
1693 Bradshaw, R. H. W.: Towards mapping the late Quaternary vegetation change of Europe,
1694 *Veg. Hist. Archaeobot.*, 23(1), doi:10.1007/s00334-012-0390-y, 2014.
- 1695
1696 Geiger, R.: The climate near the ground. Cambridge: Blue Hill Met. Observ. Harvard
1697 University 1960
- 1698
1699 Giraudi, C.: Lake levels and climate for the last 30,000 years in the fucino area (Abruzzo-
1700 Central Italy) - A review, *Palaeogeogr. Palaeoclimatol. Palaeoecol.*, 70(1–3), 249–260,
1701 doi:10.1016/0031-0182(89)90094-1, 1989.
- 1702
1703 Giraudi, C.: Climate evolution and forcing during the last 40 ka from the oscillations in
1704 Apennine glaciers and high mountain lakes, Italy, *J. Quat. Sci.*, 32(8), 1085–1098,
1705 doi:10.1002/jqs.2985, 2017.
- 1706
1707 Guido, M. A., Molinari, C., Moneta, V., Branch, N., Black, S., Simmonds, M., Stastney, P.
1708 and Montanari, C.: Climate and vegetation dynamics of the Northern Apennines (Italy)
1709 during the Late Pleistocene and Holocene, *Quat. Sci. Rev.*, 231,
1710 doi:10.1016/j.quascirev.2020.106206, 2020.
- 1711 Hansen, M. C., Potapov, P. V., Moore, R., Hancher, M., Turubanova, S. A., Tyukavina, A.,
1712 Thau, D., Stehman, S. V., Goetz, S. J., Loveland, T. R., Kommareddy, A., Egorov, A., Chini,
1713 L., Justice, C. O. and Townshend, J. R. G.: High-resolution global maps of 21st-century
1714 forest cover change, *Science (80-.)*, 342(6160), 850–853, doi:10.1126/science.1244693,
1715 2013.
- 1716
1717 Grichuk, V. P.: Main types of vegetation (ecosystems) for the maximum cooling of the last
1718 glaciation. B. Frenzel, B. Pecs, A.A. Velichko (Eds.), *Atlas of Palaeoclimates and*

1719 Palaeoenvironments of the Northern Hemisphere, NQUA/Hungarian Academy of
1720 Sciences, Budapest, pp. 123-124, doi: [10.2307/1551555](https://doi.org/10.2307/1551555), 1992.

1721

1722

1723 Guiot, J., Pons, A., Beaulieu, J. L. de, and Reille, M. A 140,000-year climatic reconstruction
1724 from two European pollen records. Nature 338, 309-313, doi:10.1038/338309a0, 1989.

1725

1726 Guiot, J., Torre, F., Jolly, D., Peyron, O., Boreux, J.J., Cheddadi, R.: Inverse vegetation
1727 modeling by Monte Carlo sampling to reconstruct palaeoclimates under changed precipitation
1728 seasonality and CO₂ conditions: application to glacial climate in Mediterranean region. *Ecol.*
1729 *Model.* 127, 119–140. doi: 10.1016/
1730 S0304-3800(99)00219-7, 2000.

1731

1732 Harrison, S. P., Yu, G. E. and Tarasov, P. E.: Late Quaternary Lake-Level Record from
1733 Northern Eurasia, *Quat. Res.*, 45(2), 138–159, doi:10.1006/qres.1996.0016, 1996.

1734

1735 Harrison, S. P., Bartlein, P. J., Brewer, S., Prentice, I. C., Boyd, M., Hessler, I., Holmgren,
1736 K., Izumi, K. and Willis, K.: Climate model benchmarking with glacial and mid-Holocene
1737 climates, *Clim. Dyn.*, 43(3–4), 671–688, doi:10.1007/s00382-013-1922-6, 2014.

1738

1739 Harrison, S. P., Bartlein, P. J., Izumi, K., Li, G., Annan, J., Hargreaves, J., Braconnot, P. and
1740 Kageyama, M.: Evaluation of CMIP5 palaeo-simulations to improve climate projections, *Nat.*
1741 *Clim. Chang.*, 5(8), 735–743, doi:10.1038/nclimate2649, 2015.

1742

1743 Heiri, O., Koinig, K. A., Spötl, C., Barrett, S., Brauer, A., Drescher-Schneider, R., Gaar, D.,
1744 Ivy-Ochs, S., Kerschner, H., Luetscher, M., Moran, A., Nicolussi, K., Preusser, F., Schmidt,
1745 R., Schoeneich, P., Schwörer, C., Sprafke, T., Terhorst, B. and Tinner, W.: Palaeoclimate
1746 records 60-8 ka in the Austrian and Swiss Alps and their forelands, *Quat. Sci. Rev.*, 106,
1747 186–205, doi:10.1016/j.quascirev.2014.05.021, 2014.

1748

1749 Heyman, B. M., Heyman, J., Fickert, T., Harbor, J. M. and Forest, B.: Paleo-climate of the
1750 central European uplands during the last glacial maximum based on glacier mass-balance
1751 modeling Bavarian Forest Republic, *Quat. Res.*, 79(1), 49–54,
1752 doi:10.1016/j.yqres.2012.09.005, 2013.

1753

1754 Hughes, A. L. C., Gyllencreutz, R., Lohne, Ø. S., Mangerud, J. and Svendsen, J. I.: The last
1755 Eurasian ice sheets - a chronological database and time-slice reconstruction, *DATED-1,*
1756 *Boreas*, 45(1), 1–45, doi:10.1111/bor.12142, 2016.

1757

1758 Hughes, P. D. and Gibbard, P. L.: A stratigraphical basis for the Last Glacial Maximum
1759 (LGM), *Quat. Int.*, 383(June 2014), 174–185, doi:10.1016/j.quaint.2014.06.006, 2015.

1760

1761 Hughes, P. D., Woodward, J. C. and Gibbard, P. L.: Late Pleistocene glaciers and climate in
1762 the Mediterranean, *Glob. Planet. Change*, 50(1–2), 83–98,
1763 doi:10.1016/j.gloplacha.2005.07.005, 2006.

1764 Huntley, B.: Dissimilarity mapping between fossil and contemporary pollen spectra in
1765 Europe for the past 13,000 years, *Quat. Res.*, 33(3), 360–376, doi:10.1016/0033-
1766 5894(90)90062-P, 1990.

1767

1768 Huntley B.: Dissimilarity mapping between fossil and contemporary pollen spectra in Europe
1769 for the past 13,000 years. *Quaternary Research* 33:360–376, 1990.

1770

1771 Huntley, B. and Allen, J. R. M.: Glacial environments III. Palaeovegetation patterns in late
1772 glacial Europe, in *Neanderthals and modern humans in the European landscape during the*
1773 *last glaciation*, edited by T. H. Van Andel and H. C. Davies, pp. 79–102, McDonald Institute
1774 for Archaeological Research, Cambridge., 2003.

1775

1776 Huntley, B. and Birks, H. J. B.: *An Atlas of Past and Present Pollen Maps for Europe: 0–*
1777 *13,000 B.P. years ago*, Cambridge University Press, Cambridge., 1983.

1778

1779 Izumi, K. and Bartlein, P., North American paleoclimate reconstructions for the Last Glacial
1780 Maximum using an inverse modeling through iterative forward modeling approach applied to
1781 pollen data, <https://doi.org/10.1002/2016GL070152>, 2016

1782

1783 Jalut, G., Andrieu, V., Delibrias, G., Fontaugne, M. and Pages, P.: Palaeoenvironment of the
1784 valley of Ossau (Western French Pyrenees) during the last 27 000 year, *Pollen et Spores*,
1785 30(3–4), 357–393, 1988.

1786

1787 Jalut, G., Marti, J. M., Fontugne, M., Delibrias, G., Vilaplana, J. M. and Julia, R.: Glacial to
1788 interglacial vegetation changes in the northern and southern Pyrénées: Deglaciation,
1789 vegetation cover and chronology, *Quat. Sci. Rev.*, 11(4), 449–480, doi:10.1016/0277-
1790 3791(92)90027-6, 1992.

1791

1792 Jankovska, V.: Vegetation cover in West Carpathians during the Last Glacial period -
1793 analogy of present day siberian forest-tundra nad taiga, *Palynol. Stratigr. geoecology*,
1794 (SEPTEMBER 2008), 282–289, 2008.

1795

1796 Janská, V., Jiménez-Alfaro, B., Chytrý, M., Divíšek, J., Anenkhonov, O., Korolyuk, A.,
1797 Lashchinskyi, N. and Culek, M.: Palaeodistribution modelling of European vegetation types
1798 at the Last Glacial Maximum using modern analogues from Siberia: Prospects and
1799 limitations, *Quat. Sci. Rev.*, 159, 103–115, doi:10.1016/j.quascirev.2017.01.011, 2017.

1800

1801 Jost, A., Lunt, D., Abe-Ouchi, A., Abe-Ouchi, A., Peyron, O., Valdes, P. J. and Ramstein, G.:
1802 High-resolution simulations of the last glacial maximum climate over Europe: A solution to
1803 discrepancies with continental palaeoclimatic reconstructions?, *Clim. Dyn.*, 24(6), 577–590,
1804 doi:10.1007/s00382-005-0009-4, 2005.

1805

1806 Juggins, S.: Quantitative reconstructions in palaeolimnology : new paradigm or sick
1807 science ?, *Quat. Sci. Rev.*, 64, 20–32, doi:10.1016/j.quascirev.2012.12.014, 2013.

1808

1809 Juggins, S.: *Rioja: Analysis of Quaternary Science Data*, [online] Available from:
1810 <https://cran.r-project.org/package=rioja>, 2020.

1811
1812 Juggins, S. and Birks, H. J. B.: Quantitative Environmental Reconstructions from Biological
1813 Data, in *Developments in Paleoenvironmental Research 5*, edited by H. J. B. Birks, pp. 431–
1814 494, Springer Science+Business Media B.V., 2012.

1815
1816 Juříčková, L., Horáčková, J. and Ložek, V.: Direct evidence of central European forest
1817 refugia during the last glacial period based on mollusc fossils, *Quat. Res. (United States)*,
1818 82(1), 222–228, doi:10.1016/j.yqres.2014.01.015, 2014.

1819
1820 Kageyama, M., Laîné, A., Abe-Ouchi, A., Braconnot, P., Cortijo, E., Crucifix, M., de Vernal,
1821 A., Guiot, J., Hewitt, C. D., Kitoh, A., Kucera, M., Marti, O., Ohgaito, R., Otto-Bliesner, B.,
1822 Peltier, W. R., Rosell-Melé, A., Vettoretti, G., Weber, S. L. and Yu, Y.: Last Glacial
1823 Maximum temperatures over the North Atlantic, Europe and western Siberia: a comparison
1824 between PMIP models, MARGO sea-surface temperatures and pollen-based reconstructions,
1825 *Quat. Sci. Rev.*, 25(17–18), 2082–2102, doi:10.1016/j.quascirev.2006.02.010, 2006.

1826
1827 Kageyama, M., Harrison, S. P., Kapsch, M. L., Lofverstrom, M., Lora, J. M., Mikolajewicz,
1828 U., ... & Zhu, J. The PMIP4 Last Glacial Maximum experiments: preliminary results and
1829 comparison with the PMIP3 simulations. *Climate of the Past*, 17(3), 1065–1089, 2021.

1830
1831 Kaltenrieder, P., Belis, C. A., Hofstetter, S., Ammann, B., Ravazzi, C. and Tinner, W.:
1832 Environmental and climatic conditions at a potential Glacial refugial site of tree species near
1833 the Southern Alpine glaciers. New insights from multiproxy sedimentary studies at Lago
1834 della Costa (Euganean Hills, Northeastern Italy), *Quat. Sci. Rev.*, 28(25–26), 2647–2662,
1835 doi:10.1016/j.quascirev.2009.05.025, 2009.

1836
1837 Kaplan, J. O., Pfeiffer, M., Kolen, J. C. A. and Davis, B. A. S.: Large scale anthropogenic
1838 reduction of forest cover in last glacial maximum Europe, *PLoS One*, 11(11),
1839 doi:10.1371/journal.pone.0166726, 2016.

1840
1841 Kehrwald, N. M., McCoy, W. D., Thibeault, J., Burns, S. J. and Oches, E. A.: Paleoclimatic
1842 implications of the spatial patterns of modern and LGM European land-snail shell $\delta^{18}\text{O}$,
1843 *Quat. Res.*, 74(1), 166–176, doi:10.1016/j.yqres.2010.03.001, 2010.

1844
1845 Kelly, A., Charman, D. J. and Newnham, R. M.: A last glacial maximum pollen record from
1846 bodmin moor showing a possible cryptic Northern refugium in Southwest England, *J. Quat.*
1847 *Sci.*, 25(3), 296–308, doi:10.1002/jqs.1309, 2010.

1848
1849 Kolodny, Y., Stein, M. and Machlus, M.: Sea-rain-lake relation in the Last Glacial East
1850 Mediterranean revealed by $\delta^{18}\text{O}$ - $\delta^{13}\text{C}$ in Lake Lisan aragonites, *Geochim. Cosmochim.*
1851 *Acta*, 69(16), 4045–4060, doi:10.1016/j.gca.2004.11.022, 2005.

1852
1853 Kovács, J., Moravcová, M., Újvári, G. and Pintér, A. G.: Reconstructing the
1854 paleoenvironment of East Central Europe in the Late Pleistocene using the oxygen and
1855 carbon isotopic signal of tooth in large mammal remains, *Quat. Int.*, 276–277, 145–154,
1856 doi:10.1016/j.quaint.2012.04.009, 2012.

1857
1858 Krebs, P., Pezzatti, G. B., Beffa, G., Tinner, W. and Conedera, M.: Revising the sweet
1859 chestnut (*Castanea sativa* Mill.) refugia history of the last glacial period with extended pollen

1860 and macrofossil evidence, *Quat. Sci. Rev.*, 206, 111–128,
1861 doi:10.1016/j.quascirev.2019.01.002, 2019.

1862

1863 Kuneš, P., Pelánková, B., Chytrý, M., Jankovská, V., Pokorný, P. and Petr, L.: Interpretation
1864 of the last-glacial vegetation of eastern-central Europe using modern analogues from southern
1865 Siberia, *J. Biogeogr.*, 35(12), 2223–2236, doi:10.1111/j.1365-2699.2008.01974.x, 2008.

1866

1867 Küster, H.: Postglaziale Vegetationsgeschichte Südbayerns. Geobotanische Studien zur
1868 Prähistorischen Landschaftskunde, Akademie Verlag, Berlin., 1995.

1869

1870 Lacey, J. H., Leng, M. J., Höbig, N., Reed, J. M., Valero-Garcés, B. and Reicherter, K.:
1871 Western Mediterranean climate and environment since Marine Isotope Stage 3: a 50,000-year
1872 record from Lake Banyoles, Spain, *J. Paleolimnol.*, 55(2), 113–128, doi:10.1007/s10933-015-
1873 9868-9, 2016.

1874

1875 Latombe, G., Burke, A., Vrac, M., Levavasseur, G. and Dumas, C.: Comparison of spatial
1876 downscaling methods of general circulation model results to study climate variability during
1877 the Last Glacial Maximum, , 2563–2579, 2018.

1878

1879 Lefort J.P., Monnier J.L., Danukalova G.: Transport of Late Pleistocene loess particles by
1880 katabatic winds during the lowstands of the English Channel. *Journal of the Geological*
1881 *Society* 176: 1169–1181, doi: [10.1144/jgs2019-07](https://doi.org/10.1144/jgs2019-07), 2019.

1882

1883 Lehmkuhl, F., Nett, J.J., Pötter, S., Schulte, P., Sprafke, T., Jary, Z., Antoine, P., Wacha, L.,
1884 Wolf, D., Zerboni, A., Hošek, J., Marković, S.B., Obrecht, I., Sümegi, P., Veres, D.,
1885 Zeeden, C., Boemke, B., Schaubert, V., Viehweger, J., Hambach, U.: Loess landscapes of
1886 Europe e mapping, geomorphology, and zonal differentiation. *Earth Sci. Rev.* 215, 103496.
1887 <https://doi.org/10.1016/j.earscirev.2020.103496>, 2021.

1888

1889 Leroy, S. A. G. and Arpe, K.: Glacial refugia for summer-green trees in Europe and south-
1890 west Asia as proposed by ECHAM3 time-slice atmospheric model simulations, *J. Biogeogr.*,
1891 34(12), 2115–2128, doi:10.1111/j.1365-2699.2007.01754.x, 2007.

1892

1893 Lev, L., Stein, M., Ito, E., Fruchter, N., Ben-Avraham, Z. and Almogi-Labin, A.:
1894 Sedimentary, geochemical and hydrological history of Lake Kinneret during the past 28,000
1895 years, *Quat. Sci. Rev.*, 209, 114–128, doi:10.1016/j.quascirev.2019.02.015, 2019.

1896

1897 Lister, A. M. and Stuart, A. J.: The impact of climate change on large mammal distribution
1898 and extinction: Evidence from the last glacial/interglacial transition, *Comptes Rendus -*
1899 *Geosci.*, 340(9–10), 615–620, doi:10.1016/j.crte.2008.04.001, 2008.

1900

1901 López-García, J. M. and Blain, H. A.: Quaternary small vertebrates: State of the art and new
1902 insights, *Quat. Sci. Rev.*, 233, doi:10.1016/j.quascirev.2020.106242, 2020.

1903

1904 Ludwig, P., Pinto, J. G., Raible, C. C. and Shao, Y.: Impacts of surface boundary conditions
1905 on regional climate model simulations of European climate during the Last Glacial
1906 Maximum, *Geophys. Res. Lett.*, 44(10), 5086–5095, doi:10.1002/2017GL073622, 2017.

1907

1908

- 1909 Luetscher, M., Boch, R., Sodemann, H., Spötl, C., Cheng, H., Edwards, R. L., Frisia, S., Hof,
1910 F. and Müller, W.: North Atlantic storm track changes during the Last Glacial Maximum
1911 recorded by Alpine speleothems, *Nat. Commun.*, 6, 27–32, doi:10.1038/ncomms7344, 2015.
1912
- 1913 Magri, D.: Persistence of tree taxa in Europe and Quaternary climate changes, *Quat. Int.*,
1914 219(1–2), 145–151, doi:10.1016/j.quaint.2009.10.032, 2010.
1915
- 1916 Magri, D. and Parra, I.: Late Quaternary western Mediterranean pollen records and African
1917 winds, *Earth Planet. Sci. Lett.*, 200(3–4), 401–408, doi:10.1016/S0012-821X(02)00619-2,
1918 2002.
1919
- 1920 Magri, D. and Sadori, L.: Late Pleistocene and Holocene pollen stratigraphy at Lago di Vico,
1921 central Italy, *Veg. Hist. Archaeobot.*, 8(4), 247–260, doi:10.1007/BF01291777, 1999.
1922
- 1923 Magyari, E., Jakab, G., Rudner, E. and Sümegi, P.: Palynological and plant macrofossil data
1924 on Late Pleistocene short-term climatic oscillations in NE-Hungary, *Acta Palaeobot. Suppl.*,
1925 2(January), 491–502, 1999.
1926
- 1927 Magyari, E. K., Kuneš, P., Jakab, G., Sümegi, P., Pelánková, B., Schäbitz, F., Braun, M. and
1928 Chytrý, M.: Late Pleniglacial vegetation in eastern-central Europe: Are there modern
1929 analogues in Siberia?, *Quat. Sci. Rev.*, 95, 60–79, doi:10.1016/j.quascirev.2014.04.020,
1930 2014a.
1931
- 1932 Magyari, E. K., Veres, D., Wennrich, V., Wagner, B., Braun, M., Jakab, G., Karátson, D.,
1933 Pál, Z., Ferenczy, G., St-Onge, G., Rethemeyer, J., Francois, J. P., von Reumont, F. and
1934 Schäbitz, F.: Vegetation and environmental responses to climate forcing during the Last
1935 Glacial Maximum and deglaciation in the East Carpathians: Attenuated response to
1936 maximum cooling and increased biomass burning, *Quat. Sci. Rev.*, 106, 278–298,
1937 doi:10.1016/j.quascirev.2014.09.015, 2014b.
1938
- 1939 Magyari, E. K., Pál, I., Vincze, I., Veres, D., Jakab, G., Braun, M., Szalai, Z., Szabó, Z. and
1940 Korponai, J.: Warm Younger Dryas summers and early late glacial spread of temperate
1941 deciduous trees in the Pannonian Basin during the last glacial termination (20-9 kyr cal BP),
1942 *Quat. Sci. Rev.*, 225, doi:10.1016/j.quascirev.2019.105980, 2019.
1943
- 1944 Margari, V., Gibbard, P. L., Bryant, C. L. and Tzedakis, P. C.: Character of vegetational and
1945 environmental changes in southern Europe during the last glacial period; evidence from
1946 Lesvos Island, Greece, *Quat. Sci. Rev.*, 28(13–14), 1317–1339,
1947 doi:10.1016/j.quascirev.2009.01.008, 2009.
1948
- 1949 Marsicek, J., Shuman, B. N., Bartlein, P. J., Shafer, S. L. and Brewer, S.: Reconciling
1950 divergent trends and millennial variations in Holocene temperatures, *Nature*, 554(7690), 92–
1951 96, doi:10.1038/nature25464, 2018.
1952
- 1953 Mauch Lenardić, J., Oros Sršen, A. and Radović, S.: Quaternary fauna of the Eastern Adriatic
1954 (Croatia) with the special review on the Late Pleistocene sites, *Quat. Int.*, 494, 130–151,
1955 doi:10.1016/j.quaint.2017.11.028, 2018.
1956

- 1957 Mauri, A., Davis, B. A. S., Collins, P. M. and Kaplan, J. O.: The influence of atmospheric
1958 circulation on the mid-Holocene climate of Europe: A data-model comparison, *Clim. Past*,
1959 10(5), 1925–1938, doi:10.5194/cp-10-1925-2014, 2014.
1960
- 1961 Mauri, A., Davis, B. A. S., Collins, P. M. and Kaplan, J. O.: The climate of Europe during the
1962 Holocene: A gridded pollen-based reconstruction and its multi-proxy evaluation, *Quat. Sci.*
1963 *Rev.*, 112, doi:10.1016/j.quascirev.2015.01.013, 2015.
1964
- 1965 MARGE Project Members.: Constraints on the magnitude and patterns of ocean cooling at
1966 the Last Glacial Maximum, , (January), 1–6, doi:10.1038/ngeo411, 2009.
1967
- 1968 Mikolajewicz, U.: Modeling mediterranean ocean climate of the last glacial maximum, *Clim.*
1969 *Past*, 7(1), 161–180, doi:10.5194/cp-7-161-2011, 2011.
1970
- 1971 Miola, A., Bondesan, A., Corain, L., Favaretto, S., Mozzi, P., Piovan, S. and Sostizzo, I.:
1972 Wetlands in the Venetian Po Plain (northeastern Italy) during the Last Glacial Maximum:
1973 Interplay between vegetation, hydrology and sedimentary environment, *Rev. Palaeobot.*
1974 *Palynol.*, 141(1–2), 53–81, doi:10.1016/j.revpalbo.2006.03.016, 2006.
1975
- 1976 Mix, A. C., Bard, E. and Schneider, R.: Environmental processes of the ice age: Land,
1977 oceans, glaciers (EPILOG), *Quat. Sci. Rev.*, 20(4), 627–657, doi:10.1016/S0277-
1978 3791(00)00145-1, 2001.
1979
- 1979 Moine, O., Rousseau, D. D., Jolly, D. and Vianey-Liaud, M.: Paleoclimatic reconstruction
1980 using mutual climatic range on terrestrial mollusks, *Quat. Res.*, 57(1), 162–172,
1981 doi:10.1006/qres.2001.2286, 2002.
1982
- 1983 Monegato, G., Ravazzi, C., Donegana, M., Pini, R., Calderoni, G. and Wick, L.: Evidence of
1984 a two-fold glacial advance during the last glacial maximum in the Tagliamento end moraine
1985 system (eastern Alps), *Quat. Res.*, 68(2), 284–302, doi:10.1016/j.yqres.2007.07.002, 2007.
1986
- 1987 Monegato, G., Ravazzi, C., Culiberg, M., Pini, R., Bavec, M., Calderoni, G., Jež, J. and
1988 Perego, R.: Sedimentary evolution and persistence of open forests between the south-eastern
1989 Alpine fringe and the Northern Dinarides during the Last Glacial Maximum, *Palaeogeogr.*
1990 *Palaeoclimatol. Palaeoecol.*, 436, 23–40, doi:10.1016/j.palaeo.2015.06.025, 2015.
1991
- 1992 Moreno, A., González-Sampériz, P., Morellón, M., Valero-Garcés, B. L. and Fletcher, W. J.:
1993 Northern Iberian abrupt climate change dynamics during the last glacial cycle: A view from
1994 lacustrine sediments, *Quat. Sci. Rev.*, 36, 139–153, doi:10.1016/j.quascirev.2010.06.031,
1995 2012.
1996
- 1997 Nogues-Bravo D, Rodríguez-Sánchez F, Orsini L, de Boer E, Jansson R, Morlon, H.,
1998 Fordham, D.A., Jackson, S.T.: Cracking the code of biodiversity responses to past climate
1999 change. *Trends Ecol. Evol.* 33:765–76, 2018.
2000
- 2001
- 2002 Nolan, C., Overpeck, J. T., Allen, J. R. M., Anderson, P. M., Betancourt, J. L., Binney, H. A.,
2003 Brewer, S., Bush, M. B., Chase, B. M., Cheddadi, R., Djamali, M., Dodson, J., Edwards, M.
2004 E., Gosling, W. D., Haberle, S., Hotchkiss, S. C., Huntley, B., Ivory, S. J., Kershaw, A. P.,
2005 Kim, S. H., Latorre, C., Leydet, M., Lézine, A. M., Liu, K. B., Liu, Y., Lozhkin, A. V.,
2006 McGlone, M. S., Marchant, R. A., Momohara, A., Moreno, P. I., Müller, S., Otto-Bliesner, B.

2007 L., Shen, C., Stevenson, J., Takahara, H., Tarasov, P. E., Tipton, J., Vincens, A., Weng, C.,
2008 Xu, Q., Zheng, Z. and Jackson, S. T.: Past and future global transformation of terrestrial
2009 ecosystems under climate change, *Science* (80-), 361(6405), 920–923,
2010 doi:10.1126/science.aan5360, 2018.

2011

2012 Normand, S., Treier, U. A. and Odgaard, B. V.: Tree refugia and slow forest development in
2013 response to post - LGM warming in North - Eastern European Russia, , 2(4), 2–5, 2011.

2014

2015 Paganelli, A.: Evolution of vegetation and climate in the Veneto-Po Plain during the Late-
2016 Glacial and Early Holocene using pollen-stratigraphical data, *Alp. Mediterr. Quat.*, 9(2),
2017 581–589, 1996.

2018

2019 Peyron, O., Guiot, J., Cheddadi, R., Tarasov, P., Reille, M., De Beaulieu, J. L., Bottema, S.
2020 and Andrieu, V.: Climatic Reconstruction in Europe for 18,000 YR B.P. from Pollen Data,
2021 *Quat. Res.*, 49(2), 183–196, doi:10.1006/qres.1997.1961, 1998a.

2022

2023 Peyron, O., Magny, M., Goring, S., Joannin, S., de Beaulieu, J.-L., Brugiapaglia, E., Sadori,
2024 L., Garfi, G., Kouli, K., Ioakim, C., Combourieu-Nebout, N., Contrasting patterns of climatic
2025 changes during the Holocene across the Italian Peninsula reconstructed from pollen data.
2026 *Clim. Past* 9 (3), 1233–1252. Doi:10.5194/cp-9-1233-2013, 2013.

2027

2028 Pons, A. and Reille, M.: The Holocene- and upper Pleistocene pollen record from Padul
2029 (Granada, Spain): A new study, *Palaeogeogr. Palaeoclimatol. Palaeoecol.*, 66(3–4),
2030 doi:10.1016/0031-0182(88)90202-7, 1988.

2031

2032 Potì, A., Kehl, M., Broich, M., Carrión Marco, Y., Hutterer, R., Jentke, T., Linstädter, J.,
2033 López-Sáez, J. A., Mikdad, A., Morales, J., Pérez-Díaz, S., Portillo, M., Schmid, C., Vidal-
2034 Matutano, P. and Weniger, G. C.: Human occupation and environmental change in the
2035 western Maghreb during the Last Glacial Maximum (LGM) and the Late Glacial. New
2036 evidence from the Iberomaurusian site Ifri El Baroud (northeast Morocco), *Quat. Sci. Rev.*,
2037 220, 87–110, doi:10.1016/j.quascirev.2019.07.013, 2019.

2038

2039 Prentice, I. C., Cleator, S. F., Huang, Y. H., Harrison, S. P., and Roulstone, I.: Reconstructing
2040 ice-age palaeoclimates: Quantifying low-CO₂ effects on plants, *Global Planet. Change*, 149,
2041 166–176, <https://doi.org/10.1016/j.gloplacha.2016.12.012>, 2017.

2042

2043 Prentice, I. C. and Harrison, S. P.: Ecosystem effects of CO₂ concentration: Evidence from
2044 past climates, *Clim. Past*, 5(3), 297–307, doi:10.5194/cp-5-297-2009, 2009.

2045

2046 Prentice, I. C., Guiot, J. and Harrison, S. P.: Mediterranean vegetation, lake levels and
2047 palaeoclimate at the Last Glacial Maximum, *Nature*, 360(6405), 658–660,
2048 doi:10.1038/360658a0, 1992.

2049

2050 Prentice, I. C., Guiot, J., Huntley, B., Jolly, D. and Cheddadi, R.: Reconstructing biomes
2051 from palaeoecological data: A general method and its application to European pollen data at
2052 0 and 6 ka, *Clim. Dyn.*, 12(3), 185–194, doi:10.1007/BF00211617, 1996.

2053

2054 Prentice, I. C., Harrison, S. P. and Bartlein, P. J.: Global vegetation and terrestrial carbon
2055 cycle changes after the last ice age, *New Phytol.*, 189(4), 988–998, doi:10.1111/j.1469-
2056 8137.2010.03620.x, 2011.

2057
2058 Prud'homme, C., Lécuyer, C., Antoine, P., Moine, O., Hatté, C., Fourel, F., Martineau, F. and
2059 Rousseau, D. D.: Palaeotemperature reconstruction during the Last Glacial from $\delta^{18}\text{O}$ of
2060 earthworm calcite granules from Nussloch loess sequence, Germany, *Earth Planet. Sci. Lett.*,
2061 442, 13–20, doi:10.1016/j.epsl.2016.02.045, 2016.
2062
2063 Prud'homme, C., Lécuyer, C., Antoine, P., Hatté, C., Moine, O., Fourel, F., Amiot, R.,
2064 Martineau, F. and Rousseau, D. D.: $\delta^{13}\text{C}$ signal of earthworm calcite granules: A new proxy
2065 for palaeoprecipitation reconstructions during the Last Glacial in western Europe, *Quat. Sci.*
2066 *Rev.*, 179, 158–166, doi:10.1016/j.quascirev.2017.11.017, 2018.
2067
2068 Puzachenko, A. Y., Markova, A. K. and Pawłowska, K.: Evolution of Central European
2069 regional mammal assemblages between the late Middle Pleistocene and the Holocene (MIS7–
2070 MIS1), *Quat. Int.*, (November), doi:10.1016/j.quaint.2021.11.009, 2021.
2071
2072 Ramstein, G., Kageyama, M., Guiot, J. and Wu, H.: How cold was Europe at the Last Glacial
2073 Maximum ? A synthesis of the progress achieved since the first PMIP model-data
2074 comparison, , 331–339, 2007.
2075
2076 Reille, M. and Andrieu, V.: The late Pleistocene and Holocene in the Lourdes Basin, Western
2077 Pyrénées, France: new pollen analytical and chronological data, *Veg. Hist. Archaeobot.*, 4(1),
2078 1–21, doi:10.1007/BF00198611, 1995.
2079
2080 Reille, M. and de Beaulieu, J. L.: History of the Würm and Holocene vegetation in western
2081 velay (Massif Central, France): A comparison of pollen analysis from three corings at Lac du
2082 Bouchet, *Rev. Palaeobot. Palynol.*, 54(3–4), 233–248, doi:10.1016/0034-6667(88)90016-4,
2083 1988.
2084
2085 Reimer, A., Landmann, G. and Kempe, S.: Lake Van, Eastern Anatolia, hydrochemistry and
2086 history, *Aquat. Geochemistry*, 15(1–2), 195–222, doi:10.1007/s10498-008-9049-9, 2009.
2087
2088 Rousseau, D. D.: Climatic transfer function from quaternary molluscs in European loess
2089 deposits, *Quat. Res.*, 36(2), 195–209, doi:10.1016/0033-5894(91)90025-Z, 1991.
2090
2091 Royer, A., Montuire, S., Legendre, S., Discamps, E., Jeannet, M. and Lécuyer, C.:
2092 Investigating the influence of climate changes on rodent communities at a regional-scale
2093 (MIS 1-3, Southwestern France), *PLoS One*, 11(1), 1–25, doi:10.1371/journal.pone.0145600,
2094 2016.
2095
2096 Ruiz-Zapata, M. B., Vegas, J., Garcia-Cortes, A., Gil Garcia, M. J., Torres, T., Ortiz, J. E.
2097 and Perez-Gonzalez, A.: Vegetation evolution during the Last Maximum Glacial Period in
2098 FU-1 sequence (Fuentillejo Lacustrin Maar, Campo de Calatrava, Ciudad Real), *Polen*, 18,
2099 37–49, 2008.
2100
2101 Salonen, J., Sanchez Goñi, M.F., Renssen, H. and Pliikk, A.: Contrasting northern and
2102 southern European winter climate trends during the Last Interglacial. *Geology* 49.
2103 10.1130/G49007.1. 2021
2104
2105 Salonen, J.S., Korpela, M., Williams, J.W., Luoto, M., Machine-learning based
2106 reconstructions of primary and secondary climate variables from North American and

2107 [European fossil pollen data. Sci. Rep. 9, 1–13. doi: 10.1038/s41598-019-](#)
2108 [52293-4, 2019.](#)
2109
2110 Salonen, J.S., Ilvonen, L., Seppä, H., Holmström, L., Telford, R.J., Gaidamavicius, A.,
2111 Stancikaite, M., Subetto, D. Comparing different calibration methods (WA/WA-PLS
2112 regression and Bayesian modelling) and different-sized calibration sets in pollen-based
2113 quantitative climate reconstruction. *The Holocene* 22, 413–424, 2012.
2114
2115 Samartin, S., Heiri, O., Kaltenrieder, P., Köhl, N. and Tinner, W.: Reconstruction of full
2116 glacial environments and summer temperatures from Lago della Costa, a refugial site in
2117 Northern Italy, *Quat. Sci. Rev.*, 143, 107–119, doi:10.1016/j.quascirev.2016.04.005, 2016.
2118
2119 Sánchez Goñi, M.F., Loutre, M.F., Crucifix, M., Peyron, O., Santos, L., Duprat, J., Malaizé,
2120 B., Turon, J.-L., and Peyrouquet, J.-P.: Increasing vegetation and climate gradient in western
2121 Europe over the Last Glacial inception (122–110 ka): Data–model comparison. *Earth and*
2122 *Planetary Science Letters*, 231, 111–130, doi: 10.1016/j.epsl.2004.12.010, 2005.
2123
2124 Sanchez Goñi, M.F., Harrison, S.P.: Millennial-scale climate variability and vegetation
2125 changes during the Last Glacial: concepts and terminology. *Quaternary Science*
2126 *Reviews* 29, 2823–2827, doi: [10.1016/j.quascirev.2009.11.014](#), 2010.
2127
2128 Sanchi, L., Ménot, G. and Bard, E.: Insights into continental temperatures in the northwestern
2129 Black Sea area during the Last Glacial period using branched tetraether lipids, *Quat. Sci.*
2130 *Rev.*, 84, 98–108, doi:10.1016/j.quascirev.2013.11.013, 2014.
2131
2132 Satkūnas, J. and Grigienė, A.: Eemian-Weichselian palaeoenvironmental record from the
2133 Mickūnai glacial depression (Eastern Lithuania), *Geologija*, 54(2), 35–51,
2134 doi:10.6001/geologija.v54i2.2482, 2012.
2135 Schäfer, I. K., Bliedtner, M., Wolf, D., Faust, D. and Zech, R.: Evidence for humid
2136 conditions during the last glacial from leaf wax patterns in the loess-paleosol sequence El
2137 Paraíso, Central Spain, *Quat. Int.*, 407, 64–73, doi:10.1016/j.quaint.2016.01.061, 2016.
2138
2139 Scourse, J. D.: Late Pleistocene stratigraphy and palaeobotany of the Isles of Scilly, *Philos.*
2140 *Trans. - R. Soc. London, B*, 334(1271), 405–448, doi:10.1098/rstb.1991.0125, 1991.
2141
2142 Spötl, C., Koltai, G., Jarosch, A. H. and Cheng, H.: Increased autumn and winter
2143 precipitation during the Last Glacial Maximum in the European Alps, *Nat. Commun.*, 12(1),
2144 doi:10.1038/s41467-021-22090-7, 2021.
2145
2146 Stewart, J. R. and Lister, A. M.: Cryptic northern refugia and the origins of the modern biota,
2147 *Trends Ecol. Evol.*, 16(11), 608–613, doi:10.1016/S0169-5347(01)02338-2, 2001.
2148
2149 Stivrins, N., Soininen, J., Amon, L., Fontana, S. L., Gryguc, G., Heikkilä, M., Heiri, O.,
2150 Kisielienė, D., Reitalu, T., Stančikaitė, M., Veski, S. and Seppä, H.: Biotic turnover rates
2151 during the Pleistocene-Holocene transition, *Quat. Sci. Rev.*, 151, 100–110,
2152 doi:10.1016/j.quascirev.2016.09.008, 2016.
2153
2154 Strahl, J.: Zur Pollenstratigraphie des Weichselspätglazials von Berlin-Brandenburg [On the
2155 palynostratigraphy of the Late Weichselian in Berlin-Brandenburg], *Brand.*
2156 *Geowissenschaftliche Beiträge*, 12, 87–112, 2005.

2157
2158 Stute, M. and Deak, J.: Environmental isotope study (14C, 13C, 18O, D, noble gases) on
2159 deep groundwater circulation systems in Hungary with reference to paleoclimate,
2160 Radiocarbon, 31(3), 902–918, doi:10.1017/s0033822200012522, 1990.
2161
2162 Svenning, J., Normand, S. and Kageyama, M.: Glacial refugia of temperate trees in Europe :
2163 insights from species distribution modelling, , (Svenning 2003), 1117–1127,
2164 doi:10.1111/j.1365-2745.2008.01422.x, 2008.
2165
2166 Tarasov, P. E., Webb, T., Andreev, A. A., Afanas'eva, N. B., Berezina, N. A., Bezusko, L.
2167 G., Blyakharchuk, T. A., Bolikhovskaya, N. S., Cheddadi, R., Chernavskaya, M. M.,
2168 Chernova, G. M., Dorofeyuk, N. I., Dirksen, V. G., Elina, G. A., Filimonova, L. V., Glebov,
2169 F. Z., Guiot, J., Gunova, V. S., Harrison, S. P., Jolly, D., Khomutova, V. I., Kvavadze, E. V.,
2170 Osipova, I. M., Panova, N. K., Prentice, I. C., Saarse, L., Sevastyanov, D. V., Volkova, V. S.
2171 and Zernitskaya, V. P.: Present-day and mid-Holocene biomes reconstructed from pollen and
2172 plant macrofossil data from the former Soviet Union and Mongolia, J. Biogeogr., 25(6),
2173 1029–1053, doi:10.1046/j.1365-2699.1998.00236.x, 1998.
2174
2175 Tarasov, P. E., Volkova, V. S., Webb, T., Guiot, J., Andreev, A. A., Bezusko, L. G.,
2176 Bezusko, T. V., Bykova, G. V., Dorofeyuk, N. I., Kvavadze, E. V., Osipova, I. M., Panova,
2177 N. K. and Sevastyanov, D. V.: Last glacial maximum biomes reconstructed from pollen and
2178 plant macrofossil data from northern Eurasia, J. Biogeogr., 27(3), 609–620,
2179 doi:10.1046/j.1365-2699.2000.00429.x, 2000.
2180
2181 Tarasov, P.E., Andreev, A.A., Anderson, P.M., Lozhkin, A.V., Haltia-Hovi, E., Nowaczyk,
2182 N.R., Wennrich, V., Brigham-Grette, J., Melles, M.: A pollen-based biome reconstruction
2183 over the last 3.562 million years in the Far East Russian Arctic e new insights on climate-
2184 vegetation relationships at the regional scale. Clim. Past 9, 2759-2775, doi: 10.5194/cp-9-
2185 2759-2013, 2013.
2186
2187 Telford, R. J. and Birks, H. J. B.: Evaluation of transfer functions in spatially structured
2188 environments, Quat. Sci. Rev., 28(13–14), 1309–1316, doi:10.1016/j.quascirev.2008.12.020,
2189 2009.
2190
2191 Turner, M. G., Wei, D., Prentice, I. C., & Harrison, S. P. The impact of methodological
2192 decisions on climate reconstructions using WA-PLS. *Quaternary Research*, 99, 341-356,
2193 2021.
2194
2195 Valero-Garcés, B. L., González-Sampériz, P., Navas, A., Machin, J., Delgado-Huertas, A.,
2196 Pena-Monné, J. L., Sancho-Marcén, C., Stevenson, T. and Davis, B.: Paleohydrological
2197 fluctuations and steppe vegetation during the last glacial maximum in the central Ebro valley
2198 (NE Spain), Quat. Int., 122(1 SPEC. ISS.), doi:10.1016/j.quaint.2004.01.030, 2004.
2199
2200 Valsecchi, V., Sanchez Goñi, M. F. and Londeix, L.: Vegetation dynamics in the
2201 Northeastern Mediterranean region during the past 23 000 yr: Insights from a new pollen
2202 record from the Sea of Marmara, Clim. Past, 8(5), 1941–1956, doi:10.5194/cp-8-1941-2012,
2203 2012.
2204
2205 Vandenberghe, J., French, H. M., Gorbunov, A., Marchenko, S., Velichko, A. A., Jin, H.,
2206 Cui, Z., Zhang, T. and Wan, X.: The Last Permafrost Maximum (LPM) map of the Northern

2207 Hemisphere: Permafrost extent and mean annual air temperatures, 25-17ka BP, *Boreas*,
2208 43(3), 652–666, doi:10.1111/bor.12070, 2014.

2209

2210 Varsányi, I., Palcsu, L. and Kovács, L. Ó.: Groundwater flow system as an archive of
2211 palaeotemperature: Noble gas, radiocarbon, stable isotope and geochemical study in the
2212 Pannonian Basin, Hungary, *Appl. Geochemistry*, 26(1), 91–104,
2213 doi:10.1016/j.apgeochem.2010.11.006, 2011.

2214

2215 Vegas-Vilarrúbia, T., González-Sampériz, P., Morellón, M., Gil-Romera, G., Pérez-Sanz, A.
2216 and Valero-Garcés, B.: Diatom and vegetation responses to late glacial and early holocene
2217 climate changes at lake estanya (southern pyrenees, NE Spain), *Palaeogeogr. Palaeoclimatol.*
2218 *Palaeoecol.*, 392, 335–349, doi:10.1016/j.palaeo.2013.09.011, 2013.

2219

2220 Vegas, J., Ruiz-Zapata, B., Ortiz, J. E., Galán, L., Torres, T., García-Cortés, Á., Gil-García,
2221 M. J., Pérez-González, A. and Gallardo-Millán, J. L.: Identification of arid phases during the
2222 last 50 cal. ka BP from the Fuentillejo maar-lacustrine record (Campo de Calatrava Volcanic
2223 Field, Spain), *J. Quat. Sci.*, 25(7), 1051–1062, doi:10.1002/jqs.1262, 2010.

2224

2225 Velasquez, P., Kaplan, J. O., Messmer, M., Ludwig, P. and Raible, C. C.: The role of land
2226 cover in the climate of glacial Europe, *Clim. Past*, 17(3), 1161–1180, doi:10.5194/cp-17-
2227 1161-2021, 2021.

2228

2229 Vicente-Serrano, S. M., Trigo, R. M., López-Moreno, J. I., Liberato, M. L. R., Lorenzo-
2230 Lacruz, J., Beguería, S., Morán-Tejeda, E. and El Kenawy, A.: Extreme winter precipitation
2231 in the Iberian Peninsula in 2010: Anomalies, driving mechanisms and future projections,
2232 *Clim. Res.*, 46(1), 51–65, doi:10.3354/cr00977, 2011.

2233

2234 Williams, J.W., Grimm, E.G., Blois, J., Charles, D.F., Davis, E., Goring, S.J., Graham, R.,
2235 Smith, A.J., Anderson, M., Arroyo-Cabrales, J., Ashworth, A.C., Betancourt, J.L., Bills,
2236 B.W., Booth, R.K., Buckland, P., Curry, B., Giesecke, T., Hausmann, S., Jackson, S.T.,
2237 Latorre, C., Nichols, J., Purdum, T., Roth, R.E., Stryker, M., Takahara, H. :The Neotoma
2238 Paleoecology Database: A multi-proxy, international community-curated data resource. *Quat.*
2239 *Res.* 89, 156-177, doi:10.1017/qua.2017.105, 2018.

2240

2241 Williams, J. W. and Jackson, S. T.: Palynological and AVHRR observations of modern
2242 vegetational gradients in eastern North America, , 4, 485–497, 2003.

2243

2244 Williams, J. W., Webb, T., Shurman, B. N. and Bartlein, P. J.: Do Low CO₂ Concentrations
2245 Affect Pollen-Based Reconstructions of LGM Climates? A Response to “Physiological
2246 Significance of Low Atmospheric CO₂ for Plant–Climate Interactions” by Cowling and
2247 Sykes, *Quat. Res.*, 53(3), 402–404, doi:10.1006/qres.2000.2131, 2000.

2248

2249 Willis, K. J. and Van Andel, T. H.: Trees or no trees? The environments of central and
2250 eastern Europe during the Last Glaciation, *Quat. Sci. Rev.*, 23(23–24), 2369–2387,
2251 doi:10.1016/j.quascirev.2004.06.002, 2004.

2252

2253 Wu, H., Guiot, J., Brewer, S. and Guo, Z.: Climatic changes in Eurasia and Africa at the last
2254 glacial maximum and mid-Holocene: Reconstruction from pollen data using inverse
2255 vegetation modelling, *Clim. Dyn.*, 29(2–3), 211–229, doi:10.1007/s00382-007-0231-3, 2007.

2256

- 2257 Wu, H., Li, Q., Yu, Y., Sun, A., Lin, Y., Jiang, W. & Luo, Y. Quantitative climatic reconstruction of
2258 the Last Glacial Maximum in China. *Sci. China Earth Sci.* 62, 1269–1278 (2019).
2259 Doi:10.1007/s11430-018-9338-3, 2019.
2260
- 2261 Yu, G. and Harrison, S. P.: Lake status records from Europe: data base documentation,
2262 NOAA Paleoclimatology Publications Series, Boulder, Colorado., 1995.
2263
- 2264 Zaarur, S., Affek, H. P. and Stein, M.: Last glacial-Holocene temperatures and hydrology of
2265 the Sea of Galilee and Hula Valley from clumped isotopes in *Melanopsis* shells, *Geochim.*
2266 *Cosmochim. Acta*, 179, 142–155, doi:10.1016/j.gca.2015.12.034, 2016.
2267
- 2268 Zanon, M., Davis, B. A. S., Marquer, L., Brewer, S. and Kaplan, J. O.: European forest cover
2269 during the past 12,000 years: A palynological reconstruction based on modern analogs and
2270 remote sensing, *Front. Plant Sci.*, 9, doi:10.3389/fpls.2018.00253, 2018.
2271
- 2272 Zech, M., Buggle, B., Leiber, K., Marković, S., Glaser, B., Hambach, U., Huwe, B., Stevens,
2273 T., Sümegi, P., Wiesenberg, G. and Zöller, L.: Reconstructing Quaternary vegetation history
2274 in the Carpathian Basin, SE-Europe, using n-alkane biomarkers as molecular fossils:
2275 Problems and possible solutions, potential and limitations, *Quat. Sci. J.*, 58(2), 148–155,
2276 doi:10.3285/eg.58.2.03, 2010.
2277
2278

2279
2280
2281

Tables

| Site | Site Name | Country/Ocean | Latitude | Longitude | Elevation | Site Type | Data Type | Samples | Source | Reference |
|------|--------------------------------|----------------|------------|------------|-----------|--------------|-----------|---------|------------------|------------------------------|
| 1 | MD95-2039 (M) | Atlantic | 40.578333 | -10.348333 | -3381 | Marine | Raw Count | 21 | EPD (E#1472) | Roucoux et al. 2005 |
| 2 | SU81-18 (M) | Atlantic | 37.77 | -9.82 | -3135 | Marine | Raw Count | 10 | ACER | Turon et al. 2003 |
| 3 | MD99-2331 (M) | Atlantic | 41.15 | -9.68 | -2110 | Marine | Raw Count | 41 | ACER | Naughton et al. 2006 |
| 4 | Carn Morval | United Kingdom | 49.926111 | -6.313889 | 5 | Lake | Digitised | 1 | Publication | Scourse 1991 |
| 5 | Gorham Cave | Spain | 36.132826 | -5.347358 | 0 | Cave | Digitised | 1 | Publication | Carrion et al. 2008 |
| 6 | Dozmary Pool | United Kingdom | 50.5347222 | -4.5358333 | 265 | Lake | Raw Count | 32 | Author | Kelly et al. 2010 |
| 7 | Bajondillo | Spain | 36.619722 | -4.496389 | 20 | Cave | Raw Count | 1 | EPD (E#1570) | Cortes-Sanchez et al. 2011 |
| 8 | Laguna del maar de Fuentillejo | Spain | 38.937996 | -4.0539 | 637 | Lake | Digitised | 1 | Publication | Ruiz-Zapata et al. 2009 |
| 9 | Padul-1 | Spain | 37.016338 | -3.608503 | 785 | Peat Bog | Digitised | 13 | Publication | Pons & Reille 1988 |
| 10 | Padul-2 | Spain | 37.010833 | -3.603889 | 726 | Peat Bog | Digitised | 1 | Publication | Camuera et al. 2019 |
| 11 | Cova di Carihuela | Spain | 37.4489 | -3.4297 | 1020 | Cave | Digitised | 1 | Publication | Carrion 1992 |
| 12 | Ifri El Baroud | Morocco | 34.75 | -3.3 | 539 | Cave | Digitised | 1 | Publication | Poti et al. 2019 |
| 13 | MD95-2043 (M) | Mediterranean | 36.14 | -2.621 | -1841 | Marine | Raw Count | 7 | ACER | Fletcher et al. 2008 |
| 14 | San Rafael | Spain | 36.773611 | -2.601389 | 0 | Peat Bog | Raw Count | 2 | EPD (E#574) | Pantaléon-Cano 1997 |
| 15 | Siles | Spain | 38.24 | -2.3 | 1320 | Lake | Digitised | 1 | Publication | Carrion 2002 |
| 16 | Torreçilla de Valmadrid | Spain | 41.4469444 | -0.895 | 570 | Colluvium | Digitised | 1 | Publication | Valero-Garces et al. 2004 |
| 17 | Navarrés-1 | Spain | 39.1 | -0.683333 | 225 | Peat Bog | Raw Count | 1 | EPD (E#469) | Carrion & Dupré-Olivier 1996 |
| 18 | Navarrés-2 | Spain | 39.1 | -0.683333 | 225 | Peat Bog | Raw Count | 1 | EPD (E#470) | Carrión & Dupré-Olivier 1996 |
| 19 | Tourbiere de l'Estarrès | France | 43.0933 | -0.3792 | 356 | Lake | Digitised | 1 | Publication | Jalut et al. 1988 |
| 20 | Cova de les Malladetes | Spain | 39.058 | -0.321 | 20 | Cave | Digitised | 1 | Publication | Dupré-Olivier 1988 |
| 21 | Lourdes | France | 43.033333 | -0.075 | 430 | Lake | Digitised | 15 | Publication | Reille & Andrieu 1995 |
| 22 | Lake Estanya | Spain | 42.0333333 | 0.5333333 | 670 | Lake | Digitised | 1 | Publication | Vegas-Villarubia et al. 2013 |
| 23 | Freychinede | France | 42.7833 | 1.4333 | 1350 | Lake | Digitised | 1 | Publication | Jalut et al. 1992 |
| 24 | Banyoles | Spain | 42.133333 | 2.75 | 173 | Lake | Raw Count | 13 | EPD (E#931) | Pérez-Obiol & Julia 1994 |
| 25 | Lac du Bouchet B5 | France | 44.916667 | 3.783333 | 1200 | Lake | Digitised | 14 | Publication | Reille & de Beaulieu 1988 |
| 26 | MD99-2348 (103) (M) | Mediterranean | 42.692778 | 3.841667 | -296 | Marine | Raw Count | 41 | EPD (E#1474) | Beaudouin et al. 2007 |
| 27 | Les Echets G | France | 45.9 | 4.93 | 267 | Peat Bog | Digitised | 136 | ACER | de Beaulieu & Reille 1984 |
| 28 | La Grotte Walou | Belgium | 50.585278 | 5.536389 | 252 | Cave | Digitised | 1 | Publication | Dambon 2011 |
| 29 | Bergsee | Germany | 47.5722222 | 7.93638889 | 382 | Lake | Digitised | 1 | Publication | Duprat-Qualid et al. 2017 |
| 30 | Garaat El-Ouez | Algeria | 36.818333 | 8.33333 | 45 | Peat Bog | Raw Count | 6 | EPD (E#1501) | Benslama et al. 2010 |
| 31 | Pian del Lago | Italy | 44.321561 | 9.485682 | 833 | Lake | Digitised | 1 | Publication | Guido et al. 2020 |
| 32 | Pilsensee | Germany | 48.0267 | 11.1883 | 534 | Lake | Digitised | 1 | Publication | Küster 1995 |
| 33 | Orgiano | Italy | 45.29 | 11.43 | 19 | Peat Bog | Digitised | 1 | Publication | Paganelli 1996 |
| 34 | Lago della Costa | Italy | 45.2702778 | 11.7430556 | 7 | Lake | Digitised | 8 | Publication | Kaltenrieder et al. 2009 |
| 35 | Lagaccione | Italy | 42.566667 | 11.85 | 355 | Lake | Raw Count | 7 | ACER | Magri 1999 |
| 36 | Lago Vico | Italy | 42.3166667 | 12.166667 | 510 | Lake | Digitised | 15 | Publication | Magri & Sadori 1999 |
| 37 | Stracciaccia | Italy | 42.13 | 12.32 | 220 | Lake | Raw Count | 2 | ACER | Giardini 2007 |
| 38 | Lago di Monterosi | Italy | 42.2166667 | 12.4333333 | 237 | Lake | Raw Count | 1 | Publication | Bonatti 1970 |
| 39 | Venice | Italy | 45.629523 | 12.654086 | 0 | Peat Bog | Digitised | 1 | Publication | Miola et al. 2006 |
| 40 | Azzano Decimo | Italy | 45.8833 | 12.7165 | 10 | Alluvial Fan | Raw Count | 6 | ACER | Pini et al. 2009 |
| 41 | Valle di Castiglione | Italy | 41.89 | 12.75 | 44 | Lake | Raw Count | 2 | ACER | Follieri et al. 1989 |
| 42 | Travesio | Italy | 46.2 | 12.87 | 220 | Lake | Digitised | 1 | Publication | Monegato et al. 2007 |
| 43 | Orvenco | Italy | 46.252088 | 13.169771 | 380 | Alluvial Fan | Digitised | 1 | Publication | Monegato et al. 2007 |
| 44 | Rio Doidis | Italy | 46.12 | 13.19 | 152 | Lake | Digitised | 1 | Publication | Monegato et al. 2007 |
| 45 | Billerio | Italy | 46.22 | 13.21 | 300 | Lake | Digitised | 1 | Publication | Monegato et al. 2007 |
| 46 | Kersdorf-Briesen | Germany | 52.333704 | 14.269142 | 44 | Lake | Digitised | 1 | Publication | Strahl 2005 |
| 47 | Lago Grande di Monticchio | Italy | 40.944444 | 15.6 | 1326 | Lake | Raw Count | 6 | EPD (E#932) | Watts et al. 1996 |
| 48 | Nagymohos | Hungary | 48.326944 | 20.436389 | 297 | Peat Bog | Raw Count | 14 | Publication | Magyari et al. 1999 |
| 49 | Safarka | Slovakia | 48.8819444 | 20.575 | 600 | Peat Bog | Digitised | 1 | Publication | Jankovska 2008 |
| 50 | Fehér Lake | Hungary | 46.45 | 20.65 | 86 | Lake | Raw Count | 10 | Publication | Magyari et al. 2014 |
| 51 | Ioannina | Greece | 39.75 | 20.85 | 470 | Peat Bog | Raw Count | 20 | ACER | Tzedakis et al. 2004 |
| 52 | Kokad | Hungary | 47.4027778 | 21.9286111 | 112 | Peat Bog | Raw Count | 2 | Publication | Magyari et al. 2019 |
| 53 | Lake Xinias | Greece | 39.05 | 22.27 | 500 | Lake | Raw Count | 5 | EPD (E#976) | Bottema 1979 |
| 54 | Mickunai | Lithuania | 54.722114 | 25.532218 | 143 | Lake | Digitised | 1 | Publication | Satkunas & Grigiene 2012 |
| 55 | Lake Sfanta Anna | Romania | 46.1263889 | 25.880556 | 946 | Lake | Digitised | 1 | Publication | Magyari et al. 2014 |
| 56 | Megali Limni | Greece | 39.1 | 26.3 | 323 | Lake | Digitised | 1 | Publication | Margari et al. 2009 |
| 57 | Straldzha | Bulgaria | 42.630278 | 26.77 | 138 | Peat Bog | Raw Count | 3 | Publication | Connor et l. 2013 |
| 58 | MD01-2430 (M) | Turkey | 40.796833 | 27.725166 | -580 | Marine | Digitised | 1 | Publication | Valsecchi et al. 2012 |
| 59 | Lake Iznik | Turkey | 40.433889 | 29.533056 | 88 | Lake | Raw Count | 7 | EPD (E#714) | Miebach et al. 2016 |
| 60 | M72/5 628-1 (M) | Black Sea | 42.1035 | 36.62383 | -418 | Marine | Raw Count | 6 | Pangaea (833387) | Shumilovskikh et al. 2014 |
| 61 | Dziguta | Georgia | 42.99 | 41.07 | 35 | Peat Bog | Digitised | 1 | Publication | Arslanov et al. 2007 |
| 62 | Lake Van LG | Turkey | 38.667 | 42.669 | 1649 | Lake | Raw Count | 10 | Pangaea (853779) | Pickarski et al. 2015 |
| 63 | Lake Zeribar | Iran | 35.533333 | 46.116667 | 1286 | Lake | Raw Count | 17 | EPD (E#714) | van Zeist & Bottema 1977 |

2282
2283
2284
2285
2286
2287

Table 1. List of selected sites

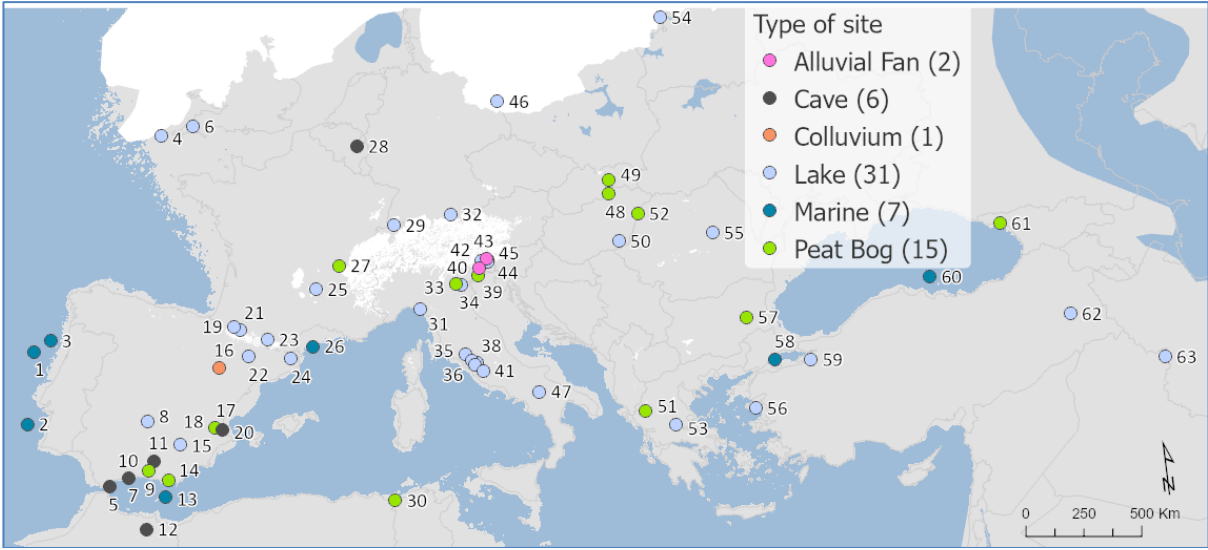
2288
2289
2290
2291
2292

| | RMSE | R2 |
|-------------------|-------------|-----------|
| TANN | 2.28 | 0.9 |
| TDJF | 3.35 | 0.91 |
| TJJA | 2.21 | 0.81 |
| PANN | 224.94 | 0.69 |
| PDJF | 78.51 | 0.69 |
| PJJA | 52.49 | 0.75 |
| Tree Cover | 21.03 | 0.52 |

2293
2294
2295
2296
2297
2298
2299
2300
2301
2302

Table 2. MAT performance statistics based on the modern pollen sample training set. This includes Mean Annual Temperature and Precipitation (TANN and PANN), Mean Winter Temperature and Precipitation (TDJF and PDJF) and Mean Summer Temperature and Precipitation (TJJA and PJJA).

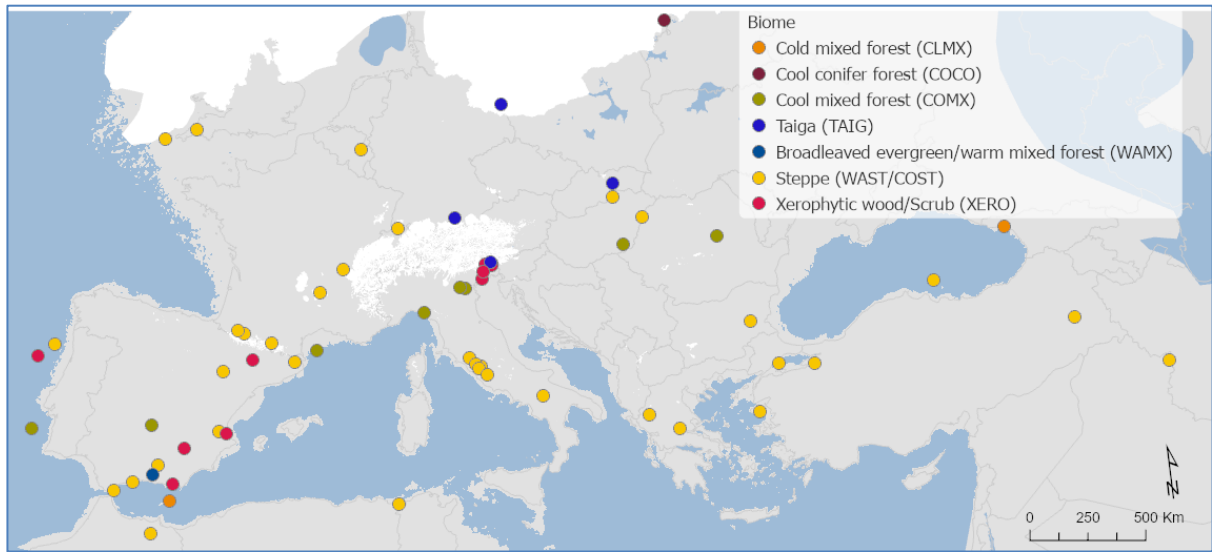
2303 **Figures**
2304
2305
2306



2307
2308
2309 **Figure 1. Site locations and archives (Site numbers are as shown in Table 1)**

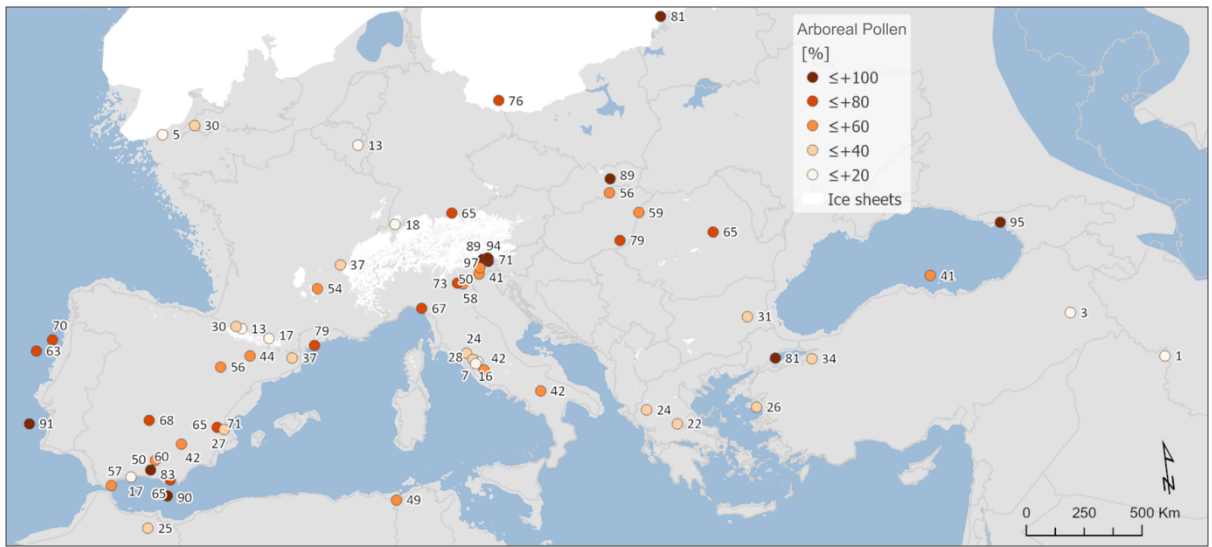
2310
2311
2312

2313

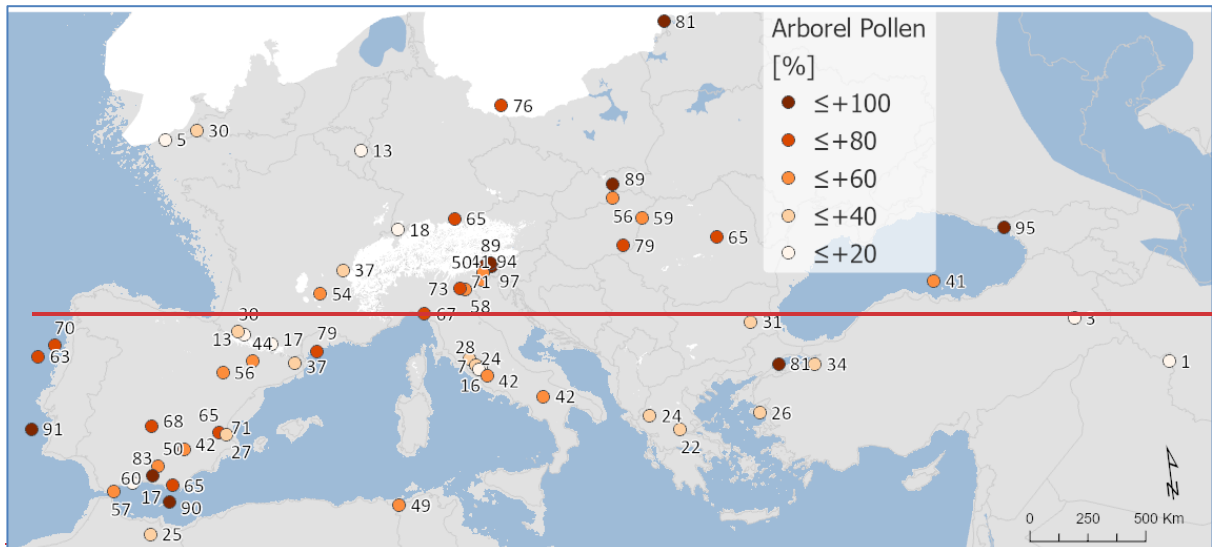


2314
2315
2316
2317

Figure 2. Pollen biomes



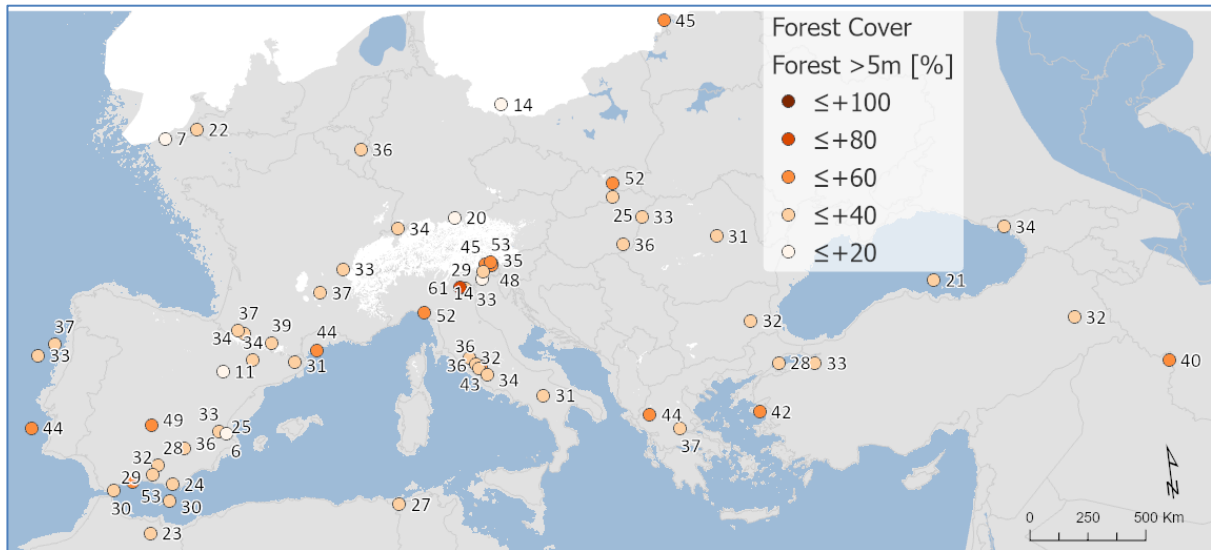
2318



2319
2320

2321 Figure 3. Arboreal Pollen (AP) % forest cover
2322
2323

2324



2325

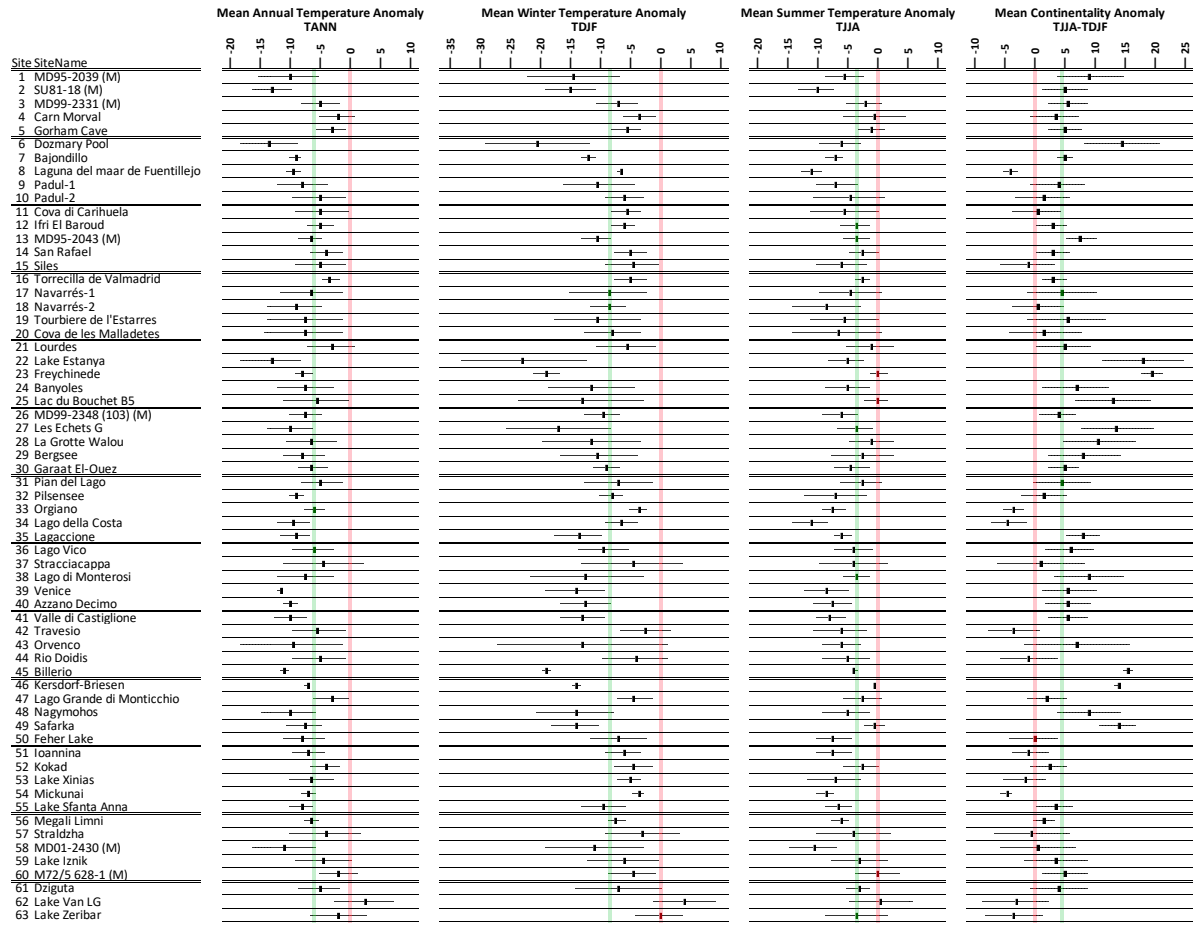
2326

2327

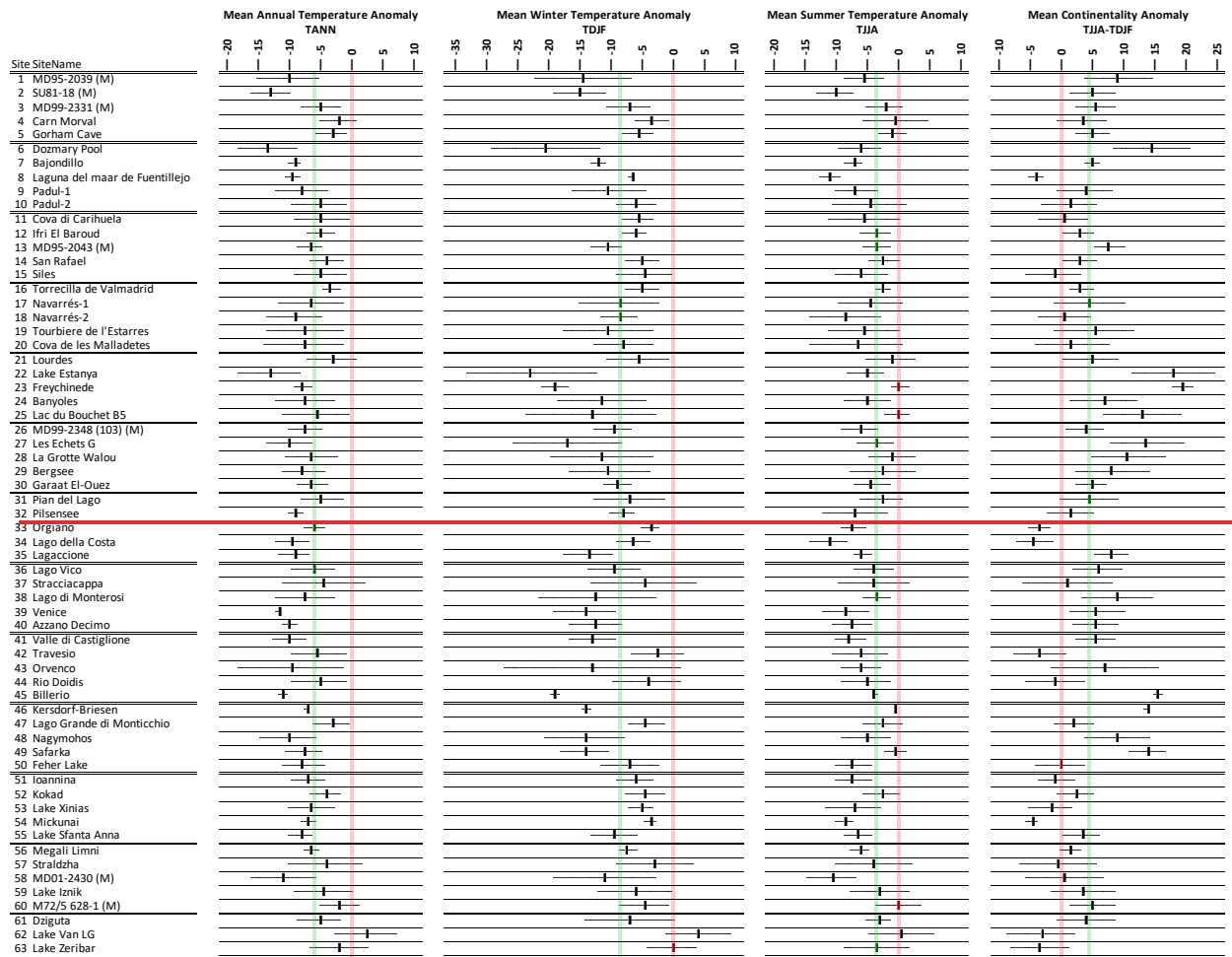
2328

2329

Figure 4. Modern Analogue Technique (MAT) % forest cover



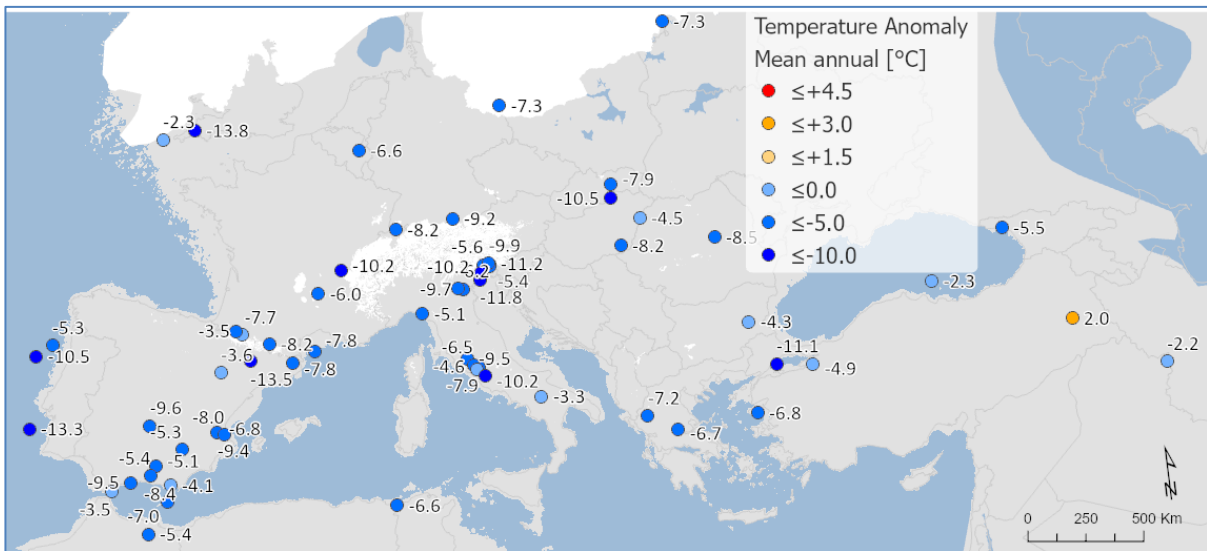
2330
2331



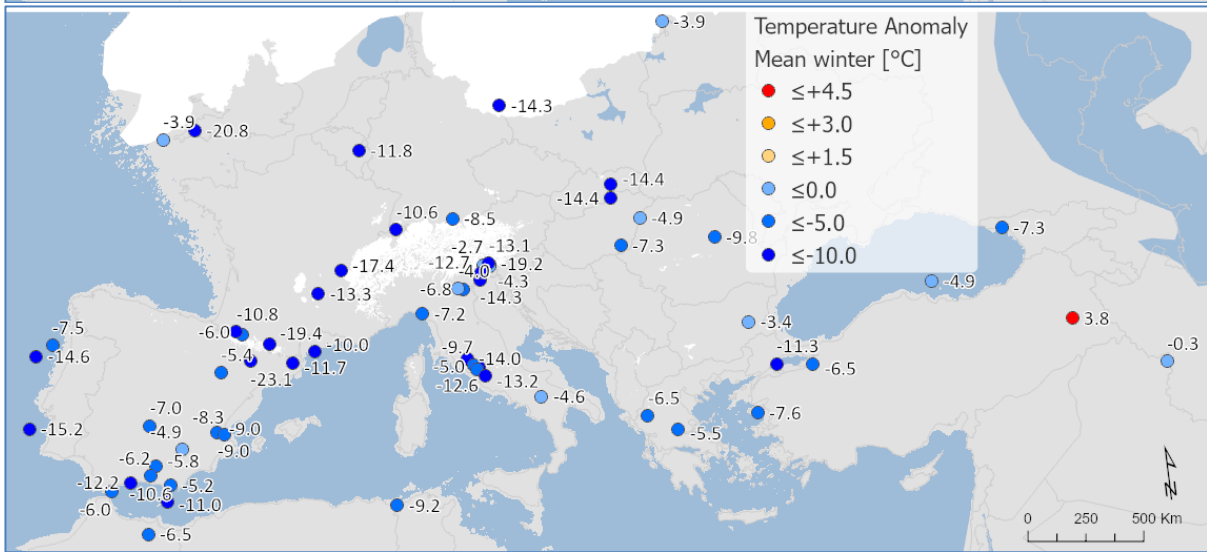
2332
 2333
 2334
 2335
 2336
 2337
 2338
 2339
 2340
 2341

Figure 5. Pollen-based MAT reconstructions for LGM annual, winter and summer temperature anomalies (uncertainties represent one standard deviation). Continentality represents the difference in temperature between summer and winter, with positive anomalies indicating an increase in the temperature difference between summer and winter. All values are expressed as anomalies compared with the present day. The green line indicates the mean for all the sites.

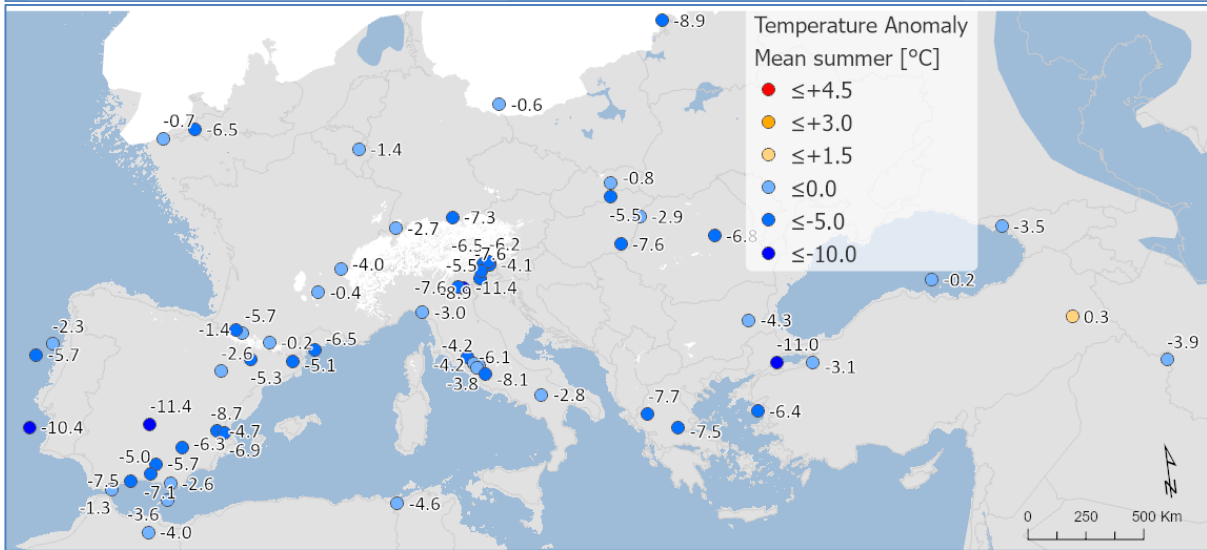
2342

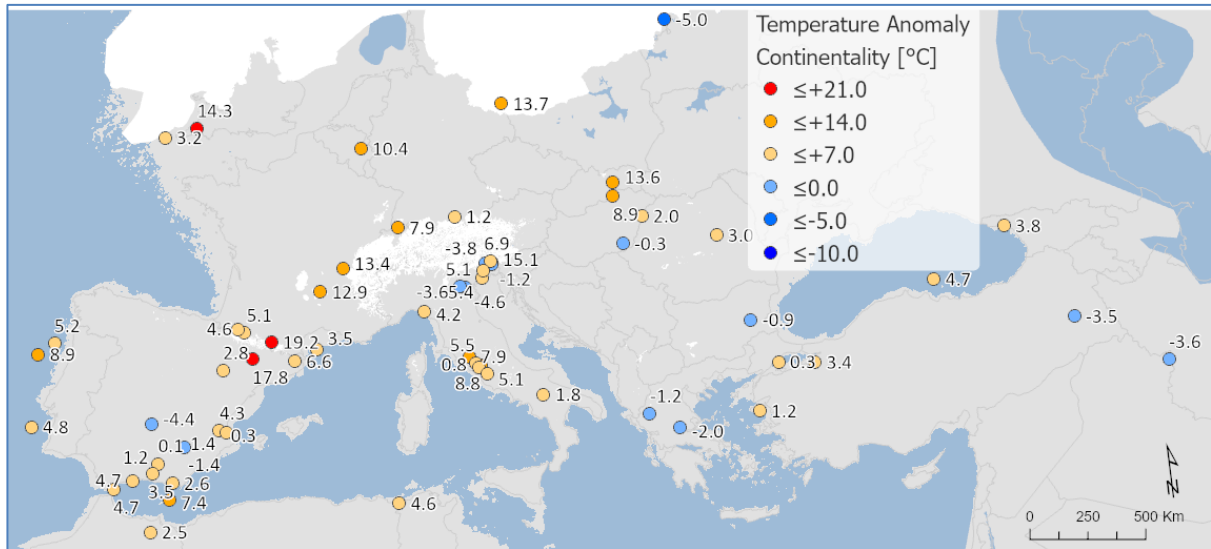


2343



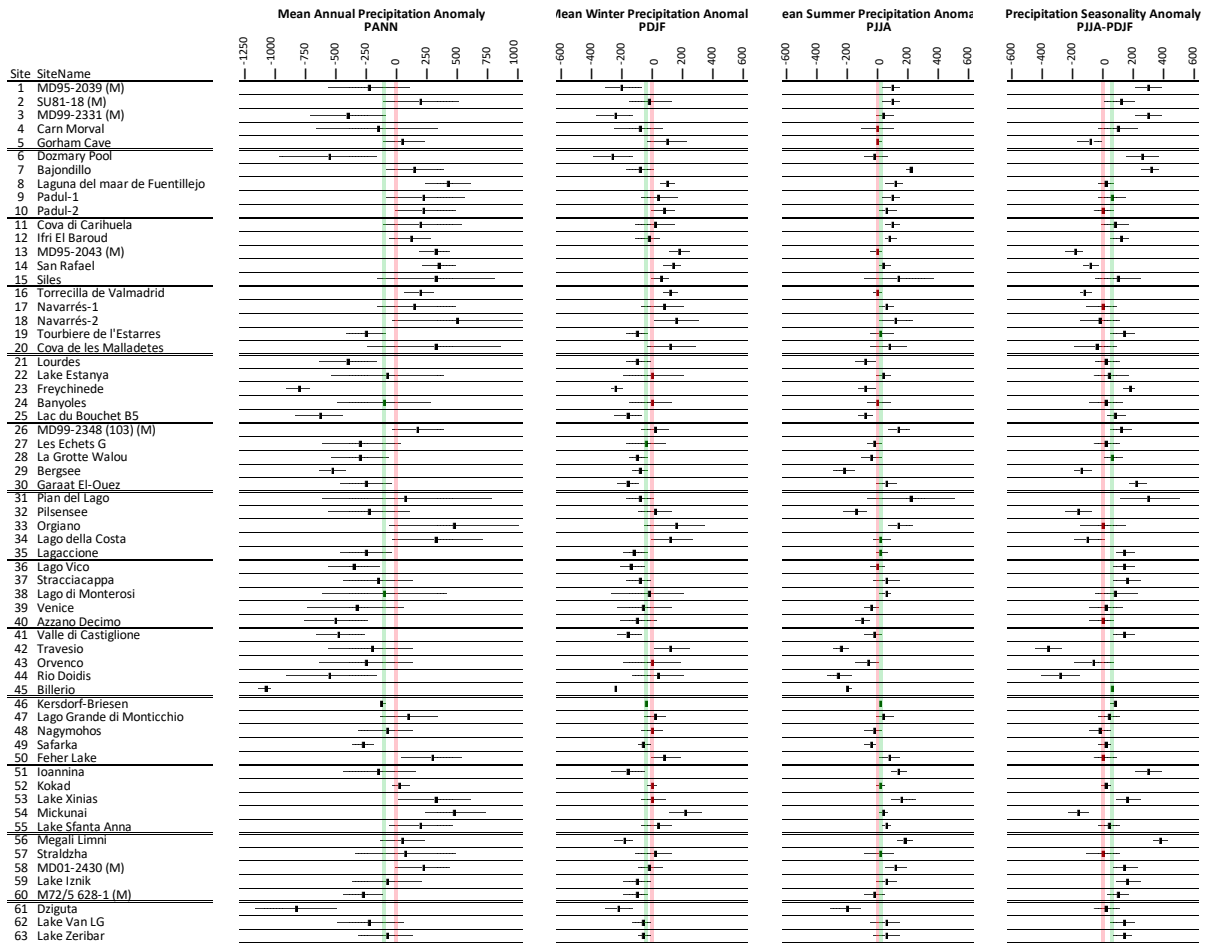
2344

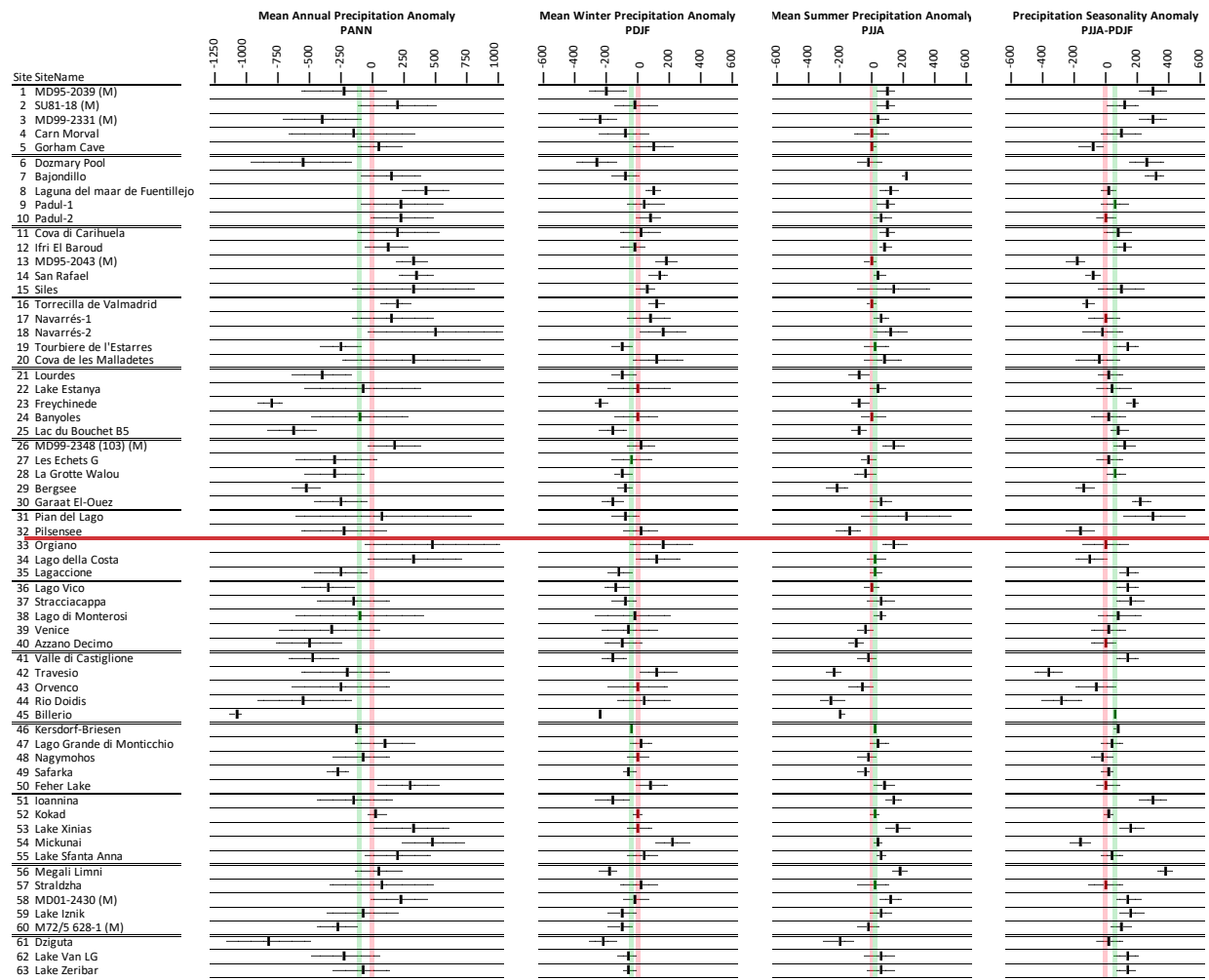




2345
 2346
 2347
 2348
 2349
 2350
 2351
 2352

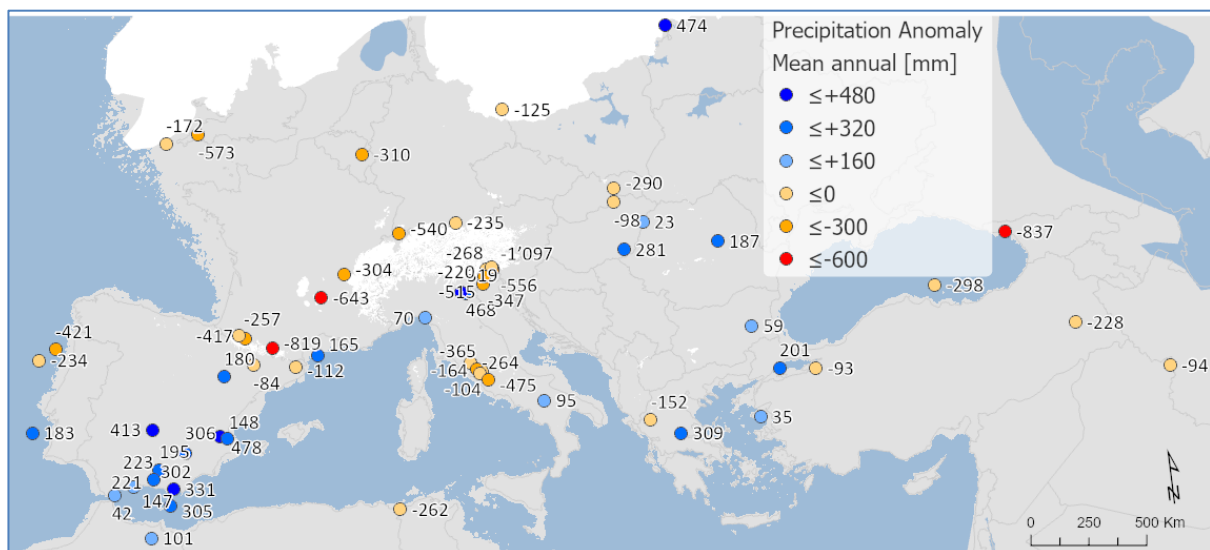
Figure 6. Maps of pollen-based MAT reconstructions for LGM annual, winter and summer temperature anomalies (as shown in figure 9). Continentality represents the difference in temperature between summer and winter, with positive anomalies indicating an increase in the temperature difference between summer and winter. All values are expressed as anomalies compared with the present day.





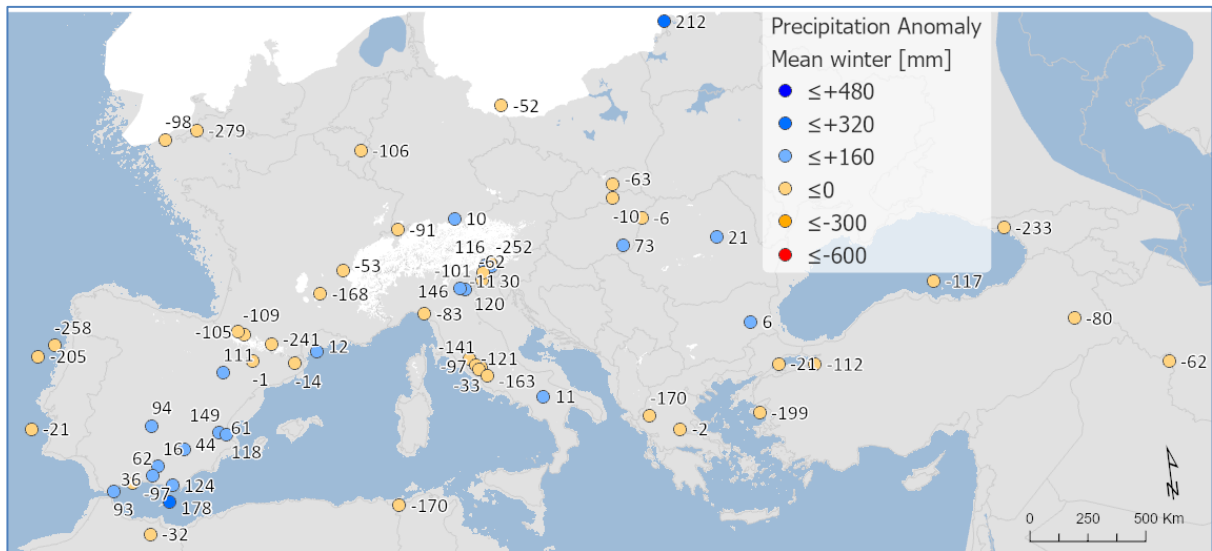
2354
2355
2356
2357
2358
2359
2360
2361

Figure 7. Pollen-based MAT reconstructions for LGM annual, winter and summer precipitation anomalies (uncertainties represent one standard deviation). Seasonality represents the difference in precipitation between summer and winter, with positive anomalies indicating an increase in summer precipitation compared to winter. All values are expressed as anomalies compared with the present day. The green line indicates the mean for all the sites.

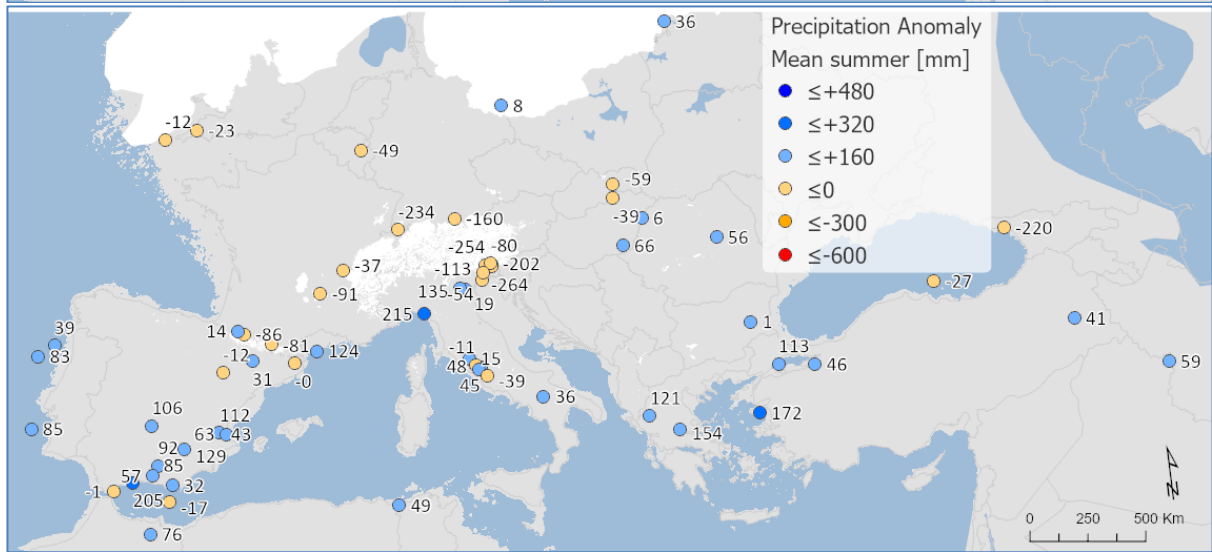


2362

2363



2364



2365

2366

2367

2368

2369

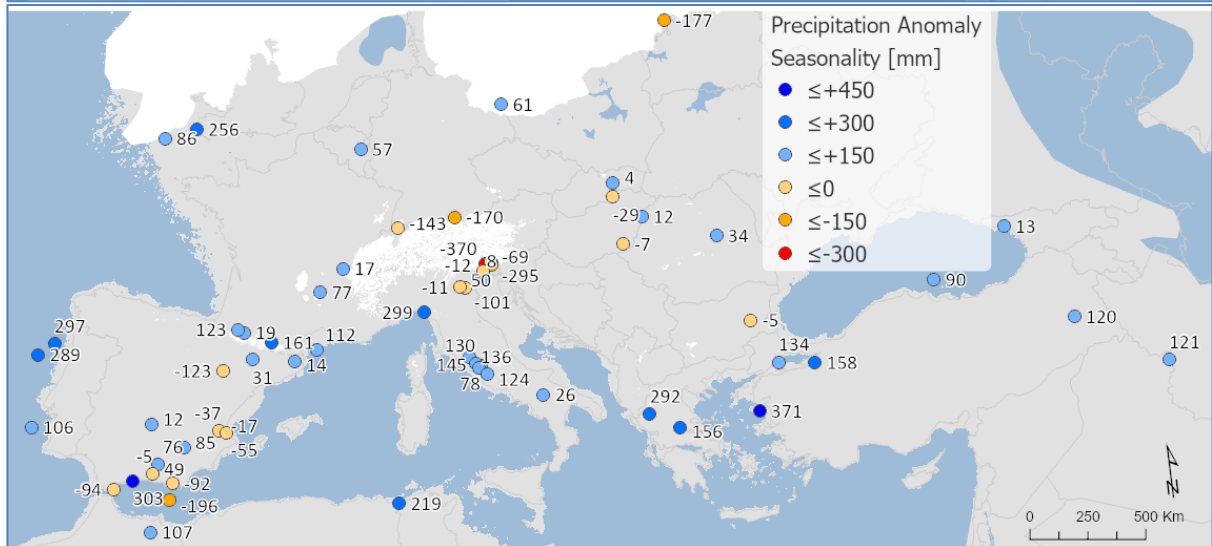
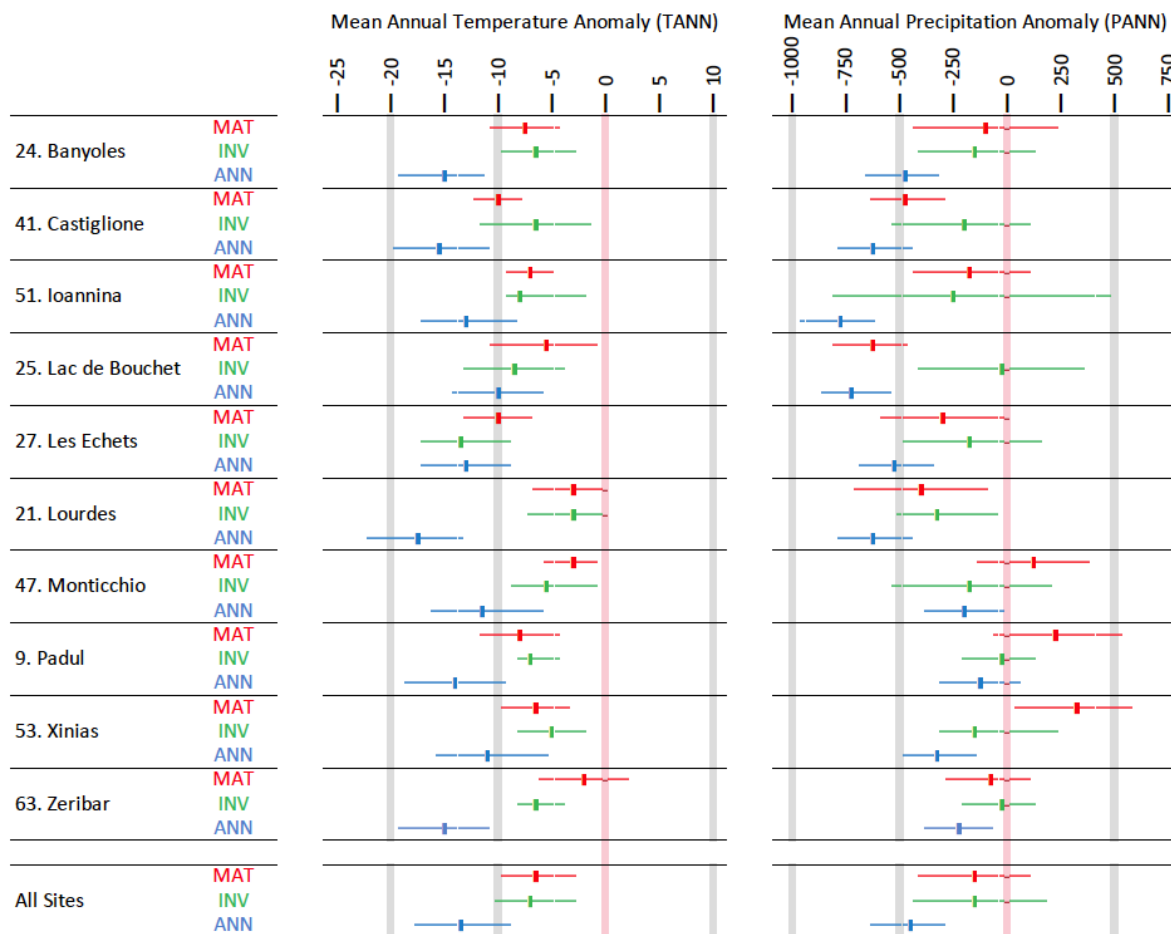


Figure 8. Maps of pollen-based MAT reconstructions for LGM annual, winter and summer precipitation anomalies (as shown in figure 11). Seasonality represents the difference in precipitation between summer and winter, with positive anomalies indicating an increase in

2370 summer precipitation compared to winter. All values are expressed as anomalies compared
2371 with the present day.
2372
2373

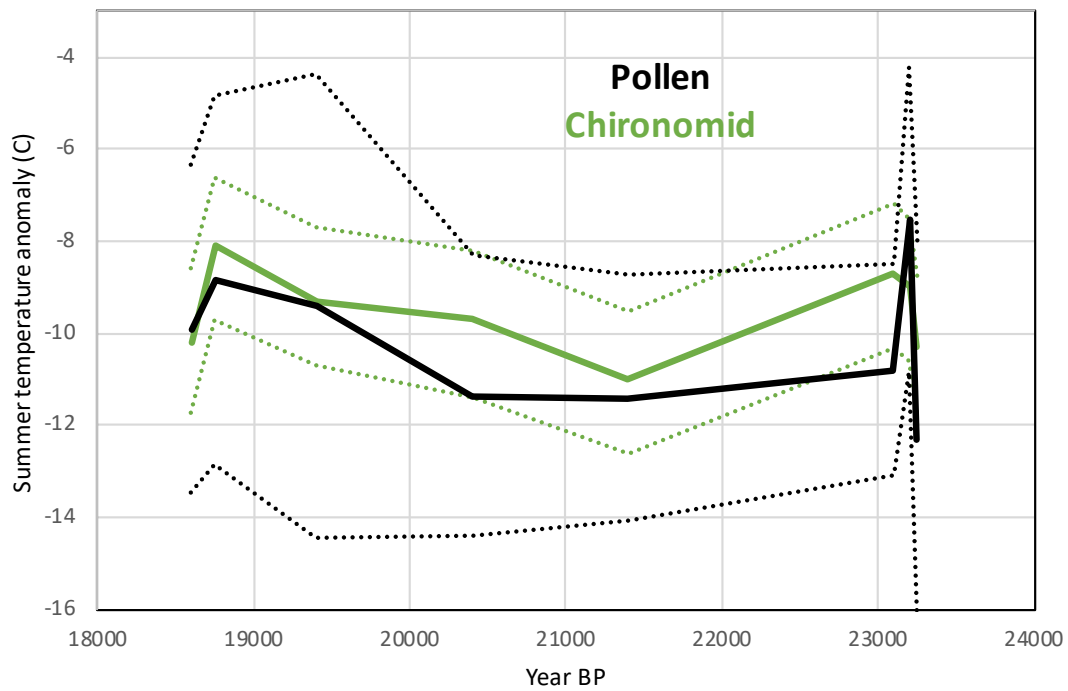
2374



2375
 2376
 2377
 2378
 2379
 2380
 2381
 2382

Figure 9. A site-by-site comparison between LGM pollen-climate reconstructions based on Modern Analogue Technique MAT (this study), neural-networks ANN (Peyron et al., 1998), and Inverse Modelling INV (Wu et al., 2007). The results show that MAT and INV give similar climate reconstructions, but ANN is significantly cooler/drier.

2383
2384
2385



2386
2387
2388
2389
2390
2391
2392

Figure 10. Comparison between LGM pollen-climate MAT and chironomid summer temperature reconstructions at Lago della Costa, Italy (chironomid reconstruction and pollen data from Samartin et al., 2016). Dash lines show uncertainties.

2393
2394
2395

Appendix

| Site | Site Name | COHMAP Quality | COHMAP | | | | | | | | | | | | Upper 14C | Upper Cal. BP | Lower 14C | Lower Cal. BP |
|------|--------------------------------|----------------|--------|-----|-----|-----|-----|-----|-----|-----|-------|--|--|------------|------------|---------------|------------|---------------|
| | | | < 17k | 18k | 19k | 20k | 21k | 22k | 23k | 24k | 25k > | | | | | | | |
| 1 | MD95-2039 (M) | 3C | | | | | | | | | | | | 14830±80 | 18166±269 | 19950±210 | 23883±374 | |
| 2 | SU81-18 (M) | 2C | | | | | | | | | | | | 17510±270 | 20952±404 | 21250±280 | 25420±441 | |
| 3 | MD99-2331 (M) | 2C | | | | | | | | | | | | 16170±130 | 19325±303 | 19770±170 | 23682±336 | |
| 4 | Carr Morval | 4C | | | | | | | | | | | | | 18600±3700 | 21500±890/800 | 25867±1127 | |
| 5 | Gorham Cave | 4D | | | | | | | | | | | | | | 18440±160 | 22055±341 | |
| 6 | Dozmary Pool | 2C | | | | | | | | | | | | 14568±129 | 17569±523 | 18325±216 | 21769±602 | |
| 7 | Bajondillo | 1C | | | | | | | | | | | | | 18701±2154 | | | |
| 8 | Laguna del maar de Fuentillejo | 5D | | | | | | | | | | | | 16540±90 | 19847±308 | | | |
| 9 | Padul-1 | 3D | | | | | | | | | | | | 18300±300 | 21821±412 | 19100±160 | 22922±308 | |
| 10 | Padul-2 | 1D | | | | | | | | | | | | | 17450±539 | | 21082±539 | |
| 11 | Cova di Carihuela | 2C | | | | | | | | | | | | 15700±220 | 18958±280 | 21430±130 | 25659±226 | |
| 12 | Ifri El Baroud | 2D | | | | | | | | | | | | 17296±87 | 20761±293 | | | |
| 13 | MD95-2043 (M) | 2C | | | | | | | | | | | | 15440±90 | 18533±294 | 18260±120 | 21951±335 | |
| 14 | San Rafael | 3D | | | | | | | | | | | | 9980±60 | 11464±133 | 16860±120 | 20083±292 | |
| 15 | Siles | 2D | | | | | | | | | | | | 17030±80 | 20345±351 | | | |
| 16 | Torreçilla de Valmadríd | 2D | | | | | | | | | | | | 17100±85 | 20456±366 | | | |
| 17 | Navarrés-1 | 4D | | | | | | | | | | | | 18360±195 | 22001±353 | 20700±295 | 24664±411 | |
| 18 | Navarrés-2 | 5D | | | | | | | | | | | | 5150±50 | 5881±85 | 16000± | 19144± | |
| 19 | Tourbiere de l'Estarres | 1C | | | | | | | | | | | | 17150±250 | 20522±470 | 18970±160 | 22847±317 | |
| 20 | Cova de les Malladetes | 5D | | | | | | | | | | | | 16300±1500 | 19686±1723 | | | |
| 21 | Lourdes | 4D | | | | | | | | | | | | 18510±130 | 22112±130 | 20025±175 | 23952±355 | |
| 22 | Lake Estanya | 5D | | | | | | | | | | | | | 9498±50 | | 19184±251 | |
| 23 | Freychinède | 3C | | | | | | | | | | | | 14800±800 | 17912±856 | 21300±760 | 25615±1030 | |
| 24 | Banyoles | 4C | | | | | | | | | | | | | 19878±100 | | 27862±3000 | |
| 25 | Lac du Bouchet B5 | 2C | | | | | | | | | | | | 15350±350 | 18513±435 | 19200±300 | 23006±384 | |
| 26 | MD99-2348 (103) (M) | 1D | | | | | | | | | | | | 17660±60 | 21065±310 | 19350±90 | 23111±271 | |
| 27 | Les Echets G | 4C | | | | | | | | | | | | 17530±270 | 20970±407 | 18030±250 | 21704±473 | |
| 28 | La Grotte Walou | 1D | | | | | | | | | | | | | | | 21200±700 | |
| 29 | Bergsee | 2D | | | | | | | | | | | | | | 17780±90 | 21244±306 | |
| 30 | Garaat El-Ouez | 2C | | | | | | | | | | | | 16010±320 | 19200±801 | | | |
| 31 | Pian del Lago | 2D | | | | | | | | | | | | | | | 21260±320 | |
| 32 | Pilsensee | 6D | | | | | | | | | | | | 15860±250 | 19073±290 | | | |
| 33 | Orgiano | 2D | | | | | | | | | | | | 17760±160 | 21221±373 | 19290±520 | 23141±621 | |
| 34 | Lago della Costa | 2C | | | | | | | | | | | | 15400±150 | 18484±330 | 19285±160 | 23052±302 | |
| 35 | Lagaccione | 2C | | | | | | | | | | | | 16080±450 | 19369±527 | 20615±940 | 24746±1201 | |
| 36 | Lago Vico | 3C | | | | | | | | | | | | 14385±140 | 17541±272 | 20500±230 | 24430±376 | |
| 37 | Stracciaccappa | 4C | | | | | | | | | | | | 12060±130 | 14093±281 | 19745±820 | 22675±955 | |
| 38 | Lago di Monterosi | 2D | | | | | | | | | | | | 17040±350 | 20398±544 | | | |
| 39 | Venice | 5D | | | | | | | | | | | | | | 18640±100 | 22277±336 | |
| 40 | Azzano Decimo | 2D | | | | | | | | | | | | 18000±300 | 21637±529 | 21025±245 | 25179±449 | |
| 41 | Valle di Castiglione | 3C | | | | | | | | | | | | 14220±145 | 17443±270 | 20300±700 | 24266±842 | |
| 42 | Travesio | 5D | | | | | | | | | | | | | | 18780±200 | 22483±406 | |
| 43 | Orvenco | 2D | | | | | | | | | | | | 17760±160 | 21221±373 | 19290±520 | 23141±621 | |
| 44 | Rio Doidis | 5D | | | | | | | | | | | | | | 18860±190 | 22390±373 | |
| 45 | Billerio | 3D | | | | | | | | | | | | | | 18165±200 | 21872±382 | |
| 46 | Kersdorf-Briesen | 1D | | | | | | | | | | | | | | 17622±94 | 21183±356 | |
| 47 | Lago Grande di Monticchio | 2C | | | | | | | | | | | | | 20204± | | 24014± | |
| 48 | Nagymohos | 2C | | | | | | | | | | | | 14246±144 | 17361±425 | 18159±247 | 21735±622 | |
| 49 | Safarka | 3D | | | | | | | | | | | | | | 18287±1512 | 21912±1781 | |
| 50 | Feher Lake | 1D | | | | | | | | | | | | 17715±250 | 21190±463 | 19911±81 | 23841±313 | |
| 51 | Ioannina | 3C | | | | | | | | | | | | 15330±140 | 18420±312 | 20760±230 | 24748±330 | |
| 52 | Kokad | 5D | | | | | | | | | | | | 14326±63 | 17433±443 | 16280±90 | 19685±538 | |
| 53 | Lake Xinias | 6C | | | | | | | | | | | | 11150±130 | 13049±160 | 21390±430 | 25671±648 | |
| 54 | Mickunai | 1D | | | | | | | | | | | | | 21000±2200 | | | |
| 55 | Lake Sfanta Anna | 1D | | | | | | | | | | | | 17626±96 | 20955±432 | | | |
| 56 | Megali Limni | 6D | | | | | | | | | | | | 19072±237 | 22906±340 | | | |
| 57 | Straldzha | 6C | | | | | | | | | | | | 14696±65 | 18022±364 | 23653±114 | 28580±390 | |
| 58 | MD01-2430 (M) | 4C | | | | | | | | | | | | 12050±75 | 14904±324 | 18310±380 | 21746±968 | |
| 59 | Lake Iznik | 7D | | | | | | | | | | | | 16910±100 | 19515±115 | | | |
| 60 | M72/5 628-1 (M) | 2C | | | | | | | | | | | | 16835±85 | 18490± | 19495±90 | 21280± | |
| 61 | Dziguta | 2C | | | | | | | | | | | | 12990±160 | 15839±483 | 20560±880 | 24666±1126 | |
| 62 | Lake Van LG | 4C | | | | | | | | | | | | | 18590±62 | | 23290±596 | |
| 63 | Lake Zeribar | 4C | | | | | | | | | | | | 13650±160 | 16610±399 | 22000±500 | 26462±880 | |

COHMAP chronological quality classification:
 1C: Bracketing dates within 2000 14C (2360 Cal.) yr interval about the time being assessed
 2C: Bracketing dates, one within 2000 14C (2360 Cal.) yr and the second within 4000 14C (4682 Cal.) yr of the time being assessed
 3C: Bracketing dates within 4000 14C (4682 Cal.) yr interval about the time being assessed
 4C: Bracketing dates, one being within 4000 14C (4682 Cal.) yr and the second being within 6000 14C (7490 Cal.) yr of the time being assessed
 5C: Bracketing dates within 6000 14C (7490 Cal.) yr interval about the time being assessed
 6C: Bracketing dates, one within 6000 14C (7490 Cal.) yr and the second within 8000 14C (9681 Cal.) yr of the time being assessed
 7C: Poorly dated
 1D: Date within 250 14C (206 Cal.) yr of the time being assessed
 2D: Date within 500 14C (684 Cal.) yr of the time being assessed
 3D: Date within 750 14C (975 Cal.) yr of the time being assessed
 4D: Date within 1000 14C (1123 Cal.) yr of the time being assessed
 5D: Date within 1500 14C (1881 Cal.) yr of the time being assessed
 6D: Date within 2000 14C (2360 Cal.) yr of the time being assessed
 7D: Poorly dated

2396
2397
2398
2399
2400
2401
2402
2403
2404
2405
2406
2407
2408
2409
2410
2411
2412
2413
2414
2415

Table A1. Chronological control

2416
2417

| Site Number | Site Name | Site Type | TANN | TDJF | TJJA | PANN | PDJF | PJJA |
|-------------|--------------------------------|--------------|------|------|------|-------|------|------|
| 1 | MD95-2039 (M) | Marine | 15.7 | 10.7 | 20.8 | 1047 | 427 | 70 |
| 2 | SU81-18 (M) | Marine | 20.8 | 15.3 | 26.5 | 629 | 282 | 25 |
| 3 | MD99-2331 (M) | Marine | 14.6 | 9.8 | 19.4 | 1239 | 507 | 88 |
| 4 | Carn Morval | Lake | 12.5 | 8.7 | 16.9 | 1183 | 392 | 206 |
| 5 | Gorham Cave | Cave | 18.3 | 13.4 | 23.7 | 740 | 336 | 25 |
| 6 | Dozmary Pool | Lake | 10.3 | 6.0 | 15.2 | 1271 | 422 | 236 |
| 7 | Bajondillo | Cave | 16.6 | 10.5 | 23.4 | 542 | 223 | 27 |
| 8 | Laguna del maar de Fuentillejo | Lake | 16.1 | 8.1 | 25.4 | 474 | 156 | 47 |
| 9 | Padul-1 | Peat Bog | 16.6 | 9.6 | 24.9 | 417 | 157 | 23 |
| 10 | Padul-2 | Peat Bog | 16.6 | 9.6 | 24.9 | 417 | 157 | 23 |
| 11 | Cova di Carihuela | Cave | 15.7 | 8.1 | 25.1 | 551 | 187 | 57 |
| 12 | Ifri El Baroud | Cave | 16.9 | 10.7 | 24.0 | 457 | 184 | 22 |
| 13 | MD95-2043 (M) | Marine | 17.9 | 12.4 | 24.0 | 214.2 | 37 | 72 |
| 14 | San Rafael | Peat Bog | 18.1 | 11.9 | 24.9 | 243 | 87 | 14 |
| 15 | Siles | Lake | 14.4 | 6.8 | 23.4 | 658 | 195 | 92 |
| 16 | Torreçilla de Valmadrid | Colluvium | 14.2 | 6.6 | 22.5 | 390 | 75 | 82 |
| 17 | Navarrés-1 | Peat Bog | 17.0 | 10.9 | 23.8 | 421 | 96 | 51 |
| 18 | Navarrés-2 | Peat Bog | 17.0 | 10.9 | 23.8 | 421 | 96 | 51 |
| 19 | Tourbiere de l'Estarres | Lake | 13.0 | 6.1 | 20.4 | 1045 | 272 | 217 |
| 20 | Cova de les Malladetes | Cave | 18.1 | 12.1 | 24.8 | 478 | 117 | 60 |
| 21 | Lourdes | Lake | 12.6 | 5.5 | 20.1 | 1002 | 256 | 212 |
| 22 | Lake Estanya | Lake | 12.8 | 5.1 | 21.0 | 641 | 125 | 152 |
| 23 | Freychinede | Lake | 10.8 | 3.9 | 19.0 | 1128 | 257 | 277 |
| 24 | Banyoles | Lake | 14.3 | 7.7 | 21.9 | 698 | 157 | 139 |
| 25 | Lac du Bouchet B5 | Lake | 8.2 | 1.3 | 15.9 | 1070 | 251 | 221 |
| 26 | MD99-2348 (103) (M) | Marine | 14.6 | 8.0 | 21.9 | 618 | 158 | 95 |
| 27 | Les Echets G | Peat Bog | 11.4 | 3.6 | 19.6 | 876 | 175 | 215 |
| 28 | La Grotte Walou | Cave | 10.3 | 3.2 | 17.0 | 903 | 215 | 249 |
| 29 | Bergsee | Lake | 9.6 | 1.4 | 17.6 | 1048 | 189 | 387 |
| 30 | Garaat El-Ouez | Peat Bog | 17.3 | 11.0 | 24.3 | 830 | 360 | 33 |
| 31 | Pian del Lago | Lake | 12.4 | 5.1 | 20.0 | 995 | 266 | 149 |
| 32 | Pilsensee | Lake | 9.3 | 0.6 | 17.7 | 947 | 151 | 374 |
| 33 | Orgiano | Peat Bog | 13.0 | 3.3 | 22.3 | 907 | 200 | 228 |
| 34 | Lago della Costa | Lake | 12.9 | 3.3 | 22.1 | 888 | 196 | 224 |
| 35 | Lagaccione | Lake | 14.2 | 7.2 | 21.7 | 705 | 203 | 109 |
| 36 | Lago Vico | Lake | 13.7 | 6.4 | 21.5 | 870 | 258 | 132 |
| 37 | Stracciacappa | Lake | 14.6 | 7.3 | 22.4 | 867 | 266 | 115 |
| 38 | Lago di Monterosi | Lake | 15.0 | 7.7 | 22.9 | 837 | 248 | 115 |
| 39 | Venice | Peat Bog | 13.4 | 4.5 | 22.1 | 1050 | 221 | 277 |
| 40 | Azzano Decimo | Alluvial Fan | 13.3 | 4.4 | 22.1 | 1170 | 241 | 311 |
| 41 | Valle di Castiglione | Lake | 16.3 | 9.1 | 24.0 | 988 | 294 | 144 |
| 42 | Travesio | Lake | 12.6 | 3.7 | 21.3 | 1415 | 281 | 375 |
| 43 | Orvenco | Alluvial Fan | 13.0 | 3.3 | 22.3 | 907 | 200 | 228 |
| 44 | Rio Doidis | Lake | 12.8 | 4.1 | 21.2 | 1529 | 315 | 392 |
| 45 | Billerio | Lake | 12.8 | 4.1 | 21.2 | 1529 | 315 | 392 |
| 46 | Kersdorf-Briesen | Lake | 8.8 | -1.0 | 17.9 | 538 | 110 | 175 |
| 47 | Lago Grande di Monticchio | Lake | 11.5 | 4.1 | 19.8 | 518 | 154 | 76 |
| 48 | Nagymohos | Peat Bog | 9.5 | -1.5 | 19.1 | 616 | 103 | 230 |
| 49 | Safarka | Peat Bog | 7.0 | -3.2 | 16.0 | 755 | 119 | 280 |
| 50 | Feher Lake | Lake | 11.0 | -0.1 | 20.7 | 546 | 112 | 185 |
| 51 | Ioannina | Peat Bog | 14.7 | 6.5 | 23.3 | 1000 | 364 | 98 |
| 52 | Kokad | Peat Bog | 10.2 | -0.9 | 19.8 | 601 | 130 | 204 |
| 53 | Lake Xinias | Lake | 15.6 | 7.5 | 24.1 | 563 | 211 | 47 |
| 54 | Mickunai | Lake | 6.0 | -5.0 | 16.3 | 682 | 131 | 230 |
| 55 | Lake Sfanta Anna | Lake | 11.6 | 5.2 | 18.4 | 867 | 253 | 172 |
| 56 | Megali Limni | Lake | 15.5 | 8.2 | 23.4 | 684 | 357 | 28 |
| 57 | Straldzha | Peat Bog | 12.5 | 2.6 | 21.8 | 591 | 158 | 135 |
| 58 | MD01-2430 (M) | Marine | 18.0 | 8.7 | 27.5 | 595 | 219 | 75 |
| 59 | Lake Iznik | Lake | 13.9 | 6.1 | 21.8 | 677 | 250 | 85 |
| 60 | M72/5 628-1 (M) | Marine | 14.5 | 8.0 | 21.6 | 857 | 251 | 156 |
| 61 | Dziguta | Peat Bog | 14.1 | 6.6 | 21.7 | 1549 | 409 | 373 |
| 62 | Lake Van LG | Lake | 12.0 | 0.9 | 23.1 | 635 | 201 | 34 |
| 63 | Lake Zeribar | Lake | 17.1 | 5.0 | 29.0 | 427 | 167 | 6 |

2418
2419
2420
2421
2422

Table A2. Modern climate values for each site used in the calculation of anomalies (taken from WorldClim 2, Fick & Hijmans 2017)

2423
2424
2425

| Biome | Change in Biome compared to the Control | | | | | | | | |
|--------------|---|-------------|--------------|---------------|---------------|---------------|----------------|----------------|----------------|
| | Control | 0 Pinaceae | +5% Pinaceae | +10% Pinaceae | +20% Pinaceae | +50% Pinaceae | +100% Pinaceae | +200% Pinaceae | +400% Pinaceae |
| CLDE | 25 | 454 | 0 | 0 | 0 | -1 | -1 | -4 | -4 |
| TAIG | 1489 | -1430 | 16 | 38 | 74 | 192 | 337 | 554 | 914 |
| CLMX | 70 | 108 | 1 | 2 | 3 | -6 | -4 | 4 | 6 |
| COCO | 388 | -388 | 0 | -1 | 3 | 6 | 25 | 50 | 74 |
| TEDE | 33 | 16 | 1 | 1 | 1 | -1 | -2 | -8 | -5 |
| COMX | 2952 | -761 | 1 | 8 | 14 | -4 | -42 | -101 | -284 |
| WAMX | 418 | -28 | -1 | 0 | -1 | -6 | -11 | -29 | -62 |
| XERO | 699 | -323 | 3 | 4 | 12 | 45 | 68 | 113 | 180 |
| DESE | 0 | 0 | 0 | 0 | 0 | 0 | 0 | 0 | 0 |
| STEP | 1752 | 1388 | -14 | -39 | -83 | -173 | -296 | -468 | -663 |
| TUND | 387 | 964 | -7 | -13 | -23 | -52 | -74 | -111 | -156 |
| Total | 8213 | 5860 | 44 | 106 | 214 | 486 | 860 | 1442 | 2348 |

2426
2427

2428 **Table A3.** This shows the results of experiment to test the sensitivity of pollen Biomes to
 2429 changes in the amount of Pinaceae in the pollen assemblage using 8213 modern pollen samples
 2430 from the EMPD2. Pinaceae can be over-represented in marine samples, and it has been
 2431 proposed that removing all Pinaceae from these samples is better than leaving the Pinaceae in
 2432 the pollen assemblage. The 'Control' column on the left shows the number of samples that were
 2433 classified for each Biome without changing the amount of Pinaceae (ie using the original pollen
 2434 assemblage). The other 8 columns to the right show the number of samples where the Biome
 2435 changed relative to the number shown in the control column as a result of either removal of all
 2436 Pinaceae ('0 Pinaceae'), or by artificially increasing the amount of Pinaceae respectively from
 2437 5 to 400% of the original count ('+5% Pinaceae' to '+400% Pinaceae'). For instance, for the
 2438 CLDE (Cold Deciduous) Biome, 25 pollen samples were classified as CLDE without any
 2439 change in Pinaceae ('Control'), but 454 more samples were classified as CLDE when all
 2440 Pinaceae was removed ('0 Pinaceae') compared to 4 fewer samples that were classified as
 2441 CLDE when Pinaceae was increased by as much as 400% ('+400% Pinaceae'). The totals along
 2442 the bottom show that out of the 8213 pollen samples included in the experiment, 5860 biomes
 2443 changed when all Pinaceae was removed, compared to up to 2348 when Pinaceae was
 2444 artificially increased by up to 400%.

2445
2446

Temperature Anomlay

| Site Name | Site Number | TANN delta | | TDJF delta | | TJJA delta | | PANN delta | | PDJF delta | | PJJA delta | |
|---------------------|-------------|------------|-------------|------------|-------------|------------|-------------|------------|-------------|------------|-------------|------------|-------------|
| | | Pinaceae | No Pinaceae | Pinaceae | No Pinaceae | Pinaceae | No Pinaceae | Pinaceae | No Pinaceae | Pinaceae | No Pinaceae | Pinaceae | No Pinaceae |
| MD95-2039 (M) | 1 | -10.5 | -12.3 | -14.6 | -17.9 | -5.7 | -5.9 | -234.3 | -236.3 | -205.4 | -196.4 | 83.1 | 63.0 |
| SU81-18 (M) | 2 | -13.3 | -21.4 | -15.2 | -23.0 | -10.4 | -17.7 | 183.3 | 703.2 | -21.1 | 124.4 | 85.1 | 167.7 |
| MD99-2331 (M) | 3 | -5.3 | -4.8 | -7.5 | -7.0 | -2.3 | -1.4 | -420.6 | -435.6 | -257.7 | -251.1 | 39.4 | 19.0 |
| MD95-2043 (M) | 13 | -7.0 | -6.0 | -11.0 | -9.9 | -3.6 | -2.7 | 304.6 | 332.5 | 178.4 | 201.9 | -17.3 | -22.9 |
| MD99-2348 (103) (M) | 26 | -7.8 | -8.8 | -10.0 | -11.5 | -6.5 | -7.3 | 164.7 | 218.0 | 12.1 | 7.6 | 124.0 | 179.5 |
| MD01-2430 (M) | 58 | -11.1 | -13.5 | -11.3 | -14.5 | -11.0 | -12.8 | 200.6 | 349.1 | -20.8 | 31.4 | 113.1 | 127.9 |
| M72/5 628-1 (M) | 60 | -2.3 | -0.5 | -4.9 | -3.0 | -0.2 | 1.7 | -298.0 | -311.1 | -116.8 | -100.1 | -27.0 | -51.7 |
| Site Average | | -8.2 | -9.6 | -10.6 | -12.4 | -5.7 | -6.6 | -14.2 | 88.5 | -61.6 | -26.0 | 57.2 | 68.9 |

Standard Deviation

| Site Name | Site Number | TANN STDEV | | TDJF STDEV | | TJJA STDEV | | PANN STDEV | | PDJF STDEV | | PJJA STDEV | |
|---------------------|-------------|------------|-------------|------------|-------------|------------|-------------|------------|-------------|------------|-------------|------------|-------------|
| | | Pinaceae | No Pinaceae | Pinaceae | No Pinaceae | Pinaceae | No Pinaceae | Pinaceae | No Pinaceae | Pinaceae | No Pinaceae | Pinaceae | No Pinaceae |
| MD95-2039 (M) | 1 | 4.6 | 3.7 | 7.5 | 4.0 | 2.9 | 4.0 | 330.6 | 268.9 | 110.5 | 96.7 | 53.6 | 55.6 |
| SU81-18 (M) | 2 | 3.1 | 4.0 | 4.0 | 3.4 | 2.8 | 4.8 | 297.1 | 149.3 | 126.6 | 58.0 | 47.3 | 28.4 |
| MD99-2331 (M) | 3 | 2.9 | 4.0 | 3.4 | 3.8 | 2.8 | 5.0 | 302.6 | 368.6 | 103.5 | 134.2 | 57.6 | 64.3 |
| MD95-2043 (M) | 13 | 2.0 | 4.7 | 2.4 | 5.6 | 2.1 | 4.1 | 115.9 | 121.5 | 59.3 | 72.1 | 36.2 | 25.2 |
| MD99-2348 (103) (M) | 26 | 2.4 | 3.8 | 3.0 | 4.2 | 2.7 | 4.6 | 192.7 | 242.9 | 75.8 | 68.2 | 58.9 | 52.1 |
| MD01-2430 (M) | 58 | 5.1 | 2.3 | 8.1 | 2.0 | 3.9 | 2.8 | 218.7 | 182.8 | 78.9 | 58.3 | 53.4 | 45.0 |
| M72/5 628-1 (M) | 60 | 3.2 | 3.9 | 3.8 | 4.0 | 3.5 | 4.6 | 149.0 | 171.9 | 67.1 | 48.2 | 56.5 | 61.8 |
| Site Average | | 3.3 | 3.8 | 4.6 | 3.9 | 3.0 | 4.3 | 229.5 | 215.1 | 88.8 | 76.5 | 51.9 | 47.5 |

2448
2449
2450
2451
2452
2453
2454
2455
2456
2457
2458
2459
2460
2461

Table A4. A comparison of the LGM reconstructed climate for marine sites showing the effect of excluding Pinaceae (shaded) from the pollen assemblage, compared to the results of including Pinaceae (unshaded, also presented in Figures 6-8). It has been proposed that because of the potential for over-representation of Pinaceae in marine pollen samples, it is better to exclude Pinaceae completely from marine pollen samples. Comparing the two approaches, temperatures are generally 1-2C cooler, and precipitation slightly higher when Pinaceae is excluded. The differences for both temperature and precipitation are significantly less than the standard deviation of their uncertainties.

| | All surface samples | | Steppe only | |
|------|---------------------|------|-------------|------|
| | RMSE | R2 | RMSE | R2 |
| TANN | 2.28 | 0.9 | 2.51 | 0.87 |
| TDJF | 3.35 | 0.91 | 3.26 | 0.88 |
| TJJA | 2.21 | 0.81 | 2.49 | 0.82 |
| PANN | 224.94 | 0.69 | 185.7 | 0.71 |
| PDJF | 78.51 | 0.69 | 66.5 | 0.66 |
| PJJA | 52.49 | 0.75 | 43.8 | 0.79 |

2462
2463
2464
2465
2466
2467
2468
2469
2470
2471
2472

Table A5. A comparison of MAT performance statistics based on the modern pollen sample training set using all surface samples from the EMPD2 used in the LGM reconstruction (as shown in Table 3), and a subset of 1588 samples from the EMPD2 that were classified as steppe. The results show little difference between the two different types of samples. The table includes Mean Annual Temperature and Precipitation (TANN and PANN), Mean Winter Temperature and Precipitation (TDJF and PDJF) and Mean Summer Temperature and Precipitation (TJJA and PJJA).

| Site Name | Site# | Pollen Biome | Modern Analogue Biome | Modern Analogue Ecoregion |
|--------------------------------|-------|--------------|---|--|
| MD95-2039 | 1 | XERO | Mediterranean Forests, woodlands and scrubs | Iberian conifer forests |
| SU81-18 | 2 | COMX | Mediterranean Forests, woodlands and scrubs | Iberian conifer forests |
| MD99-2331 | 3 | STEP | Mediterranean Forests, woodlands and scrubs | Alps conifer and mixed forests |
| Carn Morval | 4 | STEP | Temperate broadleaf and mixed forests | North Atlantic moist mixed forests |
| Gorham Cave | 5 | STEP | Mediterranean Forests, woodlands and scrubs | Cyprus Mediterranean forests |
| Dozmary Pool | 6 | STEP | Temperate Coniferous Forest | Alps conifer and mixed forests |
| Bajondillo | 7 | STEP | Temperate broadleaf and mixed forests | Central European mixed forests |
| Laguna del maar de Fuentillejo | 8 | COMX | Mediterranean Forests, woodlands and scrubs | Northwest Iberian montane forests |
| Padul | 9 | STEP | Mediterranean Forests, woodlands and scrubs | Central Anatolian steppe |
| Padul-15-05 | 10 | WAMX | Mediterranean Forests, woodlands and scrubs | Iberian sclerophyllous and semi-deciduous forests |
| Cova di Carhuela | 11 | STEP | Deserts and xeric shrublands | Azerbaijan shrub desert and steppe |
| Ifri El Baroud | 12 | STEP | Mediterranean Forests, woodlands and scrubs | Iberian sclerophyllous and semi-deciduous forests |
| MD95-2043 | 13 | CLMX | Mediterranean Forests, woodlands and scrubs | Southern Anatolian montane conifer and deciduous forests |
| San Rafael | 14 | XERO | Mediterranean Forests, woodlands and scrubs | Tyrrhenian-Adriatic Sclerophyllous and mixed forests |
| Siles | 15 | XERO | Mediterranean Forests, woodlands and scrubs | Northwest Iberian montane forests |
| Torreçilla de Valmadríd | 16 | STEP | Mediterranean Forests, woodlands and scrubs | Southern Anatolian montane conifer and deciduous forests |
| Navarres | 17 | XERO | Mediterranean Forests, woodlands and scrubs | Iberian sclerophyllous and semi-deciduous forests |
| Navarres | 18 | STEP | Temperate broadleaf and mixed forests | Pyrenees conifer and mixed forests |
| Tourbiere de Istarres | 19 | STEP | Temperate grasslands, savannas and shrublands | Eastern Anatolian montane steppe |
| Cova de les Malladetes | 20 | XERO | Mediterranean Forests, woodlands and scrubs | Pyrenees conifer and mixed forests |
| Lourdes | 21 | STEP | Temperate broadleaf and mixed forests | Gissaro-Alai open woodlands |
| Estanya | 22 | XERO | Temperate broadleaf and mixed forests | Western Siberian hemiboreal forests |
| Freychinede | 23 | STEP | Temperate grasslands, savannas and shrublands | Mongolian-Manchurian grassland |
| Lake Banyoles | 24 | STEP | Temperate grasslands, savannas and shrublands | Gissaro-Alai open woodlands |
| Lac du Bouchet B5 | 25 | STEP | Temperate grasslands, savannas and shrublands | Gissaro-Alai open woodlands |
| MD99-2348-103 | 26 | COMX | Temperate broadleaf and mixed forests | Rodope montane mixed forests |
| Les Echets G - DIGI | 27 | STEP | Temperate broadleaf and mixed forests | Western Siberian hemiboreal forests |
| La Grotte Walou | 28 | STEP | Temperate broadleaf and mixed forests | Kazakh forest steppe |
| Bergsee | 29 | STEP | Temperate broadleaf and mixed forests | Kazakh forest steppe |
| Garaat El-Ouez | 30 | STEP | Mediterranean Forests, woodlands and scrubs | Anatolian conifer and deciduous mixed forests |
| Pian del Lago | 31 | COMX | Temperate broadleaf and mixed forests | Western European broadleaf forests |
| Pilsensee | 32 | TAIG | Tundra | Kola Peninsula tundra |
| Orgiano | 33 | COMX | Temperate broadleaf and mixed forests | Western European broadleaf forests |
| Lago della Costa | 34 | COMX | Temperate Coniferous Forest | Alps conifer and mixed forests |
| Lagaccione | 35 | STEP | Temperate grasslands, savannas and shrublands | Gissaro-Alai open woodlands |
| Lago Vico | 36 | STEP | Temperate grasslands, savannas and shrublands | Gissaro-Alai open woodlands |
| Stracciaccia | 37 | STEP | Mediterranean Forests, woodlands and scrubs | Western European broadleaf forests |
| Lago di Monterosi | 38 | STEP | Temperate grasslands, savannas and shrublands | Northwest Iberian montane forests |
| Venice | 39 | XERO | Tundra | Scandinavian Montane Birch forest and grasslands |
| Azzano Decimo | 40 | XERO | Temperate broadleaf and mixed forests | Scandinavian Montane Birch forest and grasslands |
| Valle di Castiglione | 41 | STEP | Temperate broadleaf and mixed forests | Tian Shan montane steppe and meadows |
| Travesio | 42 | XERO | Mediterranean Forests, woodlands and scrubs | Iberian conifer forests |
| Orvenco | 43 | TAIG | Temperate broadleaf and mixed forests | Western Siberian hemiboreal forests |
| Rio Doidis | 44 | XERO | Mediterranean Forests, woodlands and scrubs | Cyprus Mediterranean forests |
| Billerio | 45 | TAIG | Temperate broadleaf and mixed forests | Western Siberian hemiboreal forests |
| Kersdorf-Briesen | 46 | TAIG | Temperate broadleaf and mixed forests | Western Siberian hemiboreal forests |
| Lago Grande di Monticchio | 47 | STEP | Temperate broadleaf and mixed forests | Tian Shan montane steppe and meadows |
| Nagymohos Pleistocene | 48 | STEP | Tundra | Sarmatic mixed forests |
| Safarka | 49 | TAIG | Boreal forests / Taiga | Ural montane forests and tundra |
| Feher-to | 50 | COMX | Temperate Coniferous Forest | Alps conifer and mixed forests |
| Ioannina | 51 | STEP | Temperate broadleaf and mixed forests | Central European mixed forests |
| Kokad | 52 | STEP | Temperate broadleaf and mixed forests | East European forest steppe |
| Lake Xinias | 53 | STEP | Temperate broadleaf and mixed forests | Western European broadleaf forests |
| Mickunai | 54 | COCO | Tundra | Scandinavian Montane Birch forest and grasslands |
| Lake Sfanta Anna | 55 | COMX | Temperate Coniferous Forest | Alps conifer and mixed forests |
| Lesvos ML01 Megali Limni | 56 | STEP | Temperate broadleaf and mixed forests | Rodope montane mixed forests |
| Straldzha | 57 | STEP | Temperate broadleaf and mixed forests | Aegean and Western Turkey sclerophyllous and mixed forests |
| MD01-2430 | 58 | STEP | Temperate broadleaf and mixed forests | Euxine-Colchic broadleaf forests |
| Lake Iznik | 59 | STEP | Temperate broadleaf and mixed forests | Tian Shan montane steppe and meadows |
| M72/5 628-1 | 60 | STEP | Deserts and xeric shrublands | Azerbaijan shrub desert and steppe |
| Dziguta Core 1 | 61 | CLMX | Temperate broadleaf and mixed forests | Northeastern Spain and Southern France Mediterranean forests |
| Lake Van LG | 62 | STEP | Mediterranean Forests, woodlands and scrubs | Aegean and Western Turkey sclerophyllous and mixed forests |
| Lake Zeribar | 63 | STEP | Temperate grasslands, savannas and shrublands | Pontic steppe |

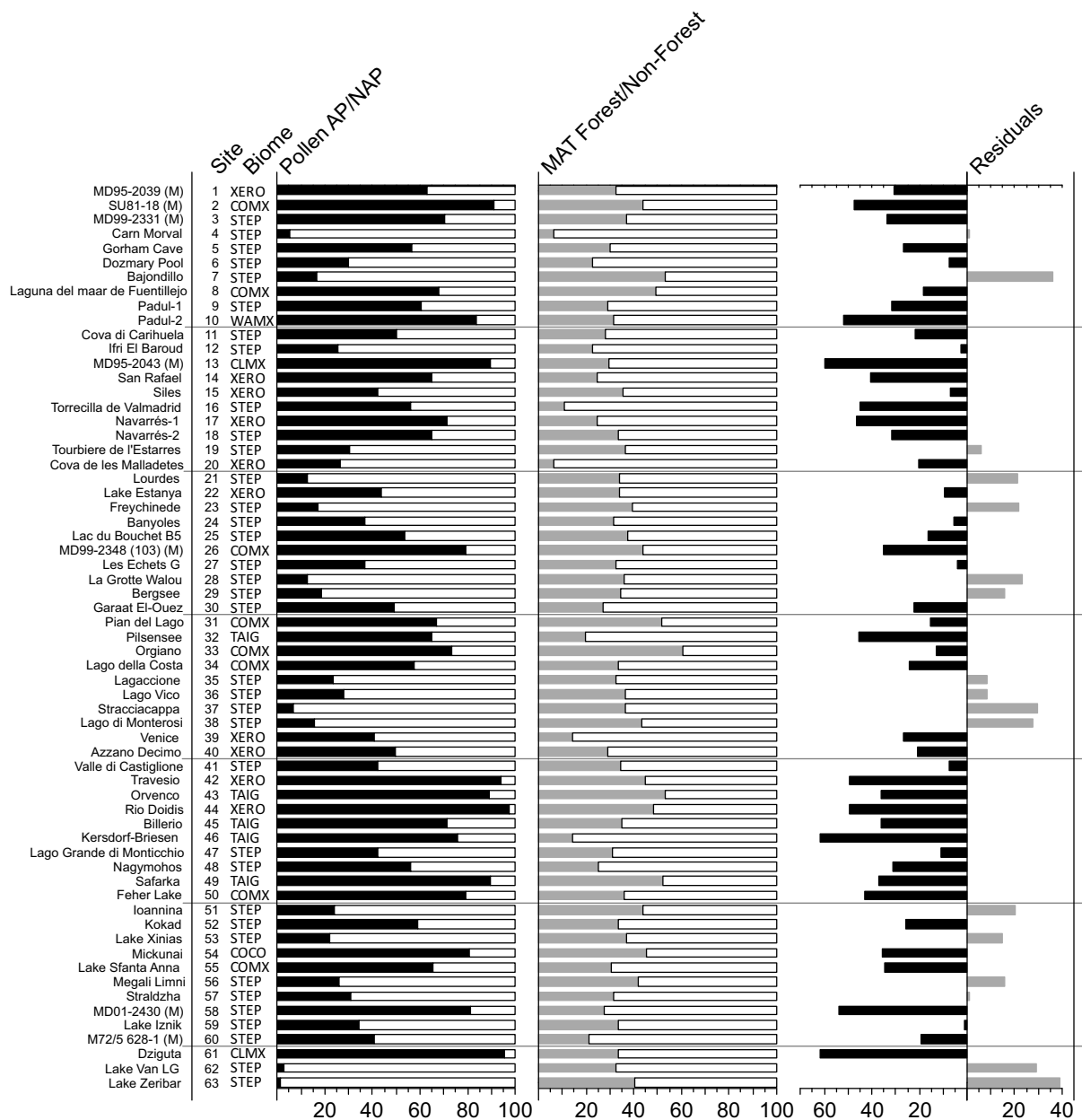
Notes: Modern analogue Biomes and Ecoregions were calculated as the most commonly occurring amongst all 6 best modern analogue pollen samples in all LGM samples for each pollen site/record. These are taken from the EMPD2 (Davis et al 2020), using the classification of Olsen et al 2001.

2473
2474
2475
2476
2477
2478
2479
2480

Table A6. The biome and ecoregion of the modern surface samples used as analogues in the pollen-climate reconstructions.

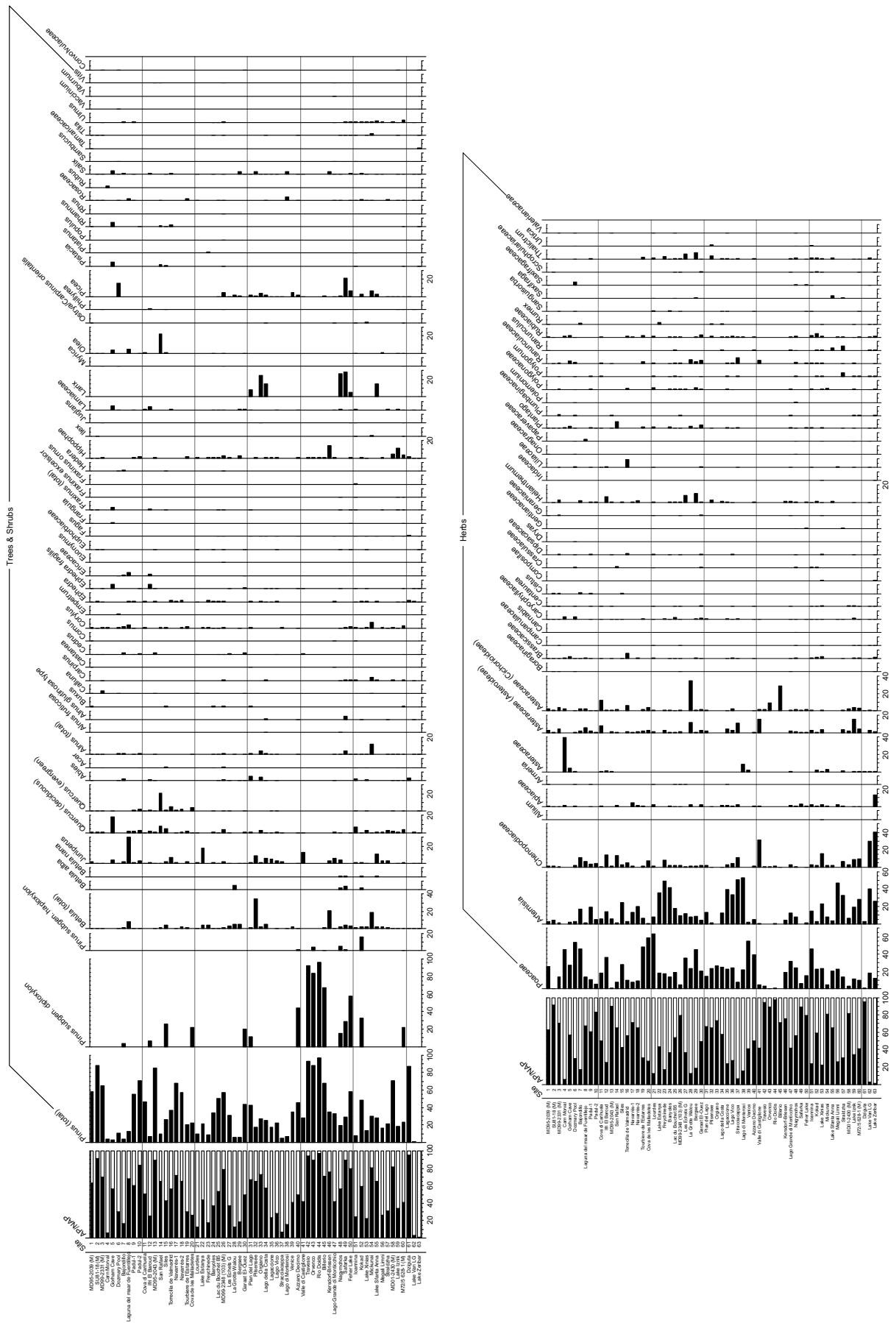
2481
 2482
 2483
 2484
 2485

Figures



2486
 2487
 2488
 2489
 2490

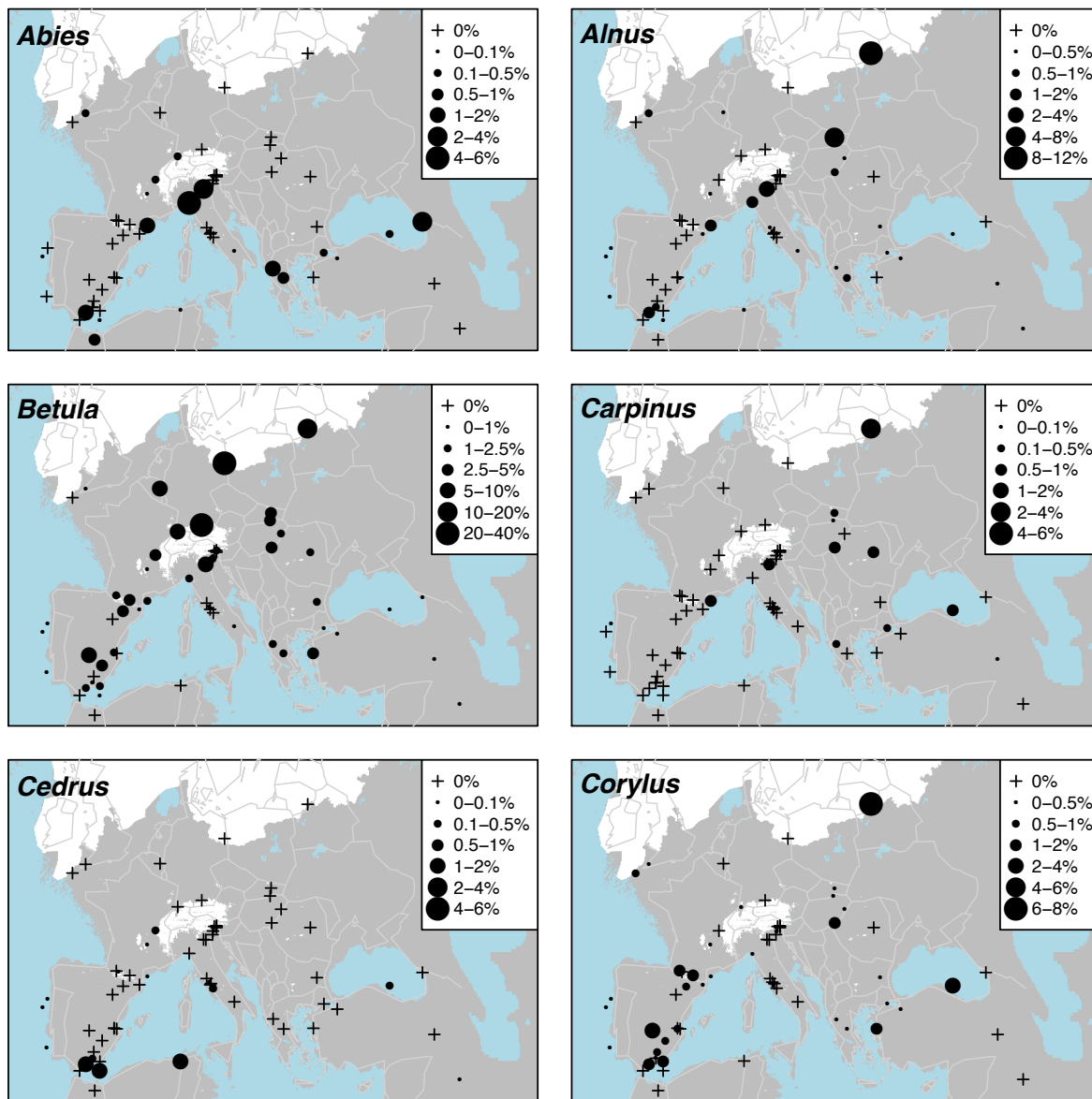
Figure A1. Pollen biomes (see figure 2 for key), Arboreal Pollen (AP) % forest cover, MAT % forest cover and residuals (AP % compared to MAT Forest %)



2491
2492

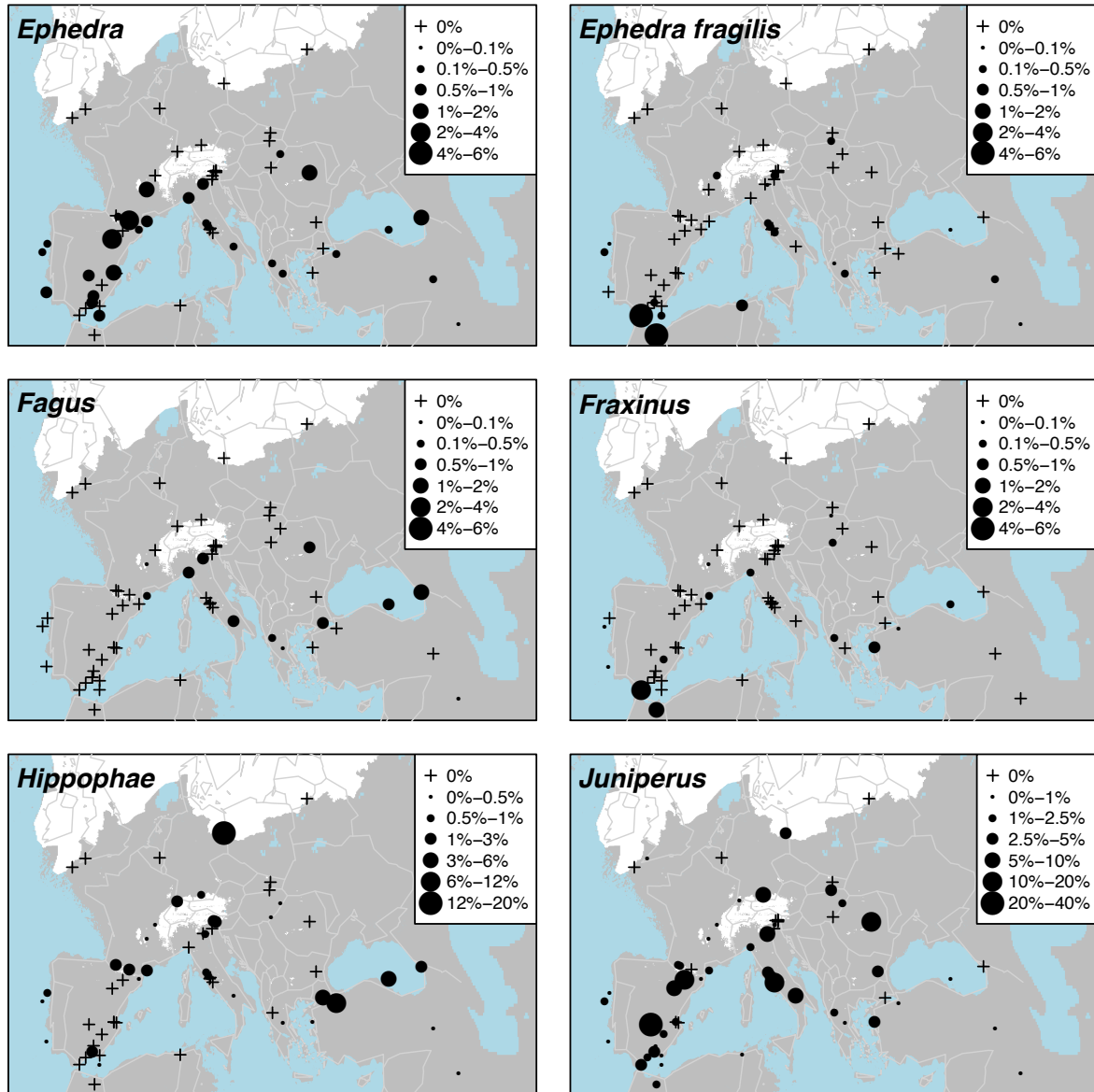
Figure A2. Pollen taxa percentages for all LGM sites/records

2493
2494
2495
2496



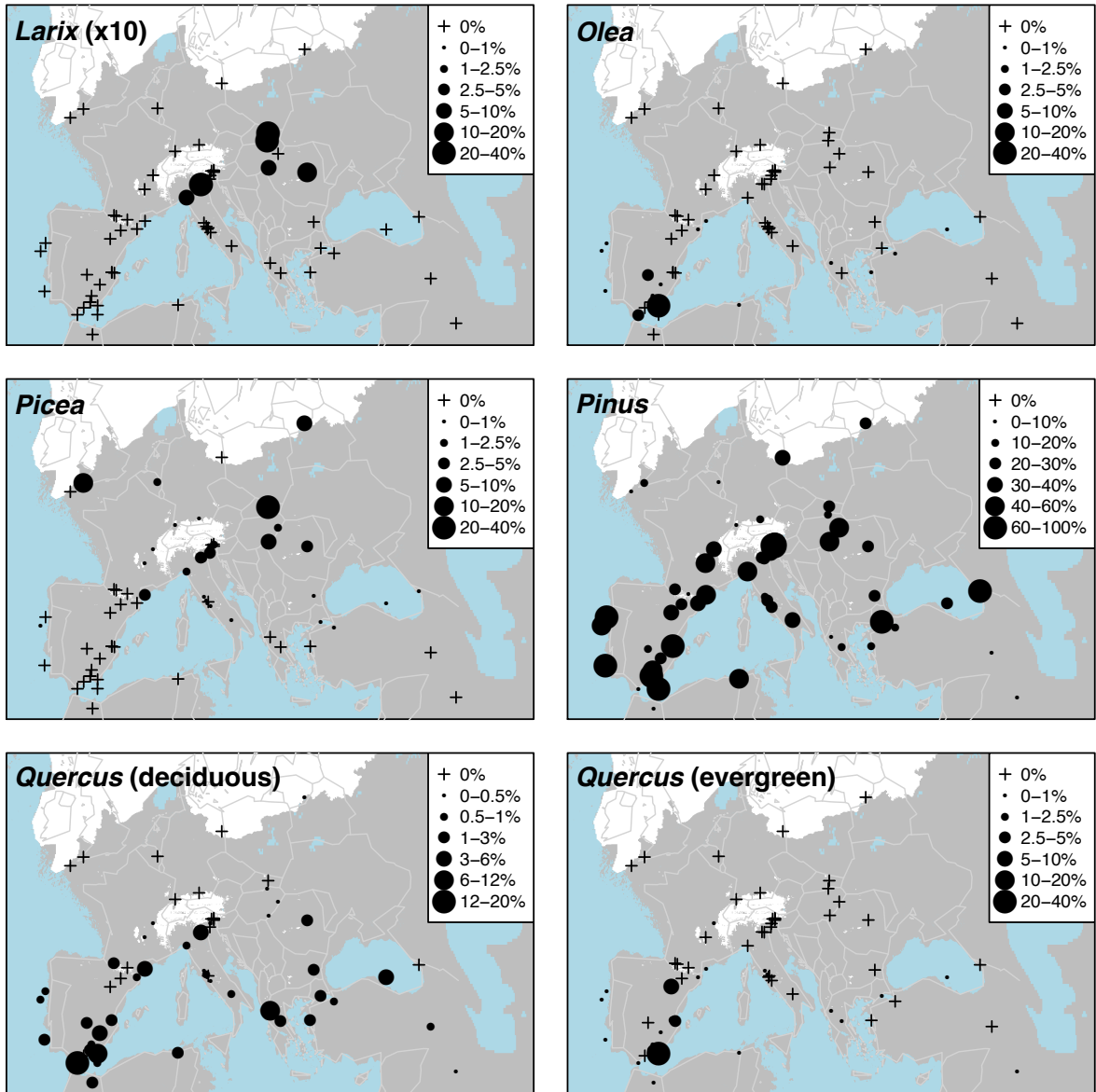
2497
2498
2499
2500

Figure A3aA3. Percentage maps of *Abies*, *Alnus*, *Betula*, *CarPinus*, *Cedrus* and *Corylus*



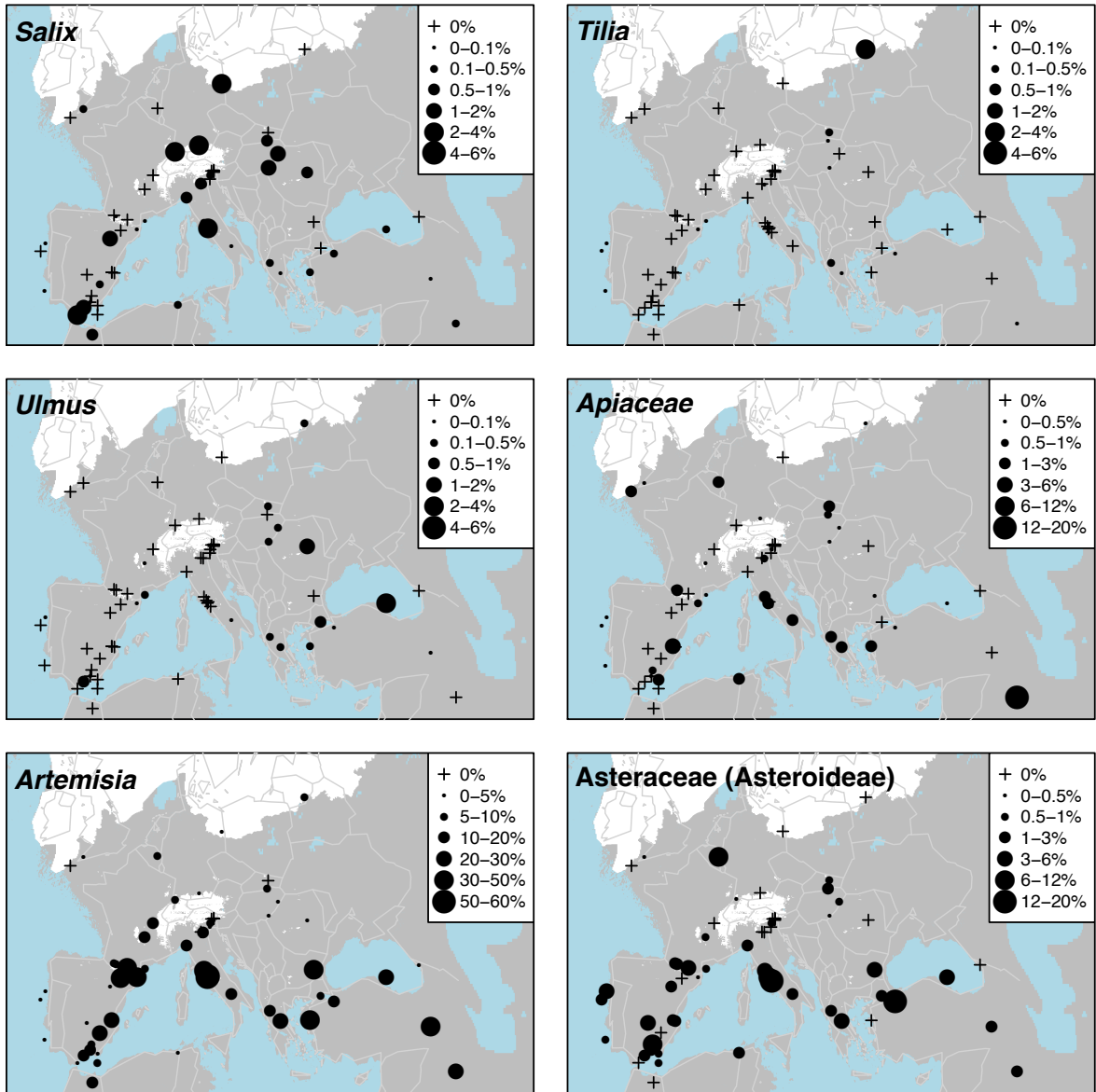
2501
 2502
 2503
 2504
 2505

Figure A3bA4. Percentage maps of *Ephedra*, *Ephedra fragilis*, *Fagus*, *Fraxinus*, *Hippophae* and *Juniperus*



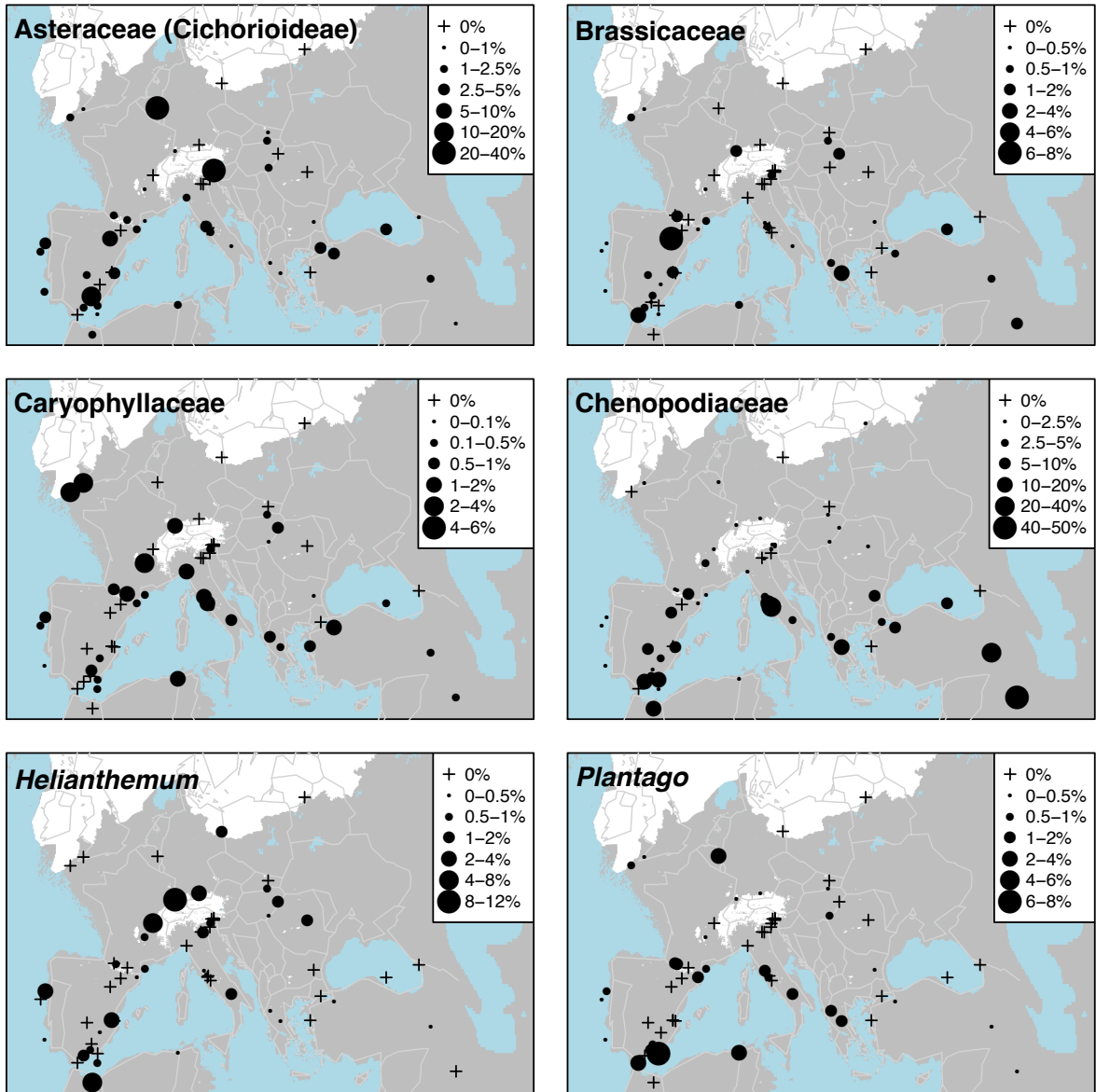
2506
 2507
 2508
 2509
 2510

Figure A3eA5. Percentage maps of *Larix* (x10 exaggeration), *Olea*, *Picea*, *Pinus*, *Quercus* (deciduous) and *Quercus* (evergreen)



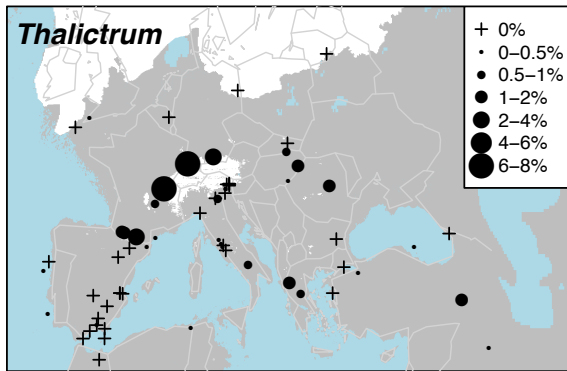
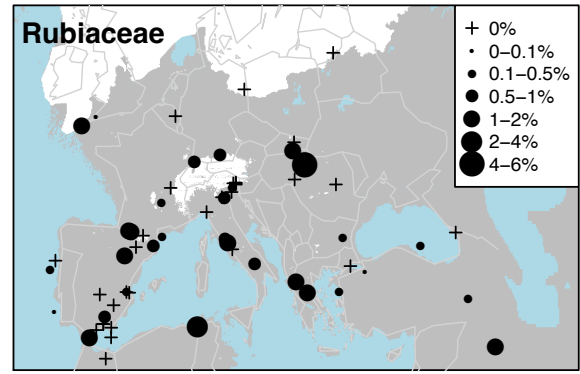
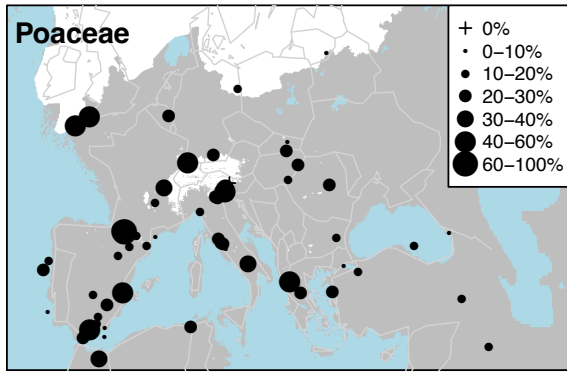
2511
 2512
 2513
 2514

Figure A3dA6. Percentage maps of *Salix*, *Tilia*, *Ulmus*, *Apiaceae*, *Artemisia* and *Asteraceae* (*Asteroideae*)



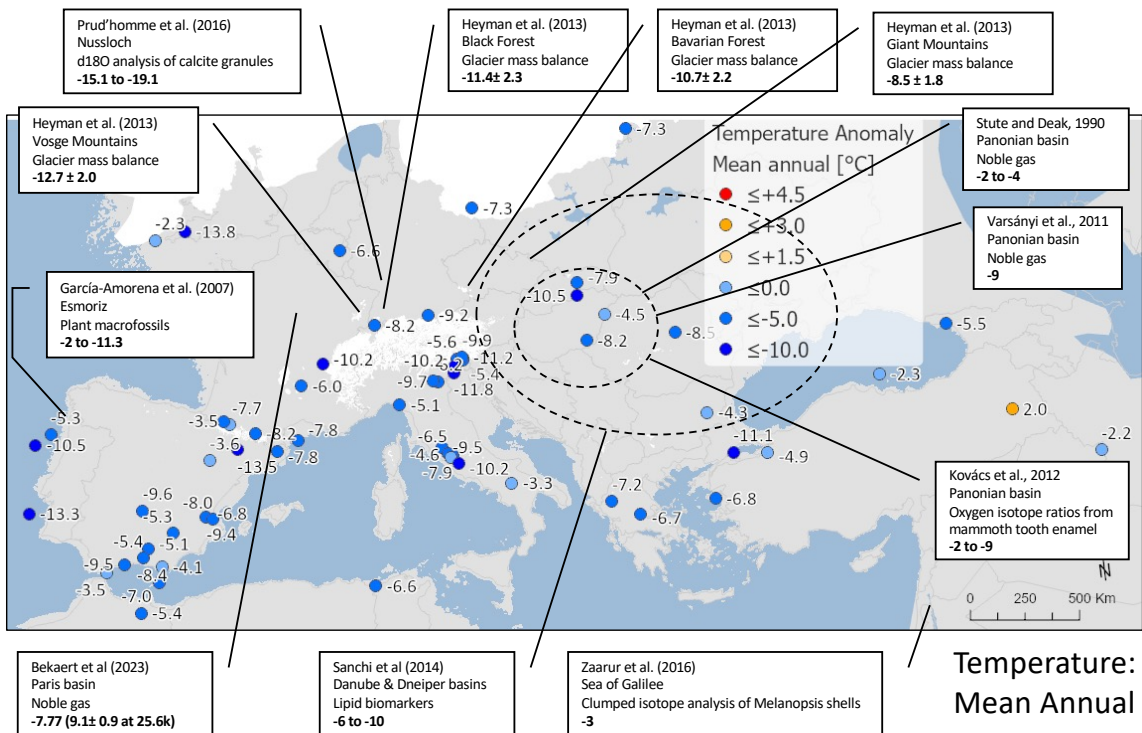
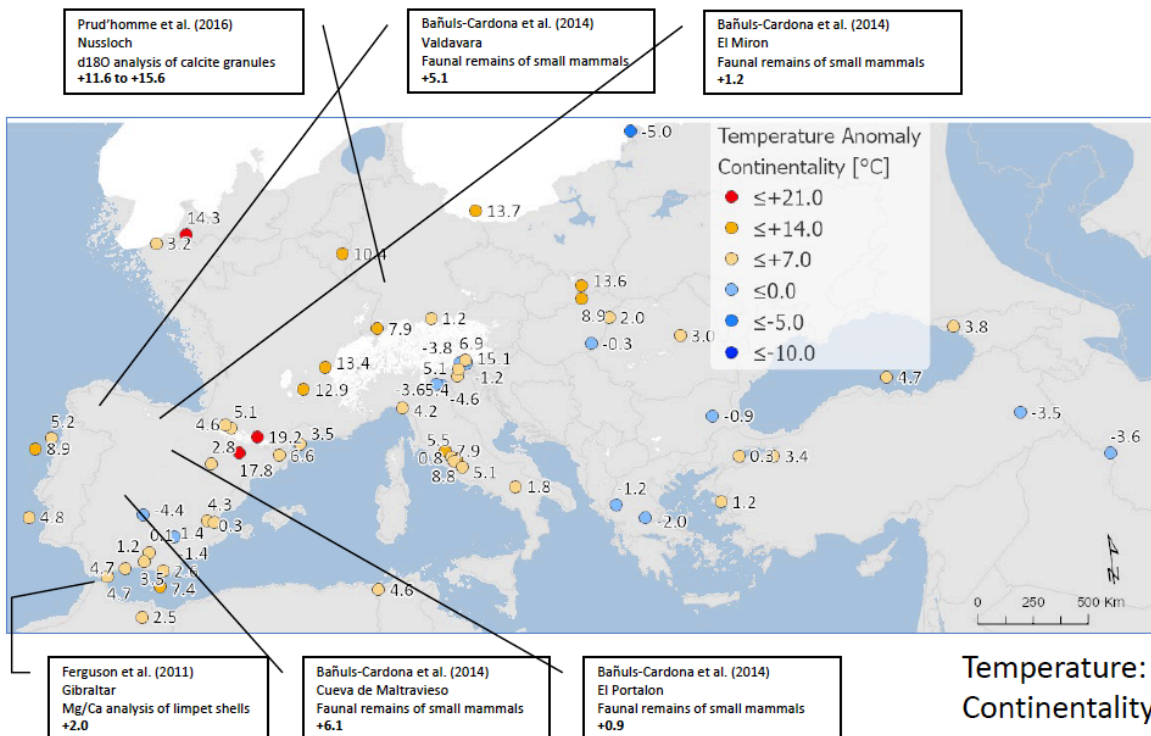
2515
 2516
 2517
 2518
 2519

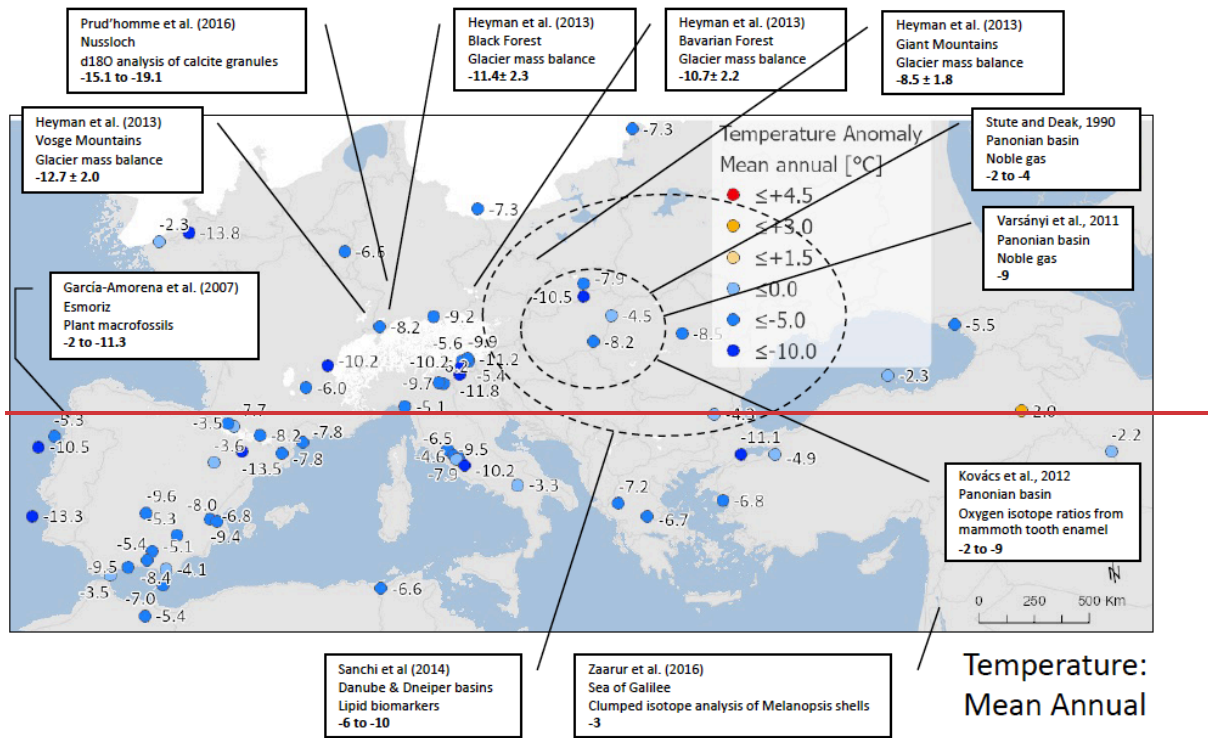
Figure A3eA7. Percentage maps of Asteraceae (Cichorioideae), Brassicaceae, Caryophyllaceae, Chenopodiaceae, Helianthemum and *Plantago*



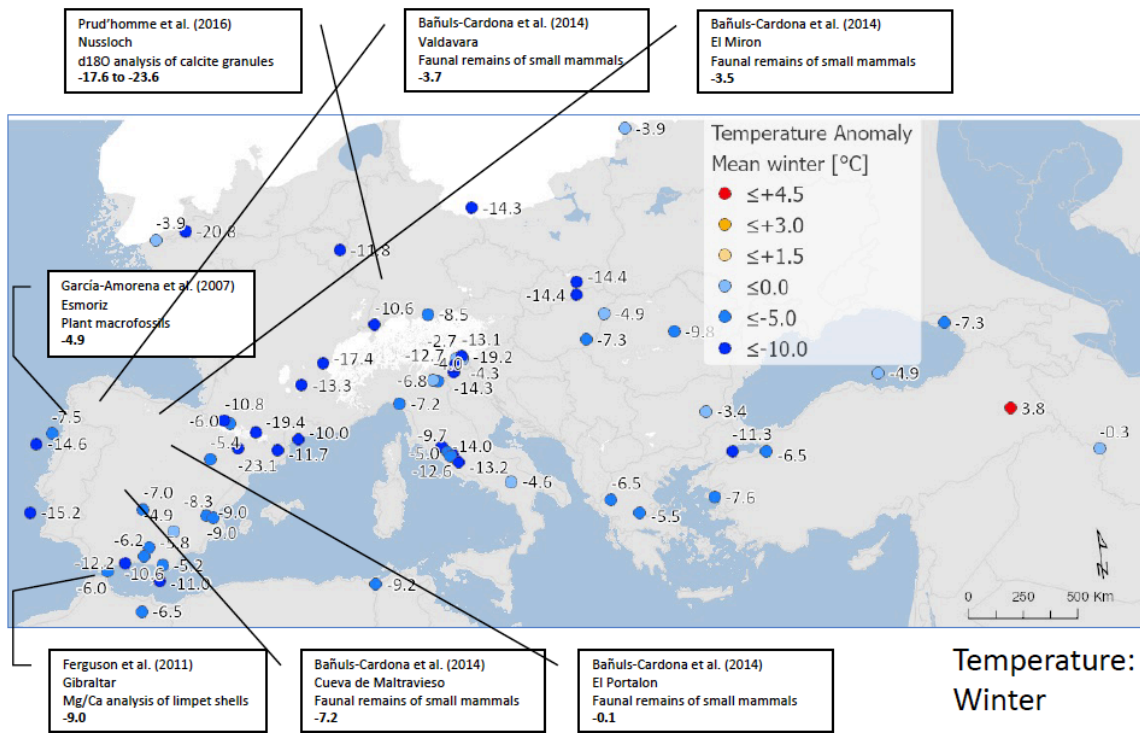
2520
 2521
 2522
 2523
 2524
 2525
 2526
 2527
 2528

Figure A3fA8. Percentage maps of Poaceae, Rubiaceae and *Thalictrum*

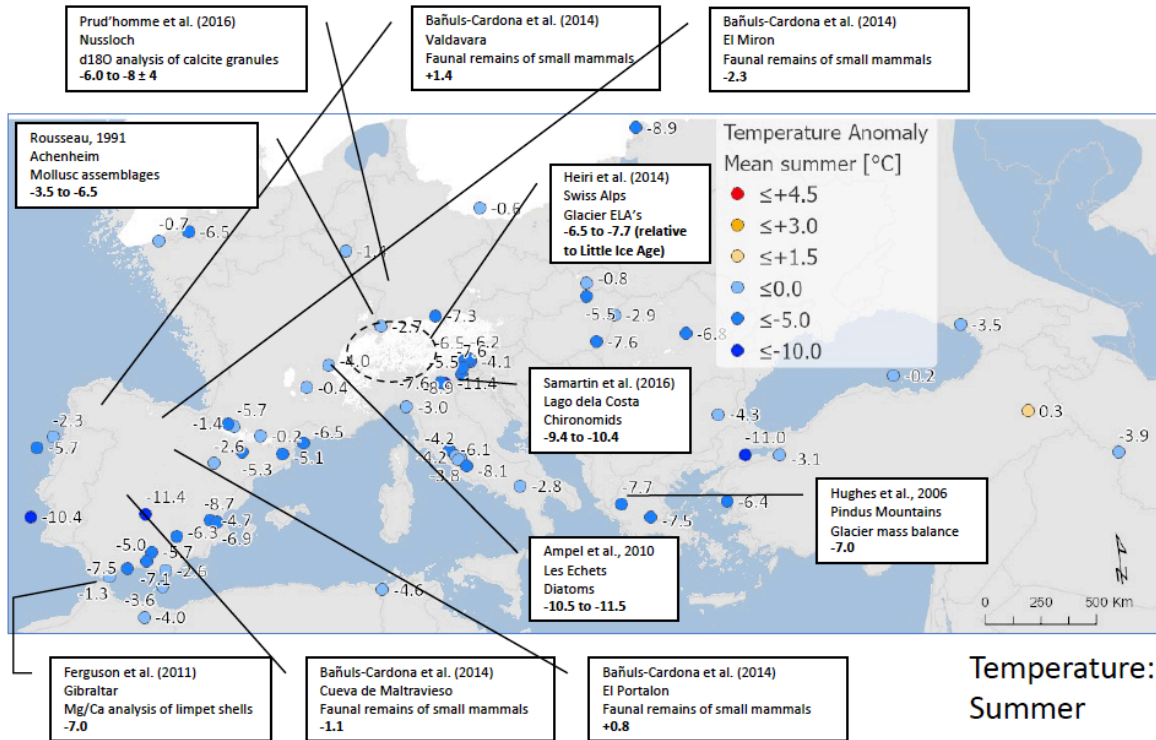




2532
2533
2534

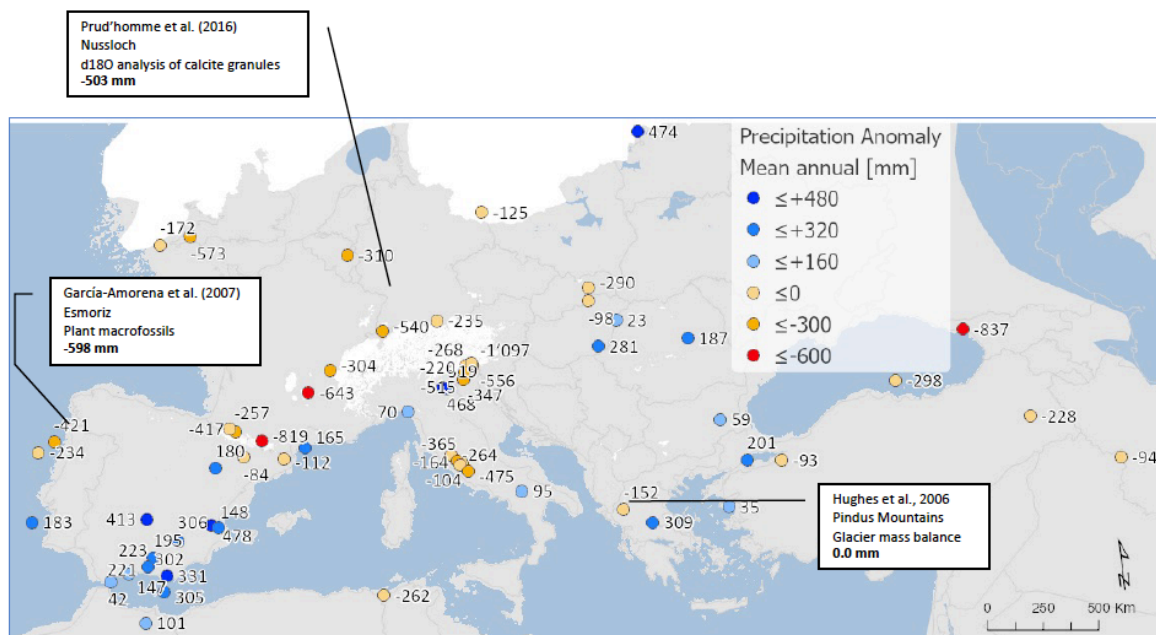


2535
2536



2537
2538
2539
2540
2541
2542
2543
2544
2545

Figure A4 Figure A9. Maps of pollen-based MAT reconstructions for LGM annual, winter and summer temperature anomalies (as shown in figure 10), shown together with the results of other published studies. Continentality represents the difference in temperature between summer and winter, with positive anomalies indicating an increase in the temperature difference between summer and winter. All values are expressed as anomalies compared with the present day unless otherwise indicated.



2546

2547
2548
2549
2550
2551

~~Figure A5~~ Figure A10. Maps of pollen-based MAT reconstructions for LGM annual precipitation anomalies (as shown in figure 12), shown together with the results of other published studies. All values are expressed as anomalies compared with the present day.

2552
2553